Development of mammalian cell display and panning techniques for the selection of HIV-1 vaccine candidates

Von der Fakultät für Lebenswissenschaften

der Technischen Universität Carolo-Wilhelmina

zu Braunschweig

zur Erlangung des Grades eines

Doktors der Naturwissenschaften

(Dr. rer. nat.)

genehmigte

D i s s e r t a t i o n

von Tim-Henrik Jens Gerhard Herbert Bruun
aus Ichenhausen

1. Referent:	Professor Dr. Stefan Dübel
2. Referent:	Professor Dr. Ralf Wagner
eingereicht am:	18.01.2012
mündliche Prüfung (Disputation) am:	20.04.2012

Druckjahr 2012

Vorveröffentlichungen der Dissertation

Teilergebnisse aus dieser Arbeit wurden mit Genehmigung der Fakultät für Lebenswissenschaften, vertreten durch den Mentor der Arbeit, in folgenden Beiträgen vorab veröffentlicht:

Tagungsbeiträge

Bruun, T-H., Kliche, A., Wagner, R.:
Cell-surface Display and Panning of HIV-1 derived Envelope proteins. (Poster)
AIDS Vaccine, Paris (2009).

Kliche, A., Schilling, K., Bruun, T-H., Wagner, R.:
Reverse vaccinology display platforms to identify novel envelope vaccine candidates. (Poster)
Keystone Symposia, Keystone Colorado, U.S.A. (2009)

Bruun, T-H., Kliche, A., Wagner, R.:
Cell-surface Display and Panning of HIV-1 derived Envelope proteins. (Poster)
GFV, Leipzig (2009)

Kliche, A., Bruun, T-H., Schilling, K., Wagner, R.:
Reverse vaccinology display platforms to identify novel envelope vaccine candidates. (Poster)
Europrise, Malta (2008)

Outline

Abstract

Development of a protective vaccine against the human immunodeficiency virus (HIV-1) has failed so far. In almost all vaccination strategies, the neutralizing antibody titers elicited against the pathogen defines protective immunity. Unfortunately, most antibody responses against HIV-1 in an acute infection are only strain-specific and quickly bypassed by escape mutations. Therefore, eliciting a broad, strain-independent immune response that affects essential portions of HIV-1 are considered crucial requirements for a valuable vaccine. An ever increasing number of broadly neutralizing antibodies (bNAb) against the HIV-1 envelope (Env) have been discovered so far. Vaccination trials designed to re-elicit bNAbs that mediate protective immunity have remained futile (reverse vaccinology). Recent discoveries suggest that a membrane-bound, trimeric state of Env used as immunogen is essential for stimulating neutralizing antibody responses.

Therefore, a discovery platform was developed in order to select trimeric envelope variants that are displayed on the surface of mammalian cells. bNAb staining of Env displaying cells was suggested to allow screening for Env variants with the highest affinity. Using iterative rounds of selection strong binding Env variants should be enriched, allowing isolation of the highest affinity Env candidate (Panning). Several display and selection techniques were evaluated, including lentiviral and cellular display, as well as microtiterplate, MACS, and FACS-based selection methods. Finally, an HIV-1 derived lentiviral vector was developed to infect HEK293T cells at a low multiplicity of infection (MOI), in order to link phenotype and genotype. The vector was designed and proven to express both GFP and Env in a constant relationship that enables indirect normalization of produced Env by detecting GFP. Hence, infected cells expressing GFP concurrently display membrane-anchored Env proteins on their surface. Subsequently to staining with an appropriate bNAb, Env-displaying cells were selected for high affinity binding via FACS sorting. A small “model” library of Env variants with distinct binding capacities against the bNAb 447-52D was used for evaluation. In a proof-of-concept study, it was demonstrated that the Env variant with the highest affinity to the applied bNAb was enriched in two rounds of selection (up to ~10-fold). Hence, the technique provides the possibility to screen for membrane-bound Env variants with high binding capacities against the bNAb applied.

Nevertheless, the lenti-cellular display and FACS-mediated panning platform developed in this thesis needs further optimization, it needs to be challenged by libraries of larger diversity, and selected candidates should be evaluated in vaccination trials.

Zusammenfassung

Die Entwicklung eines wirksamen Impfstoffs gegen das humane Immundefizienz-Virus (HIV-1) gilt bis heute als ein ungelöstes Problem. Bei fast allen gängigen Impfstoffen beruht die Wirksamkeit auf der Bildung von Pathogen-neutralisierenden Antikörpern. Die Antikörper, die bei einer akuten HIV-1-Infektion überwiegend entstehen, erreichen jedoch nicht die gewünschte Neutralisation, weil die Ziel-Epitope aufgrund der bei HIV in hohem Maße auftretenden Mutationen schnell verändert werden.

Als zwingende Eigenschaft für ein erfolgreiches Vakzin gilt daher, dass es eine Immunantwort gegen essentielle Bestandteile des HI-Virus auslöst und somit ein möglichst breites Wirkspektrum aufweist. Einige sogenannte „breit neutralisierende Antikörper“ (bNAbs) sind bereits länger bekannt und wurden ausgiebig charakterisiert. In jüngster Zeit wurden in steigendem Maße weitere vielversprechende bNAbs isoliert und Ihre Eigenschaften sind derzeitiger Bestandteil vieler Forschungsbemühungen. Diese Antikörper sind in der Lage, das Oberflächenprotein (Env) von nahezu allen bekannten HI-Viren zu binden und den Infektionsmechanismus zu unterbrechen. Eine Vielzahl von Versuchen, Antikörper mit ähnlichen Eigenschaften durch Impfungen zu induzieren, blieb jedoch bisher erfolglos („reverse vaccinology“). Neueren Erkenntnissen zufolge sind vermutlich membrangebundene, trimere Env-Proteine als Vakzin nötig, um die gewünschte Immunantwort zu vermitteln.

In der vorliegenden Arbeit wurde eine Selektionsmethode entwickelt, bei der Varianten trimerer Env-Proteine auf der Oberfläche von Säugetierzellen präsentiert werden. Die unterschiedlichen Bindungsstärken der verwendeten Env-Varianten zu einem gegebenen bNAb sollten es hierbei ermöglichen, auf Env-Varianten mit der höchsten Affinität zu selektionieren. Durch Wiederholungen des Prozesses sollten Env-Varianten mit höherer Affinität angereichert und schließlich die Variante mit höchster Affinität isoliert werden (Panning).

Es wurden verschiedene Methoden sowohl zur nativen Env-Präsentation als auch Selektion evaluiert. Hierbei wurde Env entweder direkt auf HI-Viren oder HEK293T Zellen präsentiert und mittels Mikrotiterplatten-, MACS- oder FACS-basierten Methoden selektioniert. Dies mündete in einem sogenannten „lenti-cellular display“ und FACS-basierten Panning. Um hierbei die Verknüpfung von Phäno- und Genotyp zu gewährleisten wurde ein lentiviraler Vektor genutzt, und HEK293T Zellen wurden mit einer geringen Infektionsrate (low MOI) infiziert. Dieser Vektor wurde dahingehend konstruiert, dass ein ebenfalls auf dem Vektor codiertes GFP in konstantem Verhältnis zu dem präsentierten Env exprimiert wird. Dadurch wurde es möglich, das GFP-Signal zu nutzen, um indirekt auf die Mengen des produzierten Env zu normalisieren und

spezifisch mit einem bNAb nach hoch affinen Env-Varianten mittels FACS zu selektionieren.

Der entwickelte Anreicherungsprozeß wurde mit einer Modell-Bibliothek evaluiert, die aus Env-Varianten mit bekannten Affinitäten zu bNAb 447-52D besteht. In dieser Studie konnte die Anreicherung der Env-Variante mit der höchsten Affinität zum verwendeten 447-52D Antikörper gezeigt werden (bis zu ~10-fache Anreicherung). Die entwickelte Panning-Methode eignet sich demnach zur Anreicherung und Isolierung von denjenigen Varianten einer Bibliothek von zelloberflächengebundenen Proteinen, welche die höchste Affinität zu dem eingesetzten Antikörper aufweisen.

Nach weiterer Optimierung des vorgestellten Anreicherungsprozesses sollen zukünftig Bibliotheken mit höherer Variabilität eingesetzt werden, um Env-Varianten zu selektionieren, die in präklinischen und klinischen Studien auf ihr Potential zur bNAb-Induktion untersucht werden sollen.

1. Introduction

1.1 The HIV-1 epidemic

Nearly 30 years have passed since the first reports and final identification of the human immunodeficiency virus-1 (HIV-1), as the cause for “Acquired Immune Deficiency Syndrome“ (AIDS) were published [1]. The “Joint United Nations Programme on HIV AIDS” (UNAIDS) [2] estimates that 33.3 million people were living with an HIV-1 infection at the end of 2009. That same year an estimated 2.6 million people became newly diagnosed with HIV-1 and 1.8 million AIDS-related deaths occurred. Sub-Saharan Africa continues bearing the biggest share of people living with HIV-1 infection (68% of the global total). Despite these high numbers the rate of AIDS-related deaths decreased from a peak value of 2.1 million in 2004 to 1.8 million in 2009. This decline reflects the increased availability of antiretroviral therapy (ART) [3]. Especially in Sub-Saharan Africa an estimated 20% less people died of AIDS-related causes in 2009 compared to 2004 due to a dramatically expansion of ART.

To further control and finally end the HIV pandemic three essential steps are considered; (I) accelerating the implementation of available treatment and prevention tools such as ART and prevention methods tailored to local risk factors; (II) pursuing innovative research with the goal of eradication or control of HIV-1 in infected people without the need for lifelong ART treatment; (III) development of potent prevention tools that most likely are applied in various combinations depending on the target population [4,5].

The outstanding impact of ART on the decrease of AIDS-related deaths is illustrated by the calculations provided by UNAIDS, and the estimation that an HIV-1 diagnosis with subsequent ART treatment, to date likely results in a life expectancy close to that of a healthy person [6]. Despite the advances in therapy, care and support, a lifelong treatment with daily dosing is associated with undesirable side effects, threat of chemoresistance and high economic costs, which limits part of the benefit to high-income countries. Therapy and prevention tools like ART but also condoms and progress in microbicides [7] are very important, but requires both, a professional health care system asides a high level of compliance [8].

With the exception of one case-report [9], a true cure of an HIV-1 infected person still remains elusive. Different therapeutic strategies are being developed, but remaining challenges are especially latently infected resting cells, from which a rebound of virus replication can occur [10]. Therefore, the prevention of HIV infection with the use of a

safe, efficacious vaccine affords the best long-term solution to ending the HIV-1 pandemic [11].

1.2 HIV-1

The human immunodeficiency virus 1 (HIV-1) is an enveloped retrovirus of spherical morphology and 100-120 nm in diameter. The virus is enclosed by a lipid bilayer membrane that surrounds a cone-shaped capsid (core) encasing the viral genome consisting of two identical 9.2 kb RNA (+) strands (Fig. 1.1).

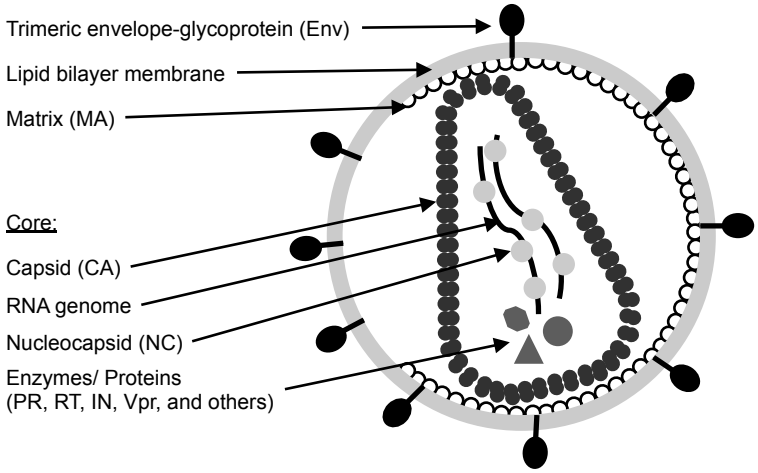

Fig. 1.1 Schematic represantation of a mature HIV-1 particle
The lipid bilayer membrane is of host origin and includes approximately 10 trimeric envelope proteins (Env) [12]. The inner layer of the membrane is lined with matrix protein (MA), illustrated with a suggested gap at the position of budding. Capsid (CA) protein forms a cone-shaped core that bears two copies of nucleocapsid (NC)-stabilized RNA genomes. The viral protease (PR), reverse transcriptase (RT), Integrase (IN) as well as Vpr and several other viral and host cell components with known or unknown functions are also located inside the virion core. Adapted from [13,14].

Immature virus particles assemble at the membrane of an infected cell and subsequently are released surrounded with the lipid bilayer membrane of the cell in a process called budding [15]. Each particle is equipped with approximately 10 trimeric envelope (Env) proteins (see 1.3) [12,16,17] together with various host membrane proteins [18]. With a scheduled cleavage at 5 distinct sites of the Gag polyprotein by the viral Protease (PR), multiple domains (MA, CA, NC, p6, SP1, SP2) are separated and a rearrangement of the viral interior is induced. The complete process is called maturation and leads to a mature, infectious virus particle [14] (Fig. 1.1).

The infection of a target cell is initiated by the attachment of the viral envelope glycoprotein (Env) to the cellular receptors CD4 and to one of the co-receptors (CCR5

or CXCR4) of T-cells and macrophages. After endocytotic uptake and fusion of the viral and endosomal membranes [19], the viral core is released into the cytoplasm of the cell. Following an uncoating of the core, the viral genomic RNA is enzymatically reverse transcribed into double-stranded DNA by the viral RT. A preintegration complex is formed, by recruiting host cell proteins to the viral DNA genome, and is shuttled into the nucleus. The infection process is finalized with the integration of viral DNA into the host genome mediated by the viral enzyme Integrase (IN). Intrinsic host cell antiviral factors, such as TRIM5α [20], APOBEC3 [21] and Tetherin [22], are bypassed by HIV-1 acquired escape mutations [23], accessory proteins Vif (viral infectivity factor) [24] and Vpu (viral protein u) [22].

The replication of integrated provirus starts with a collaborative process of cellular and viral proteins. The cellular RNA-polymerase II mediates the transcription of full-length viral pre-mRNA that is spliced into several intron-free mRNAs coding for Tat, Rev and Nef. An enhanced transcription of viral mRNA is mediated by binding of the transcription factor Tat towards the viral LTR promoter [25]. Nef is an important factor for the pathogenicity of HIV-1 and the progression to AIDS, influencing multiple host cell processes [26]. The binding of Rev towards an mRNA intron element, the so-called “Rev responsive element” (RRE), facilitates the export of singly and un-spliced mRNAs through the nuclear membrane [27] via the CRM-1 [28] export pathway. Thus, the synthesis of the structural proteins and enzymes Gag (MA-CA-SP1-NC-SP2-p6) [14], Gag-Pol (MA-CA-SP1-NC-SP2-p6*-**PR-RT-IN**) [29,30] and the envelope glycoprotein (Env) is enabled. Correspondingly, the localization of full-length viral genome RNA into the cytoplasm is ensured.

The Env proteins are synthesized in the endoplasmic reticulum (ER) and migrate via the Golgi-Complex to the cellular plasma membrane, while Gag and Gag-Pol also locate to the plasma membrane, where they induce the assembly of virus particles. The formed particles comprise the viral enzymes, full-length viral RNA genome, cellular ^{lys3}tRNA (as primer) and several cellular compounds. By budding from the cellular membrane, the virions are surrounded with the Env containing lipid bilayer of the host cell. Thus, Env is like in all retroviruses the only viral protein that is accessible at the virion surface [31].

1.3 HIV-1 envelope glycoprotein (Env)

The HIV-1 Env is translated as a precursor protein (gp160), which is heavily glycosylated in the ER and the Golgi providing a glycan-shield against neutralization [32]. Further on, it is cleaved into two subunits (gp120, gp41) by host furin proteases at the Golgi apparatus [31,33]. Trimeric complexes of non-covalently associated heterodimers consisting of a surface (gp120) and transmembrane (gp41)-subunit are incorporated into the host cell membrane. Therefore, Env is the only viral protein that is exposed on both the host cellular and viral membrane (Fig. 1.2).

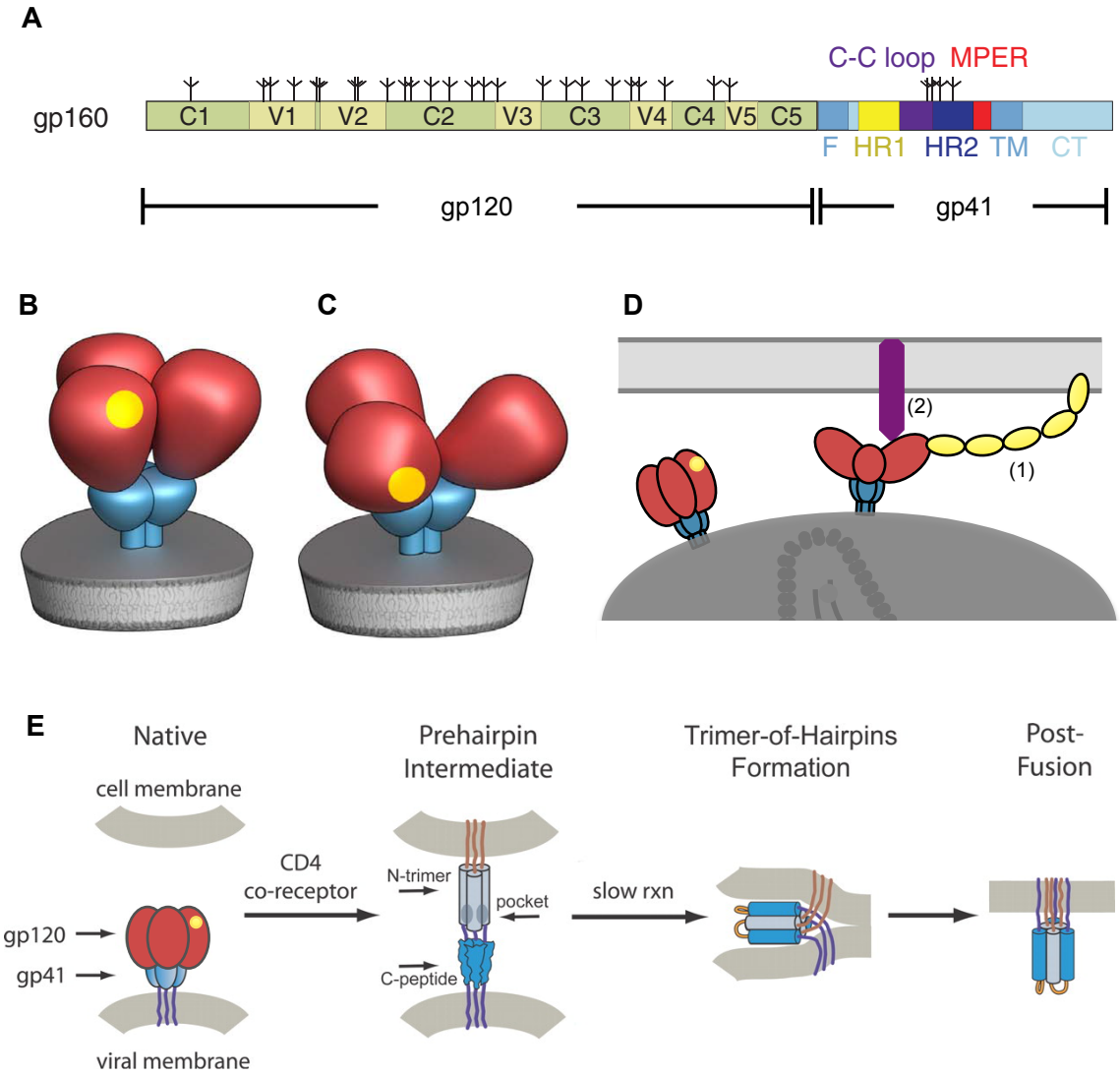

Fig. 1.2 HIV-1 envelope glycoprotein (Env)
A The full-length Env precursor gp160 is shown. Segments of gp120 and gp41 are designated as: C1–C5, conserved regions 1–5 / V1–V5, variable regions 1–5 / F, fusion peptide / HR1, heptad repeat 1 / C-C loop, the immunodominant loop with a conserved disulfide bond / HR2, heptad repeat 2 / MPER, membrane proximal external region / TM, transmembrane anchor / CT, cytoplasmic tail. Glycans are represented by tree-like symbols. Adapted from [34]. **B-D** Schematic representation of an HIV-1 Env protein incorporated into a lipid bilayer membrane, adapted from

White et al. [35]. Trimeric Env consist of the non-covalently bound subunits gp120 (red) and gp41 (blue). The position of the CD4 receptor-binding site is indicated in yellow. The induced conformational change after the binding of Env towards the CD4 receptor is proposed as a **B** "closed" and **C "**open" state. **C** The attachment process of HIV-1 to a $CD4^+$ target cell is illustrated. (1) Binding to the CD4 receptor (yellow) induces the "open state" conformation of Env and (2) enables for the subsequent binding to the co-receptor (purple) (CCR5 or CXCR4). **E** Upon cellular receptor recognition, gp120 and gp41 undergo conformational changes resulting in exposure of the N-trimer and its hydrophobic pocket in the prehairpin intermediate. Formation of the trimer-of-hairpins structure juxtaposes cellular and viral membranes and causes fusion. The gp41 fusion peptide (orange) and transmembrane domain (purple) are also shown. Note that gp120 is omitted for clarity reasons from the prehairpin intermediate. Adapted from [36]**.**

Comparison of Env gene sequences from multiple HIV-1 isolates identified a high degree of variability in the gp120 subunit, referring to as five variable domains (V1–V5) interspersed with five relatively constant domains (C1–C5) (Fig.1.2. A). Typically, gp120 comprises 18 Cysteine (Cys) residues that are covalently bound to form 9 disulfide bridges. V1 is separated from V2 by two disulfide bonds, while the two loops are contained in a larger loop by another disulfide bond. V3 and V4 loops are also delimited by a disulfide bond [33]. The V1/ V2 loop can range in length between 50 to 90 aa, while the length variation of V4 and V5 loops ranges from 19 to 44 aa and from 14 to 36 aa, respectively. The V3 loop and C2, C3, and C4 domains show relatively little length variation. Furthermore, a correlation exists between an increase in length and number of glycosylation sites in V1/V2 and disease progression, suggesting that modification of V1/ V2 length may promote escape from the host humoral immune response [37].

Approximately half of the molecular mass of gp120 is composed of N-linked glycans, [38] with a small additional contribution from O-linked sugars [39] (see Fig. 1.2 A). There are 20–35 N-linked glycosylation sites in gp120 and 3–5 N-linked glycosylation sites in gp41 that mask Env from host immune recognition [40], contribute to Env folding [41], and help virions bind to the host cell surface [42].

The target cell tropism is determined by the sequentially binding of the subunit gp120 to CD4 and a coreceptor CCR5 or CXCR4. The CD4 receptor-binding site is formed from the conserved residues in discontinuous regions that are folded into proximity in the Env tertiary structure. Particularly C1, C3, and C4, were found to be the principal Env determinants that bind CD4 [43]. Notably, it was recently shown that the contact sites of CD4 can also comprise all constant regions C1-C5, utilizing an Alanin-based library of gp120 mutants (primary isolate: JRCSF) as demonstrated by Li et al. [44].

Several studies have shown that the V3 loop is important for membrane fusion [45] and coreceptor specificity [46]. It also contains dominant epitopes recognized by neutralizing antibodies [47,48]. The switch from CCR5 to CXCR4 tropism driven by V3

mutation has been linked to an increase in the net positive charge of V3, allowing an interaction with the negatively charged surface of CXCR4 [49].

The fusion of the viral lipid envelope with the host cell membrane is mediated by the gp41 subunit, subsequently to the attachment of gp120 to the target cell receptors. Gp41 is composed of ~345 aa, organized into three major domains: an extracellular-, transmembrane- (TM), and a C-terminal (CT) -domain (Fig. 1.2 A). The extracellular-domain comprises the major fusion determinants, known as the fusion peptide (F) [50], an immunodominant C-C loop [34], two hydrophobic regions that form α-helical coiled-coil structures referred to as the heptad-repeat regions HR1 and HR2 [51], and a Trp-rich domain referred to as the membrane-proximal external region (MPER) [52]. A disulfide bridge within the hydrophilic C-C loop connects HR1 and HR2, and their interaction drives the fusion process. The fusion peptide is usually buried in the gp120/ gp41 quaternary complex.

Recently, there has been great progress in the visualization of protein assemblies combining two methods, medium-resolution cryo-electron tomography (cryo-ET; macromolecular architecture) [53] and high-resolution X-ray crystallography (molecular structure) [53,54]. Utilizing this combination of methods by fitting the available crystal structures of Env into the corresponding density maps of cryo-ET extended the knowledge about the structural organization of native, trimeric and membrane-bound Env. Comparative analyses of both CD4-dependent and -independent strains, derived from HIV-1 and SIV (Simian immunodeficiency virus) showed different ”open” or “closed” quaternary conformations [35] (Fig. 1.2 A/B). It is proposed that the CD4 dependent Env “spike-opening” process is an evolutionarily adapted mechanism to protect Env sites prone to be targeted by neutralizing antibodies, until the attachment to the target cell occurs. This model is supported by strains bearing CD4-independent Env that are more sensitive to neutralization than CD4-dependent strains. Taken together, these results are a further hint to the proposed model that the requirement of a sequentially two-step binding process to CD4 and subsequently to CCR5 or CXCR4 (Fig. 1.2 C), is an evolutionary adaptation to protect the virus from the host immune system [35,55]. Upon binding to its receptors several conformational changes are induced that trigger refolding events in gp41. (I) The prehairpin intermediate is an extended conformation of gp41 and allows inserting its N-terminal hydrophobic fusion peptide (F) into the target cell membrane, thus initiating the fusion process. (II) The Trimer-of-hairpins (six-helix bundle) conformation is reconstituted, by forming a bundle of three HR1 motifs and fold over a hydrophobic pocket antiparallel to three HR2 domains. Therefore, the fusion peptide and the transmembrane domain of gp41 are placed at the same end of the molecule. This irreversible refolding of gp41 effectively

brings the two membranes together, thus causing membrane fusion [36]. (III) The Post-fusion conformation is the most stable state and probably serves as a decoy for the host immune system, as it induces ineffective antibody responses in infected people [34] (Fig. 1.2 E) [36,56].

1.4 Vaccination

In general a vaccine mediates the protection of an organism from an infection with the respective pathogen or at least from the disease caused by the pathogen. Therefore, vaccination is mainly used as a prophylactic method establishing immunity that protects enduringly against the respective pathogen. Generally, two strategies, the *passive* and *active* immunizations, are distinguished. (I) For *passive* immunizations, immunoglobulin is administered to deactivate the pathogen before it infects the organism. Thus, it has to be administered within a certain timeframe and with an effective dosage and sometimes in combination with *active* vaccines [57]. (II) For an *active* immunization, a vaccine is administered mediating a long-lasting protection by activating the organism's immune system and leading to immunological memory.

The concepts of an innate and adaptive immune response have been reviewed extensively, though not completely explored [58-63].

Here, only the adaptive immune system with its main concepts is described to highlight how vaccination is related to protection. The T- and B-cell compartments of the immune system generally work in concert to provide such a protective immunity against pathogens.

B-cells develop from hematopoietic stem cells located in the bone marrow of adults and are genetically committed to express antibodies distinct from that of accompanying B-cells. Early in development the contact with autologous peptides lead to apoptosis, thus a self tolerance is achieved [64]. Immature B-cells characteristically display membrane-bound IgM via the B-cell-receptor (BCR) and migrate from the bone marrow. They can be divided into two subsets of cells (B1/ B2), referring to their location and mode of activation. Further development through intermediate stages results into mature naïve B-cells that express both membrane-bound IgM and IgD [65]. Besides some cells that settle at the marginal-zone of the spleen, most cells continue circulating until they encounter their cognate antigen (follicular B-cells), or undergo apoptosis. Stimulation by a related antigen induces apoptosis or activates the B-cell, depending on the development stage and if additional signals are present. Once activated, the cells display membrane-bound fragments of the antigen and enable the

binding of specific T helper cells ($CD4^+$). Upon attachment, those cells help inducing the transition of B-cells to form germinal-centers in which their antibody-genes are heavily rearranged. This includes so-called class-switch recombination and somatic hypermutations, leading to a self-antigen cleared and affinity enhanced IgG antibody secretion [58]. From this state cells can develop into: (I) long-lived memory B-cells, which have cell-surface-, not-secreting- antibody, and are quick responding to recurring antigen activation events, (II) short-lived plasma cells, which are stationary and antibody secreting. Upon a recurring activation, memory cells differentiate into rapidly dividing, migratory plasmablast (secondary immune response). These cells already secrete antibodies and are competent to form long-lived plasmacells, producing large volumes of antibodies. Notably, plasmablasts can also develop from any other type of activated B-cell, as well as class-switch and hypermutation events were reported to occur outside germinal-centers, but remained unclear in their efficacy [66]. The maintenance of serum antibody concentrations is a characteristic of the secondary immune response, due to the quick responding memory- and development of long-lived plasma-cells [59]. An immediate protection in the case of an infection is mediated by long-lived plasma cells that are present in the bone marrow and secrete antibodies in an antigen-stimulus independent fashion, thus maintaining sufficient amounts in serum and body fluids [60].

Similar functionalities apply to $CD8^+$ cytotoxic T lymphozytes (CTL). A specific T-cell receptor (TCR) mediates the contact to its cognate antigen. Infected cells display target antigens on their surface via MHC class I molecules. Upon detection by CTLs, targeted cells undergo apoptosis or get lysed. As an example, in the case of acute HIV-1 infections, though no sterile immunity is reported, a correlation between the appearance of specific CTLs and a decline of primary viremia were demonstrated [67,68].

The detailed interplay between the cellular (T-cell) and humoral (B-cell) immunity is still not entirely understood. Yet, basically CTLs ($CD8^+$) are considered necessary to control viral replication. Whereas T-helper-cells ($CD4^+$) “help” stimulating B-cells, thus inducing antibody secretion that can prevent viral infections of host cells.

To date, almost all licensed vaccines against viral pathogens, protect due to the induction of pathogen specific antibodies by B-cells. Whereas T-cells, besides their help to B-cells, are more important in the control of an established infection. This paradigm is not strict, as demonstrated for the *varicella-zoster* virus [69,70], but rather a relative and statistical truth and subject to variation from one infection to another. Shortly, the importance of either B-cell or T-cell immunity is still subject of considerable research and debate [62,63]. Despite the widespread practice of determining antibody

titers to predict the efficacy of vaccines, exploration of the immunological mechanisms of vaccinations, defining correlates of protective immunity and their efficacy are still ongoing, as reviewed in Pulendran et al. [61,71].

To induce neutralizing antibodies (humoral immunity), several strategies in the generation of vaccines were developed (Fig. 1.3), ideally together with T-cell (cellular immunity) responses [72].

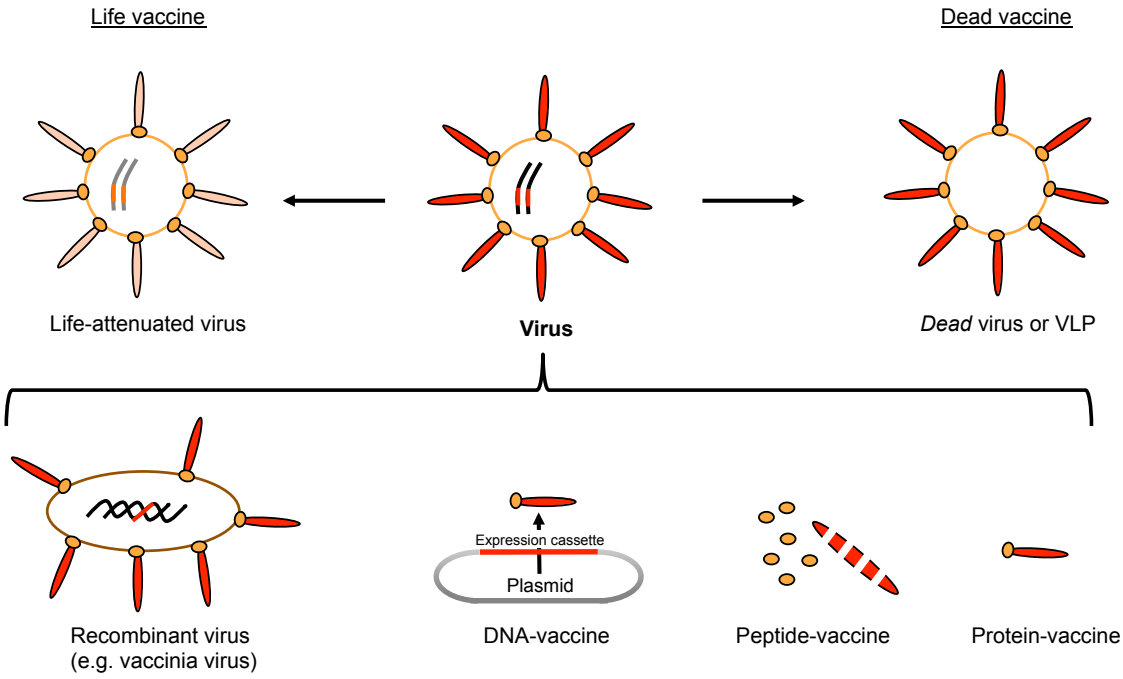

Fig. 1.3 Immunization strategies
Schematic overview of the basic strategies for immunization against a viral pathogen (adapted from [72]). A non-pathogenic but replication-competent virus is generated e.g. by mutation (top-left). Subunit vaccines: Antigens of the respective pathogen are transferred to another non-pathogenic viral background MVA (Modified Vaccinia Ankara virus) (bottom-left). A dead vaccine in its simplest definition is a non-replicating virus or virus-like particle (VLP) without genome (top-right). Recent attempts utilize combinations of antigens as part of a recombinant virus, expression plasmids, peptides or proteins (bottom).

Neutralizing antibodies are targeted towards virus envelope structures, and therefore inhibit the virus from infecting its target cells. Generally, pathogen-antibody complexes can (I) activate the complement system (CDC; complement-dependent cytotoxicity), (II) get lysed by natural killer cells (NK-cells) (ADCC; antibody dependent cellular cytotoxicity), (III) or get phagocytized or lysed by phagocytes as well as granulocytes [73]. In contrast, infected cells display foreign viral peptides in complex with MHC class-I molecules and therefore can be targeted by CTL responses. Vaccines based on replication competent viruses (*Life* vaccine) have the advantage to mostly induce both humoral and CTL responses [74,75]. To encounter a possible recombination to

an again virulent virus, modified (attenuated) recombinant viruses were developed. Therefore non-pathogen viral vectors (e.g. MVA [76]) were combined with antigens of the respective pathogen (subunit vaccine). *Dead* vaccines, comprising all variants of a non-replication competent attempt, makes use of different subunits of a virus and is applied as VLP [77], plasmid, peptides or proteins.

It was demonstrated that plasmid DNA based vaccines elicit low-level, but protective immunity against the influenza virus [78,79], a combination with other vectors was suggested [80]. Therefore, a consecutive vaccination strategy was developed comprising a DNA vaccination that may prime for enhanced responsiveness of a following boost using a viral vector. Several combinations consisting of so-called prime/ boost regimens are under development and adapted specifically to each pathogen [81,82].

1.5 Seeking for HIV-1 vaccines and broadly neutralizing antibodies

Developing a vaccine that is capable of mediating protection against the HI-virus has failed until now. Fundamental barriers that have precluded the development of a potent vaccine so far, are the exceptional properties of HIV-1 featuring its preferred entry in human $CD4^+$ T-cells, building rapidly a persistent reservoir of latently infected cells, masking of functional envelope trimers to evade humoral immune responses [40] (see 1.3) and its rapid mutation rate. The latter resulted in genetic sequence variability that is globally classified in different subtypes or clades. In addition to the global evolution of HIV-1 that lead to multiple subtypes, the transmitted (founder) virus undergoes rapid mutations resulting in multiple closely related genetic variants (quasispecies) within each infected individual [83-86]. Since the development of nonhuman primate models [87] to examine the effects of vaccine candidates, more than 30 have also been tested in human clinical trials [88,89]. These studies included both, replication-competent or incompetent viral vaccines containing HIV-1 gene inserts, HIV-1 VLPs, HIV-1 DNA-vaccines, and soluble HIV-1 proteins and peptides (as described in 1.2), with or without adjuvant formulation and with diverse combinations in Prime/Boost regimens [8,11,89,90]. The only trial with a positive outcome in reduction of infection rates (31%), was the RV144 trial in Thailand [91], using recombinant canarypox-HIV virus prime and gp120 envelope protein boost (adjuvant: alum [92,93]). Taken together, strategies that have successfully worked for other pathogens have failed to elicit similar immunity to HIV-1 infection, so far. Although the exact type needed for an

immune response is still not known, it is a wide consensus that an effective vaccine will need to induce both, B-cell and T-cell ($CD4^+$ and $CD8^+$) responses [11]. Further evidence for the need of a balanced cellular and humoral immune response was recently shown by vaccination experiments in rhesus macaques, where one third of the vaccinated animals remained virus-free during a repeated low-dose challenge. Furthermore, both cellular and humoral immunity has been inversely correlated to the degree of protection [94].

However, especially an early neutralization of HIV-1, before the infection of target cells occurs, seems highly attractive, considering the fact that HIV-1 integrates genetically into cells and forms latently infected reservoirs [95-97]. Thus, it is likely that a vaccine that induces broadly neutralizing antibodies (bNAbs) in concentrations that effectively neutralize HIV-1 of a broad spectrum of clades, can protect from infection as seen in nonhuman primate studies [98,99]. Therefore, eliciting bNAbs turns out to be a critical and obtainable component for immunization efforts [88]. Recently, multiple screening studies revealed several new bNAbs (VRC01 [44,100], PG9 / PG16 [101]) with exceptional breadth and potency (i.e. low inhibitory concentration (IC) values) in neutralizing HIV (Table 1.1).

Table 1.1 Characteristics of representative types of human bNAbs [11,98]

Antibody	Specificity	Median IC_{50} * (µg/mL)
PGT128	Env glycans associated**	0.02
2G12	Env glycans	2.38
PGV04	CD4 binding site	0.20
VRC01	CD4 binding site	0.32
b12	CD4 binding site	2.82
HJ16	CD4 binding site/ DMR***	#
PG9	Quaternary epitope gp120	0.23
PG16	Quaternary epitope gp120	#
2F5	gp41 MPER	#
4E10	gp41 MPER	3.41

* Mean of IC_{50} values obtained, using a panel of 162-pseudoviruses representing all major HIV-1 subtypes [98]
** Exact epitope uncertain [98]
*** Aa D474, M475, R476 of gp120; frequently targeted epitope of neutralizing antibodies [102]
\# Not determined in that study.
Highlighted rows separate groups of similar specificities.
BNAb references are to be withdrawn from text.

Further findings about novel antibodies (PGT128 [98]) with even higher (up to 10 fold) potency than found before, indicate the enormous progress that is made in this discipline. Previously to the recent discoveries of quaternary-epitope-specific antibodies, there were three distinct structural regions known to be targeted by the

widely known bNAbs [11,103]: (I) b12 [104] targeting the CD4 binding site, (II) 2F5 [105] and 4E10 [106] targeting separate epitopes within the membrane proximal external region (MPER) of gp41 and (III) 2G12 [107] targeting a cluster of glycans on the gp120 outer domain. Another distinct region of known high immunogenicity is the variable loop V3 [108]. Thus antibodies that are directed to epitopes of the V3 region of Env (see 1.3) are commonly among the earliest antibody-responses against HIV-1 infection [109]. Despite high titers of antibodies, which are elicited from the V3 region, only few antibodies were found to be of broad reactivity. Interestingly, such antibodies are generally poor effectors of neutralization of primary viruses, due to the masking [110-112] of V3 epitopes by V1/V2 domains [111] on the native Env trimer, as demonstrated by Davis et al. [110]. One among the best characterized antibodies directed against a conformation-sensitive epitope [113-115] (core epitope: GPGR) at the crown [47] of V3 is the bNAb 447-52D [116-118]. Particularly, the 447-52D antibody features cross clade neutralization capacities, even against primary isolates [113,119] and is used as part of a prototypical panning procedure during the course of this thesis (see 3.3).

However, one of the main barriers in eliciting adequate antibodies is represented by the fact that the structure of an envelope, which is capable of inducing bNAbs, remains unknown. All immunization-effort-derived envelope proteins resulted in antibody responses towards immunogenic parts of the applied envelope, but with non- or only vaccine-specific neutralizing capacities [120], so far. In order to avoid these problems and to shift the immune response [108] to an epitope of interest, several approaches [121] recently led to promising results. These “reverse vaccinology” [122] -based approaches utilized libraries of chimeric envelope sequences [123] or redirected the immune response to more efficacious neutralizing regions on the envelope [124,125]. In summary, a chimeric gp120 Env construct (ST-008) with improved neutralizing antibody responses was identified using rabbits, as demonstrated by Du et al. [123]; Multiple heterologous or the complete deletion of the V1 loop dampened the immunogenicity of V3 and differentially altered the immunogenicities of several other potential epitopes, as shown by Ching et al. [124]; hyperglycosylation of the variable loops showed dampening of their immunogenicity in the context of trimeric Env, but not to the cost of target epitopes at the CD4 binding site, demonstrated by Selvarajah et al. [125].

Nevertheless, the proof-of-concept for a vaccine that can elicit antibodies with sufficient breadth and potency to protect from infection with heterologous clades remains out of reach [121]. On the other hand, there are strong hints that mimicking the native, viral, membrane-bound, trimeric envelope complex could elicit antibodies

against conserved quaternary structures, facilitating an effective neutralization of the virus [123,126]. Thus, getting access to an Env-structure reflecting the antibody-neutralized state in a physiologically relevant context is likely to be required for successful vaccine design [35,127]. A technique to identify those membrane-bound envelope trimers with enhanced properties for the binding to bNAbs may therefore lead to the identification of envelope structures capable of inducing antibodies with similar properties [98,101,121,128,129].

1.6 Display technologies

Available display systems allow the selection of proteins or peptides out of millions of candidates and are the methods of choice to identify optimally binding antigen-antibody complexes. The variety of display techniques reflects the broad benefit and potency of display-based screening methods throughout the various fields of application. Each attempt of screening has to match its own unique specifications, thus comprising multiple strategies of display systems. The most popular technologies are phage [130-134] and yeast [135,136] display, but also bacterial [137], mammalian cell [138], eukaryotic virus [139-141], ribosome [142,143], mRNA [144-146] and covalent DNA [144,147] -display systems have been developed (Table 1.2).

Table 1.2 Characteristics of representative types of display systems

Display technique	Type of phenotype and genotype linkage	Library specificities	Expression
 **Phage display**	Expression as a fusionprotein with a coat protein of the phage. The gene is coded on a phagemid packaged in the same particle.	Any protein secretable to the periplasmic space of *E.coli*. Potential size: ~10^{11} [148]	Prokaryotic
 **Retroviral display**	Expression in fusion with a cell surface molecule encoded on a viral genome. The host membrane surrounds arising viruses. Particles comprise the surface protein and the gene encoded on the viral genome.	Various sizes of proteins, fully functional, incl. folding and modifications in the ER. Mammalian cell membrane is present. Potential size: ~10^{8} [149]	Mammalian
 **Bacterial display**	Transfection of bacteria with library plasmids and expression of library proteins in fusion with a cell membrane protein.[150]	Any protein secretable to the periplasmic space of *E.coli*. Potential size: ~10^{11}	Prokaryotic
 **Cell display**	Expression in fusion with a cell surface molecule encoded on DNA, which the cell receives in order to be transformed.	Various sizes of proteins, fully functional, incl. folding and modifications in the ER. Surface: Mammalian, cell membrane/ Yeast, cell wall. Potential sizes: ~10^{10} (Yeast) [135,151,152] ~10^{7} (HEK293T) [138]	Eukaryotic: Yeast / Mammalian (HEK293T)
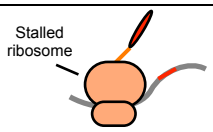 **Ribosomal display**	Stabilization of complexes comprising ribosome, mRNA and the nascent peptide upon termination of elongation using Mg^{2+} concentrations and low temperature.[153]	Methods applied to the range from short polypeptides up to antibody mimicing proteins. Potential size: >10^{13} [153]	Cell-free *In vitro*
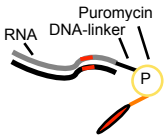 **mRNA display**	A puromycin (P) molecule is covalently bound to the 3' end of mRNA via a single stranded DNA linker. At the end of the peptidyl transferase reaction, P is bound to the nascent peptide as if it were a tRNA.		Cell-free *In vitro*
 **DNA display**	Expression as a fusionprotein with the DNA-binding protein P2A (phage P2 derived). P2A catalyzes a single strand nick and covalently binds to the 5' end of the coding DNA strand.[147]	Applied for antibody fragments (scFv). Potential size: >10^{13} [147]	Cell-free *In vitro*

library gene (red) encoded on DNA (black)
library gene (red) encoded on RNA (grey)
membrane protein/ peptide linker
library peptide/ protein

Figures are not depicted in scale

In viral display systems, the most widespread technique is M13-derived phage display. Though restricted to the expression capacities of *E.coli,* screenings can be done *in vitro* bearing the advantage to possibly select against toxoid agents like tetanus toxoid [154]. Various therapeutic antibodies against a variety of diseases, as well as the

bNAb b12 (see 1.5), were discovered using this technology [155]. For a bacterial display, proof-of-principle experiments comprising functional enzymes, vaccine antigens and polypeptide libraries [156] were successfully realized. However, in comparison to the phage-based platform it turns out that phage may be advantageous in its performance [157].

If eukaryotic properties, such as folding and posttranslational modifications are desired, yeast cell-wall surface display can be utilized [152]. Furthermore, several mammalian cell-surface display systems, which enable for a membrane-association, were developed for various types of cells, like HEK293T [138,139], BHK [158], HeLa [159], Jurkat-e [160] or DT-40 (chicken B-cell line) [161]. Retroviruses are among the most efficient mammalian viral vectors and are widely used to stably integrate genetic information into the genome of mammalian cells [162]. The potential as a vehicle for the display of various peptides as well as antibody-fragments and their selection against different target molecules has been demonstrated using murine leukemia virus (MLV) [163], avian leucosis virus (ALV) [149] and human immunodeficiency virus (HIV-1) [139].

Cell-free *in vitro* display systems (ribosomal-, m-RNA- and DNA-based, see Table 1.2) comprise the potential advantage of bearing no limitations in library diversity [153]. Additionally, the lack of transfection or infection steps should make these methods more amenable for automation processes. The non-dependence on *in vivo* expression also gives rise to screen both with or against toxoid agents, such as antibiotics or tetanus toxoid [145,147]. An overriding principle between the different display techniques is the linkage of the phenotype and genotype of the individual elements within a library of broad diversity (Fig. 1.4).

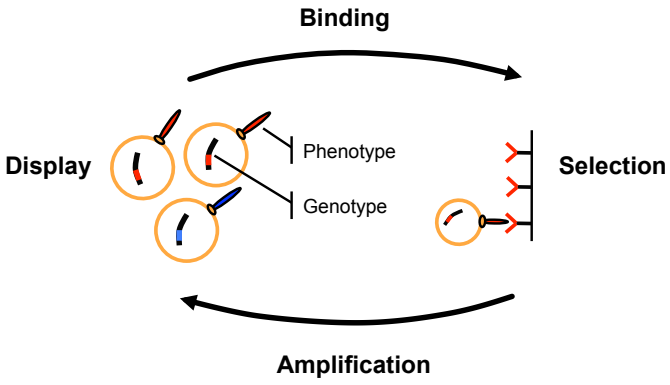

Fig. 1.4
Display and screening
Schematic overview of the common principle of display and selection procedures. A protein or peptide (phenotype) is expressed and spatially linked with its genotype (Display). After a binding step to a molecule of interest, followed by an appropriate screening procedure, interacting partners are enriched. Since the phenotype is linked to the genotype, genes of selected proteins are amplified and analyzed or utilized for another selection round.

One of the most utilized examples is given by recombinant antibody libraries that are displayed on *E.coli* bacteriophages and screened towards target antigen binding of

interest by iterative selection rounds (panning-procedure) [134,144,164,165]. Briefly, antibody fragments are cloned and expressed in fusion with the coat protein pIII of the M13 derived filamentous bacteriophage (phage). During the phage assembly process assisted by a helperphage, the fusion proteins as well as single stranded DNA encoding for the fusion protein are incorporated into the phage particle. Thus, phage produced by *E.coli* display an antibody-fragment (phenotype) linked to its DNA-sequence (genotype) [130]. A screening (panning) is applied by an iterative series of a phage selection procedure towards a target of interest and the subsequent de-novo production of selected phage after the infection of *E.coli*. Since phage-display is working superior for the screening of antibody fragments such as scFv (single chain variable fragment), other mammalian proteins, which can not be expressed in *E.coli* or which have to be displayed with native properties in structural, post-translational modification, membrane association or folding, demands for a display-system based on mammalian cells or viruses [139,140] (see Section 3.1/ 2).

1.7 Objective

Broadly neutralizing antibodies (bNAbs) like those recently discovered by extensive screenings [98,100], and the search for a safe, practical and effective vaccine able to re-elicit those bNAbs, are among the main HIV-1 vaccine research aims [11,118]. It has been suggested that a stable Env variant with a conformational state that allows optimal binding of existing bNAbs may be able to elicit complementary antibodies [127,166].

The objective of this study was to develop a lentiviral vector system and suitable mammalian display technique that enables screening of trimeric membrane-bound envelopes. This necessitated designing and generating a model Env library in order to adjust the panning parameters. Furthermore, the developed system should be evaluated by bNAb-mediated enrichment of the highest affinity Env variant from the model library applied.

2. Material and Methods

2.1 Molecular Biology

Unless otherwise specified, processing of all tasks was done using common protocols of molecular biology or of the respective manufacturers. All DNA constructs and oligonucleotides are listed in appendix 5.2. Inserts were generated by PCR, fusion PCR or restriction of plasmids. PCR for preparative purposes was performed using Finnzymes **Phusion** polymerase. PCR for analytic purposes was performed with Promega **GoTaq** Green Master Mix. For the restriction of DNA either NEB (New England Biolabs) or Fermentas endonucleases were used. Depending on the experiment, amplified DNA was purified with **purification** columns, or by separation on a 0.75 - 1 % agarose gel and subsequent gel extraction (**Qiaquick**). Ligations were processed using a three fold molar excess of the insert related to the target vector according to the standard protocol of the used **QuickLigation** Kit from NEB. Transformation of chemical- or electro-competent bacteria **DH10B** or **DB3.1** was carried out as described in 2.1.5. Plasmids were isolated after growth of bacterial cultures in **TB medium** containing the appropriate antibiotic by alkaline lysis or by using Qiagen **Plasmid Kits**. The purity and concentration of DNA was measured using a **NanoDrop** Instrument. DNA correctness was verified by obtaining restriction patterns or by **sequencing**.

Phusion® High-Fidelity DNA Polymerase	Finnzymes, F-530
GoTaq® Green Master Mix	Promega, M7112
QIAquick Gel Extraction Kit	Qiagen, 28706
QIAquick PCR Purification Kit	Qiagen, 28106
QIAGEN Plasmid Midi/Maxi Kit	Qiagen, 12145/12165
QIAamp DNA Blood Mini Kit	Qiagen, 51104
QuickLigation Kit	New England Biolabs, M2200
E.coli DH10B	Invitrogen, 18297-010
E.coli DB3.1	Invitrogen, 11782-018
TB medium	Terrific Broth medium (12 g Bacto tryptone, 24 g Bacto yeast extract, 4 ml Glycerol, 100 ml 0.17 M KH2PO4 and 0.72 M K2HPO4, adjust to 1L)
NanoDrop 1000	Thermo Fisher scientific
Sequencing Service	Geneart

2.1.1 Nested PCR

To amplify small amounts of DNA two PCR reactions were combined. A portion of 5 µL of the first reaction serves as template for the second reaction. The second PCR amplifies a region within the amplification area of the first PCR. The reactions protocol and amounts are given in Table 2.1.

Table 2.1 Nested PCR

PCR 1	
Volume (μL)	Material
36-X	Sterile water
10	HF Buffer
1	dNTPs 10mM each
1.5	DMSO
0.5	Primer 8H1
0.5	Primer 8H2
X	Genomic DNA
0.5	Phusion polymerase
50	Total amount

PCR 2	
Volume (μL)	Material
30	Sterile water
10	HF Buffer
1	dNTPs 10mM each
1.5	DMSO
1	Primer 5I3
1	Primer 5I4
5	PCR 1
0.5	Phusion polymerase
50	Total amount

Cycler schedule PCR1		
98°C	10 min	
98°C	10 sec.	|
53°C	30 sec	25x
72°C	100 sec	|
72°C	5 min	
4°C	∞	

Cycler schedule PCR2		
98°C	10 min	
98°C	10 sec.	|
		40x
72°C	75 sec	|
72°C	5 min	
4°C	∞	

The PCR2 reactions were loaded on a 0,75 % agarose gel, optically analyzed by **UV** light and gel slices containing fluorescent DNA with the length of envelope genes (2.2 kb) were excised and purified according to manufactures instructions. Elution of DNA was limited to 12 μL **Tris buffer** to enhance the concentration. The primers used in PCR2 contain overhanging sequences recognized by Esp3I followed by NheI (5I3) or XhoI (5I4) sites (5.2.1). Inserts equipped with these recognition sites can directly be introduced to QL (Quick Ligation) CcdB cloning (2.1.4).

UV source	310 nm
Tris buffer	10 mM Tris HCl, pH 8,5
PCR reagents	Finnzymes, F-530
dNTPs	NEB N0447
Primer concentrations	10 μM each in Tris buffer

2.1.2 Realtime PCR (RT-PCR)

To determine the efficiency of a specific PCR reaction a Realtime PCR standard curve analysis using a **StepOnePlus** device with a 5 fold dilution series of genomic or plasmid sample DNA was performed according to the manufacture's **manuals** (Applied Biosystems, Finnzymes). To determine the amount of different envelope coding genes in a mixture of DNA, a Realtime PCR reaction containing one specific Primer (5.2.1) for each gene to be analyzed was designed. The probe and forward primer was designed to bind to all different envelope variants. One reverse primer was designed to also match all envelope genes and therefore was used as reference. The

amount of the sample DNA varies according to the experimental setting. For both SYBR® Green chemistry or probe-based chemistry the manufacture's reaction protocols were used (**DyNAmo** Kits, Finnzymes).

DyNAmo™ Flash SYBR® Green qPCR Kit	Finnzymes, F-415
DyNAmo™ Flash Probe qPCR Kit	Finnzymes, F-455
StepOnePlus™ Real-Time PCR System	Applied Biosystems

2.1.3 Reverse transcription (RT)

To assess the genetic information of transcribed genes a reverse transcription assay was used. First, total RNA of transfected or infected cells was extracted using the **RNeasy** Plus Kit (Qiagen) according to the manufacture's protocol. Subsequently a reverse transcription of envelope specific RNA into cDNA was done using the **QuantiTect** Kit (Qiagen) modified from the standard protocol (Table 2.2).

Table 2.2 Reverse transcription (RT) in two reactions

Reaction 1 (Elimination of gDNA)	
Volume (µL)	Material
15-x	RNAse free water
2.5	gWipeout Buffer
x	500 ng total RNA
15	Total Volume

Reaction 2 (RT)	
Volume (µL)	Material
4	RT Buffer (5x)
1	RT
0.5	Primer 5G5
14.5	From reaction mix 1

Cycler schedule	
42°C	10 min
4°C	10 min

Cycler schedule	
50°C	30 min
95°C	3 min
4°C	∞

To amplify the generated cDNA, portions of the reaction 2 as well as 0.5 µL of the reaction 1 as a negative control were applied to a PCR reaction (Table 2.3).

Table 2.3 cDNA PCR reaction

cDNA PCR mixture	
Volume (µL)	Material
14,3-x	Sterile water
5	HF Buffer
0,5	10 mM dNTPs
0,5	Primer 5F3
0,5	Primer 5G5
0,2	Phusion
x	Reaction mix 1 or 2

cDNA PCR Cycler schedule		
98°C	30 sec.	
98°C	10 sec.	30x
65°C	30 sec.	
72°C	45 sec.	
72°C	10 min	
4°C	∞	

RNeasy Plus Mini Kit	Qiagen, 74136
QuantiTect Rev. Transcription Kit	Qiagen, 205311

2.1.4 Quick Ligation (QL) and CcdB cloning

For cloning of DNA into plasmids containing the QL extension (see 3.5.1) a combined restriction and ligation process was used [167]. The reaction is divided into two steps. At first a restriction mixture containing the QL plasmid (containing CcdB marker [168]) and the DNA fragment to be inserted (Insert) was incubated in a PCR cycler for 45 min at 37°C. Meanwhile a second reaction for the ligation was prepared and subsequently mixed with the first reaction mixture. The combined reactions were incubated as given in Table 2.4. The final incubation step at 65°C inactivates the enzymes in the reaction mixture.

Table 2.4 QL reaction mixture and incubation schedule

Reaction 1: Restriction mixture	
Volume (μL)	Material
14-x	Sterile water
2	10 x Tango Buffer
2	10 mM DTT
1	100 ng/μL Target QL Vector
X	100 ng Insert DNA
1	Esp3I restriction enzyme

Reaction 2: Ligation mixture	
Volume (μL)	Material
4	Sterile water
3	10 mM ATP
1	10 x Tango Buffer
1	10 mM DTT
1	T4 Ligase

QL reaction schedule	
45 min	37°C
Adding reaction 2	
45 min	25°C
45 min	37°C
45 min	25°C
10 min	65°C

2.1.5 Transformation of bacteria

DNA plasmids were introduced into bacteria by transformation of either chemical- [169] or electro-competent *E.coli* cells. A complete ligation mixture or pure plasmid DNA was applied if chemical competent cells were used. Prior to transformation, electro-competent cells were prepared and divided into 50 μL aliquots and frozen at -80°C according to the given protocol (Table 2.5). The cells were slowly thawed on ice, 1-3 μL of QL reaction mixture were applied and mixed cautiously only by stirring with the pipette tip. The mixture of cells and QL reaction was incubated for 1 min on ice, subsequently transferred into a precooled cuvette, pulsed with 1.6 kV, 25 µF, 200 Ω (GenePulser, BioRad) and immediately transferred into 500 μL 37°C pre-warmed TB medium by flushing the medium into the cuvette and pipetting up and down once. The bacteria were incubated at 37°C, 600 rpm for 30 min and subsequently plated on a LB

Agar plate containing a corresponding antibiotic for the selection of transformed bacterial clones.

Table 2.5 Preparation of electro-competent bacteria

Protocol for the preparation of electro-competent bacteria	
1	Starter culture: 5 mL LB medium was inoculated and incubated over night at 37°C, 220 rpm with bacteria (of a glycerin stock).
	All materials were precooled at 4°C
2	200 mL LB medium without antibiotics was inoculated with the starter culture to a OD(600) = 0.1
3	The bacterial culture was incubated at 37°C, 220 rpm until OD(600) reached 0.5
4	The bacteria were centrifuged at 4°C, 3220xg for 10 min
5	The supernatant was discarded and the pellet resuspended in 10 mL sterile 7% DMSO
6	The suspension was centrifuged at 4°C, 2000xg for 5 min
7	The supernatant was discarded and the pellet resuspended in 5 mL sterile 7% DMSO
8	Repeat step 6 and 7
9	The suspension was centrifuged at 4°C, 2000xg for 5 min
10	The supernatant was discarded and the pellet resuspended in 0.5 mL sterile 7% DMSO
11	The suspension was frozen in liquid nitrogen in portions of 50 µL

2.1.6 Preparation of DNA using Microtiter plates (MTP)

For the preparation of 94 separate bacterial clones, an **MTP** was filled with 190 µL of **TB medium** including **ampicillin** per well. Bacterial clones were transferred by picking with a sterile pipette tip and short stirring in the target well to be inoculated. Once the complete MTP was inoculated, it was transferred onto a **Microplate shaker**, sealed with a "**breathable seal**" and incubated over night at 37°C at 800 rpm. The next day the supernatant was discarded after 30 min of centrifugation at 4°C and 3000 x g. The pellets were resuspended in 30 µL **P1** by shaking the MTP at RT for 5 min at 1000 rpm. After complete resuspension, 30 µL of **P2** was added to each well and mixed shortly by shaking at RT, 1000 rpm for 5 sec. and incubated for 3 min at RT. Subsequently 30 µL of ice cooled **P3** was added to neutralize the lysis and mixed shortly by shaking at RT, 1000 rpm for 5 sec. and incubated for 15 min at 4°C. After 30 min of centrifugation at 4°C, 3000 x g up to 90 µL of supernatant was transferred into a fresh MTP by pipetting carefully without disturbing the pellet. 0,7 x volume of isopropanol was added and mixed by shaking shortly at 800 rpm. After 30 min of centrifugation at 4°C, 3000 x g the supernatant was discarded carefully by overturning the plate in one swinging move. The remaining pellet was washed by addition of 100 µL ethanol (70 %) to each well and shaking shortly at 800 rpm. After 30 min of centrifugation at 4°C, 3000 x g the supernatant was discarded carefully by overturning the plate in one swinging move and immediately placing the plate onto a tissue without

turning the plate in the meanwhile. After 5 min of incubation the dried DNA pellets were resuspended by adding 50 μL **Tris-Buffer**. Concentration of DNA was calculated as the mean concentration of three randomly measured wells.

Ampicillin concentration	100 μg/mL
E.coli DH10B	Invitrogen, 18297-010
Microplate shaker	IKA, MTS 2/4
Breathable seal	GBO, 676050
MTP, U-form untreated	GBO, 650201
TB medium	Terrific Broth medium (12 g Bacto tryptone, 24 g Bacto yeast extract, 4 ml Glycerol, 100 ml 0.17 M KH2PO4 and 0.72 M K2HPO4, adjust to 1L)
P1, P2, P3	Qiagen, 19051, 19052, 19053
Tris buffer	10 mM Tris HCl, pH 8,5

2.2 Protein biochemistry

2.2.1 p24-ELISA

The amount of p24 capsid peptide in a cell culture supernatant of HIV-1 infected HEK293T cells, was determined by a p24-ELISA. Since p24 is part of the capsid of HIV-1, its amount directly correlates to the amount of virus in the solution.

After 10 min of centrifugation at RT and 500 x g, the supernatant was inactivated by adding 0.1 x volume 5 % (v/v) Triton-X-100 in PBS and incubation at RT for 1 h. The solution was directly used or stored at -20°C until usage in the ELISA. Since the concentration of the solution was unknown, dilutions of 1:10, 1:100, and 1:1000 were used. Standard **p24** peptide control dilutions were prepared by pipetting eight 1:2 serial dilutions, starting with 5 ng/μL, that were treated like normal samples in the experiment. The ELISA was processed as given in Table 2.6.

Table 2.6 p24 ELISA

Protocol	
1	Coating: 100 μL of capture antibody solution was added to each well. Incubation over night at 4°C
2	Washing: ELISA-washer, program p24_3x_A
3	Capture: 100 μL of sample solution was added to each well. Incubation for 1 h at 37°C
4	Washing: ELISA-washer, program p24_6x_A
5	Detection: 100 μL of secondary antibody solution was added to each well. Incubation for 1 h at RT
6	Washing: ELISA-washer, program p24_10x_A
7	Detection: 100 μL of Streptavidin-HRP solution was added to each well. Incubation for 30 min at RT
8	Washing: ELISA-washer, program p24_10x_A
9	Signal processing: 100 μL of TMB solution was added to each well. Incubation for 5 min at RT
10	Reaction stop: 50μL of H_2SO_4 solution was added to each well.
11	Measuring: The signals were detected as the absorption at 450 nm

The p24 concentrations for the samples were calculated in relationship to the values from the standard curve (standard curve: absorption/concentration, fitted curve in linear range, correlation coefficient: $R^2 > 0,99$).

Coating buffer	100 mM $NaHCO_3$, pH 9.5
p24	Stock solution: 50 ng/μL
Capture solution	M01- antibody,1:1000 in coating buffer, Polymun AB006
PBS	137 mM NaCl, 2.7 mM KCl, 10 mM Na_2HPO_4, 1.47 mM KH_2PO_4, pH 7.4
BSA	AppliChem, A1391
Blocking buffer	PBS, 1 % (w/v) BSA
Secondary antibody	37G12 antibody biotinylated, 1:5000 in blocking buffer, Polymun AB005
Streptavidin-HRP solution	Streptavidin-HRP 1:10000 in blocking buffer, Roche 11089153001

HEK293T	Ad5-transformed embryonic kidney fibroblast cell line (ATCC CRL-11268)
FCS	GIBCO, 10270-106
Pen/Strep	10000 U/ml Penicillin, 10 mg/ml Streptomycin, PAN Biotech P06-07100
DMEM medium	DMEM (Invitrogen 41966) + 50 ml FCS, 5 ml Pen/Strep
ELISA plate	Maxisorp, Nunc 442404
ELISA washer	Hydroflex, Tecan Wash buffer (WB): PBS 0.05 % (v/v) Tween-20 Programs: - Aspiration - Dispensing: 300 µl WB each Well, 300 µl/s - Continuous washing with (400 µl/s): 1 ml WB program p24_3x_A 2 ml WB program p24_6x_A 3 ml WB program p24_10x_A 2x 3 ml WB program p24_20x_A - final aspiration
TMB solution	20 x volume A + 1 x volume B mixed before use: A: 30 mM Kalium-Citrat, pH 4.2 B: 10 mM 3,3',5,5' - tetramethylbenzidine, 10 % (v/v) Acetone, 90 % (v/v) Ethanol, 80 mM H_2O_2

2.2.2 Virus binding assay

To capture viruses with high affinity to specific antibodies immobilized on **MTP**s, a virus binding assay comparable to ELISA was established.

Table 2.7 Virus binding assay

Protocol	
1	Coating: 100 µL of capture antibody solution was added to each well. Incubation over night at 4°C
2	Washing: ELISA-washer, program p24_3x_A
3	Blocking: The wells were completely filled with DMEM for 2 h at RT
4	Washing: ELISA-washer, program p24_3x_A
5	Capture: 100 µL of virus sample solution was added to each well. Incubation for 2 h at RT.
6	Washing: ELISA-washer, program p24_3x_A using PBS
7	Lysis: 100 µL of lysis solution was added to each well. Incubation for 1 h at RT
8	The lysed mixture was treated as a sample in a p24-ELISA as described in 2.2.1.

Coating buffer	100 mM $NaHCO_3$, pH 9.5
Capture antibody solution	10 µg/mL in coating buffer, broad neutralizing antibody depending on the experiment
Blocking buffer	DMEM, 10% FCS
MTP	Maxisorp, Nunc 442404
ELISA washer	Hydroflex, Tecan Wash buffer (WB): PBS, 0.05 % (v/v) Tween-20 Program: Aspiration Dispensing: 300 µl buffer each Well, 300 µl/s Continues washing with (400 µl/s): 1 ml buffer program p24_3x_A final aspiration

2.3 Cell biology

2.3.1 Cultivation of cell lines

Eukaryotic cells were cultivated at 37°C and 5 % CO_2 according to common protocols. Adherent **HEK293T** cells were split in a ratio of 1:10 at day 2-3 of cultivation by washing once with **PBS**, detaching with **Trypsin-EDTA** solution and subsequent resuspension of 1/10 of the cells with **DMEM** to avoid complete confluence.

HEK293T	Ad5-transformed embryonic kidney fibroblast cell line (ATCC CRL-11268)
PBS	137 mM NaCl, 2.7 mM KCl, 10 mM Na_2HPO_4, 1.47 mM KH_2PO_4, pH 7.4
FCS	GIBCO, 10270-106
Pen/Strep	10000 U/ml Penicillin, 10 mg/ml Streptomycin, PAN Biotech P06-07100
DMEM medium	DMEM (Invitrogen 41966) + 50 ml FCS, 5 ml Pen/Strep
Trypsin-EDTA	Pan Biotech, P10-023500

2.3.2 Transfection

DNA was introduced into eukaryotic cells using a common transfection protocol [170]. Shortly, HEK293T cells were seeded to reach 80% confluence on the day of transfection. Therefore, 5 x 10^5 cells in 2 mL **DMEM** medium were seeded into a 6-well plate the day before transfection. Directly before transfection, the medium was replaced by 1 mL of DMEM without supplements and incubated as before until transfection. A transfection mixture was prepared by diluting 2 μg of DNA into 100 μL DMEM without supplements, adding 8 μL **PEI solution** and incubation of 10 min at RT after vigorously mixing on a vortex instrument. The prepared mixture was pipetted to the cells by lifting the plate on one side and releasing the mixture directly below the surface of the medium, mixed by swirling and incubated for 6 h before the medium was replaced by 2 mL DMEM. After 24 to 72 h the cells or the supernatant were harvested. If smaller or greater vessels were used, the amount of cells, DNA, PEI and the amount of medium were scaled in relation to the surface of the vessel.

PEI solution	Polyethylenimine in sterile water at 1 mg/mL
FCS	GIBCO, 10270-106
Pen/Strep	10000 U/ml Penicillin, 10 mg/ml Streptomycin, PAN Biotech P06-07100
DMEM medium	DMEM (Invitrogen 41966) + 50 ml FCS, 5 ml Pen/Strep

2.3.3 Virus production

Transfection (2.3.2) of either proviral plasmids, or a three-component (5.2.2/3) **plasmid mixture** (i.e. plasmids for: packaging / envelope / VSV-G) into HEK293T cells initiated production of viruses. HEK293T cells were transfected in a 15 cm dish according to the protocol given in 2.3.2. After 72 h of incubation the supernatant was cleared by centrifugation at 4°C, 3000 x g for 15 min, and transferred onto a 30% sucrose cushion by pipetting the sucrose solution carefully below the supernatant. After **ultracentrifugation** at 4°C, 100000 x g for 2h the pellet was resuspended in 300 µL of **DMEM** medium over night at 4°C and stored in 50 µL portions at -80°C. The amount of p24 was measured by a p24 ELISA (2.2.1).

Ultracentrifuge	BD, Optima L90K
Centrifuge tubes	BD, 326823
Plasmid mixture	Total amount 30 µg DNA Ratio: 4 parts pTN-pack 3 parts pQL 1 part pVSV-G
DMEM medium	DMEM (Invitrogen 41966) + 50 ml FCS, 5 ml Pen/Strep

2.3.4 Infection and multiplicity of infection (MOI)

The day before infection 13 x 10^6 cells in 30 mL **DMEM medium** were seeded into 15 cm dish, or 2.5 x 10^4 cells in 0.5 mL into each well of a 6-well plate. Directly before infection the medium was replaced by freshly prepared 20 mL, or 0.5 mL, DMEM containing 10 µg/mL **Polybrene**. Virus was thawed slowly on ice or used directly after production (2.3.3). Various amounts of virus were pipetted to the cells depending on the experiment by lifting the dish or plate on one side and releasing the virus directly below the surface of the medium, mixed by swirling and incubated for 24 h before the medium was replaced by 30 mL or 0.5 mL fresh DMEM medium. The cells were assayed 48 h after infection. If cells were transduced using low MOI amounts of virus, MOI was deduced by infection of cells (2.3.4) with different amounts of virus and counting for GFP positive cells after 48 h post infection using FACS analysis (2.3.6) in relation to the volume of virus applied. MOI was estimated to be in a range of highest probability for singly infected cells (low MOI: < 0.2) by correlating the measured infection rate (% positive cells) and the expected multiplicity of infection (MOI) according to the Poisson distribution (5.3). Briefly, at MOI 0.2 the probability (P(n)) that a cell is infected by 0 (n) virus is 81.87 % (the negative cells). The rest of the cells are

infected by 1 (n) virus 16.37 %, 2 (n) viruses 1.64 % and so on. Therefore, most cells getting infected at MOI < 0.2 are singly infected cells.

DMEM medium	DMEM (Invitrogen 41966) + 50 ml FCS, 5 ml Pen/Strep
Polybrene	10 μg/μL Hexadimethrine bromide in sterile water, Sigma H9268

2.3.5 HIV replication assay

Manipulations in the viral genome of HIV-1 were proven not to affect the functionality of essential viral mechanisms by a comparison of the replication potency to its predecessor. Because the HIV-1 viruses tested in this assay were in general infection incompetent for the targeted HEK293T cells they had to be pseudotyped by an heterologous envelope which mediates the infection. The envelope of vesicular stomatitis virus (**VSV-G**) [171] was used to produce a pseudotyped batch of viruses. Since VSV-G is a superior envelope for mediating infections, it is known to be toxic if constitutively expressed by HEK293T cells [172]. Another envelope glycoprotein, the one of baculovirus *Autographa californica* (**gp64**) is described [173] to also mediate infections in HEK293T cells, but not to be toxic in those cells [172]. A constitutive expressing stable **HEK293-wtgp64** cell line was kindly provided by S.Bredl. HEK293-wtgp64 and HEK293T (negative control) cells were seeded in equal amounts and were infected with VSV-G pseudotyped viruses at an MOI of 0.1 (2.3.4). At different time points, 90 μL of supernatant were collected from each infected dish and analyzed in a p24-ELISA for the release of new viruses (2.2.1). Fresh **DMEM medium** was added to compensate for volume changes of the supernatant in every dish.

Flp-In-293	Invitrogen, R750-07
VSV-G	Envelope glycoprotein of vesicular stomatitis virus
gp64	Envelope glycoprotein of baculoviruses
HEK293-wtgp64	HEK293 FlpIn cell line constitutively expressing wtgp64 from its integration site (FRT).
DMEM medium	DMEM (Invitrogen 41966) + 50 ml FCS, 5 ml Pen/Strep
Polybrene	10 μg/μL Hexadimethrine bromide in sterile water, Sigma H9268

2.3.6 MACS sorting

Cells were detached with **PBE** and centrifuged at 300 x g for 5 min at 4°C. Preparation for MACS sorting was done according to Table 2.8.

Table 2.8 MACS sorting

Protocol	
1	Binding: incubation with 10 μg/mL 447-52D antibody diluted in PBE for 1 h at 4°C
2	Washing: 2 x with 1 mL ice cold PBE, centrifugation at 300 x g for 5 min at 4°C
3	Capture: 20 μL magnetic beads added to 80 μL resuspended cells in PBE for 15 min at 4°C
4	Washing: 2 x with 1 mL ice cold PBE, centrifuged at 300 x g for 5 min at 4°C
5	Staining: incubation with 1:500 anti-human-IgG antibody conjugated with APC in PBE
6	Washing: 2 x with 1 mL ice cold PBE, centrifuged at 300 x g for 5 min at 4°C
7	Cells were suspended in 500 μL PBE and applied to separation according to manufacture's protocol
8	Columns: Preparation of MS columns according to manufacture's protocol
9	Elution: Flush out cells with 1 mL PBE by firmly applying the plunger, supplied with the column.

PBE	PBS + 0.5 % FCS, 2 mM EDTA, 1 mg/mL NaN_3
Magnetic beads (Mouse anti-human)	Miltenyi Biotech, 130-047-501
MS column	Miltenyi Biotech, 130-042-201
anti-human IgG APC	BD, 555787

2.3.7 Flow cytometry analysis

In flow cytometry, cells are injected in a laminar flow through a capillary and thereby scattered to allow a single cell analysis. Passing the measuring system one or more beams of laser light of different wave lengths allows a multiparametric analysis of each cell according to its shape and fluorescence by various detection units [174,175].
Cells were detached with **PBE** and centrifuged at 200 x g for 5 min at 4°C. Preparation for cytometric analysis using **FACS Canto II or FACS Aria** is shown in Table 2.9.

Table 2.9 Flow cytometry

Protocol	
1	Binding: incubation with primary antibody diluted in PBE at 4°C
2	Washing: 3 x with 1mL ice cold PBE, centrifuged at 200xg for 5 min at 4°C
3	Staining: incubation with secondary antibody diluted in PBE for 1 h at 4°C
4	Washing: 3 x with 1mL ice cold PBE, centrifuged at 200xg for 5 min at 4°C
5	Cells were suspended in PBE and subjected to cytometric analysis

---

FACS Canto II and FACS Aria	Becton Dickinson (BD)	
PBE	PBS + 0.5 % FCS, 2 mM EDTA, 1 mg/mL NaN_3	
Primary antibodies:		
447-52D	0.001 - 10 μg/mL, 60 - 15 min, 4°C	Polymun, AB014
5F3	5 μg/mL, 1 h, 4°C	Polymun, AB010
2G12	10 μg/mL, 1 h, 4°C	Polymun, AB002
4E10	10 μg/mL, 1 h, 4°C	Polymun, AB004
HJ16	10 μg/mL, 1 h, 4°C	Corti et al. [176]
Secondary antibody:		
anti-human-IgG PE / APC	1:500, 1 h, 4°C	Jackson, 109-136-098

2.3.8 FACS (fluorescence activated cell sorting)

Cells were prepared according to the protocol given in 2.3.7 but finally resuspended in 1mL **PBE** per one 15 cm dish and filtered with a 30 μm **pre-separation filter**. Cells were subjected to cytometric sorting by a **FACS Aria** instrument. The instrument was set to "single cell mode" to obtain the most accurate counts for the sorting procedure (see 3.3.). In this mode drops containing two target events are discarded. When a particle is detected matching the criteria for separation, an electrical charge is applied just as the droplet containing this particle breaks off from the stream. As the charged droplet passes strongly charged deflection plates, it can be separated and collected [177,178]. The genomic DNA of the sorted cells and a portion of cells before sorting were prepared according to the manufacture's instructions but without addition of carrier DNA and limited to 20 μL Tris buffer for elution to increase the DNA concentration. To amplify viral integrated envelope genes (2.3.4) the genomic DNA was used as a template for Nested PCR (2.1.1).

PBE	PBS + 0.5 % FCS, 2 mM EDTA, 1 mg/mL NaN3
447-52D	0.2 μg/mL, 15 min, 4°C
	Polymun, AB014
anti-human-IgG APC	1:500; Jackson, 109-136-098
Pre-Separation Filters	Miltenyi Biotech, 130-041-407
FACS Aria	Becton Dickinson (BD)

3. Results

3.1 HIV-1 envelope display and panning

The objective to identify an effective immunogen against HIV-1 is one of the biggest challenges in the global scientific community as discussed in detail in the introduction (1.1-4). One way to identify a to date unavailable immunogen against HIV-1 might be the screening for a native and trimeric envelope with strong binding capabilities towards an existing bNAb [101,123,128,129]. The display of envelopes on a cellular membrane is a further step to its native appearance. In the following experiments a procedure to display native, trimeric and membrane-associated envelopes as prerequisite for the selection of binding (panning) with high affinity towards applied bNAbs is described.

3.1.1 General display and panning strategy for HIV envelope libraries

Since HIV-1 envelopes should not only be expressed natively and trimeric, but also displayed on a eukaryotic cell membrane a direct adaptation of existing panning methods was not possible, since the Lentivirus display of Taube et al. [139] was not present at the beginning of this thesis. However, the overall principle of panning procedures like phage display and others remains the same: The phenotype of a library has to be linked to its genotype and somehow displayed towards a binder-molecule. The resulting binder-molecule / library-binding-partner complexes have to be selected in a way that the genotype of the selected binding partner can be amplified. With iterative rounds of selections strong binding partners can enrich and are identified by poly- and monoclonal screening assays (Fig. 3.1).

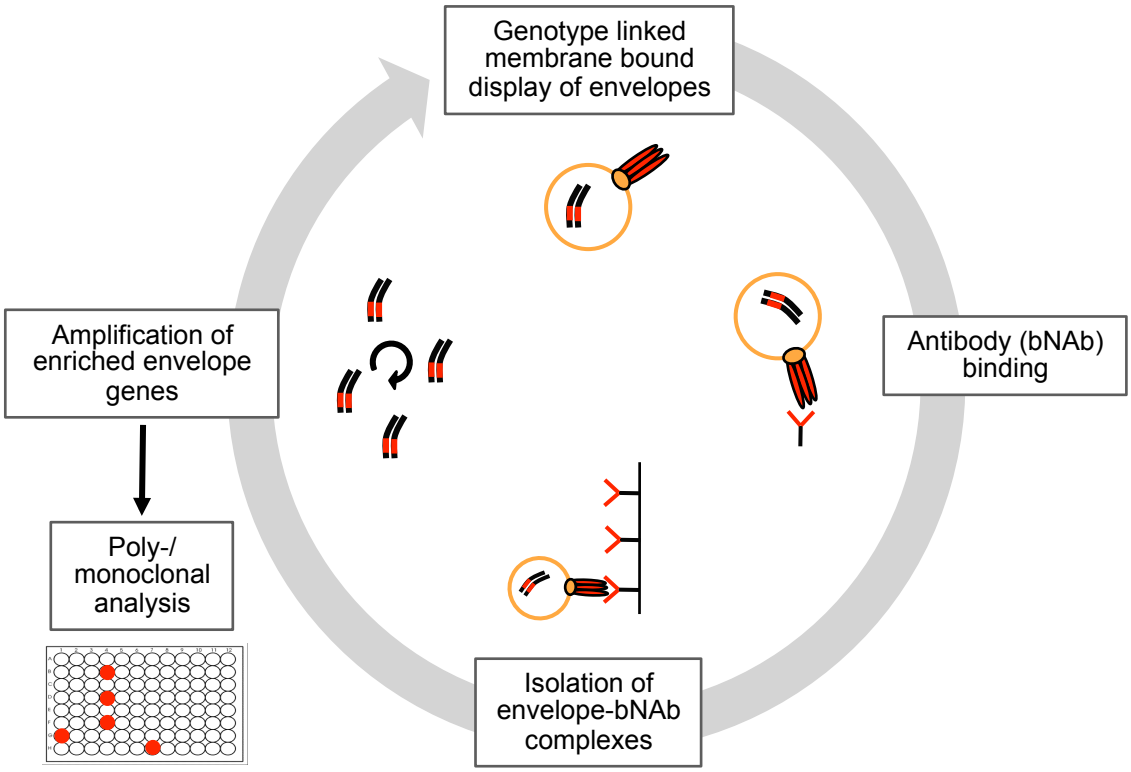

Fig. 3.1 General panning procedure
Schematic overview of the basic principle of the panning methods of this study. An envelope is displayed in its native, trimeric, membrane bound form. The particle contains the genetic information of the envelope displayed (top). A broad neutralizing antibody (bNAb) is incubated together with the displayed envelopes (right). Bound antibody-envelope complexes are isolated (e.g. immobilizing the antibodies and wash away unbound envelopes) (bottom). Isolation and amplification of the enriched genetic information by standard molecular biology techniques (left). Characterization of the enriched envelopes with either poly- or monoclonal analysis techniques such as sequencing, ELISA or FACS (bottom left).

Based on those common rules for panning, a procedure that includes proposed prerequisites for an optimal envelope presentation, as well as the use of bNAbs was developed in several steps.

3.1.2 Summary

Based on recent findings and insights into characteristics of broadly neutralizing antibodies and their capabilities to mediate protection against HIV-1 infections, a strategy is proposed to screen for optimal HIV-1 envelope binding partners against bNAbs. Recent findings of bNAbs restricted to trimeric envelopes [98,101] suggests that a native membrane-bound trimeric HIV-1 envelope with high affinity toward bNAbs might be a good vaccine candidate.

3.2 All in One (AIO) viral display and panning

Choosing HIV-1 viruses as a vector equals the criteria of a native display of envelopes the most, because the viral particles are the native environment of the envelopes *in vivo*. Since very productive display strategies exists (e.g. phage display) [165] that make use of a viral vector which carries both the phenotype and genotype of a protein library, it was straight-forward to choose a similar system for HIV-1 envelopes. Taking only one construct encoding for both, a heterologous Env and the components to form a functional HIV-1 particle, the approach was called “All-in-One“ or short “AIO”.

3.2.1 AIO display and panning procedure

Referring to the well established phage display technologies [130,179] a procedure based on HIV-1 viral particles, instead of phage, and HEK293T cells, instead of bacteria, was intended. Hence, an HIV-1 based display and panning procedure similar to the existing ALV (avian leukosis virus) display of Khare et al. [140,149] (see 1.6) was designed (Fig. 3.2).

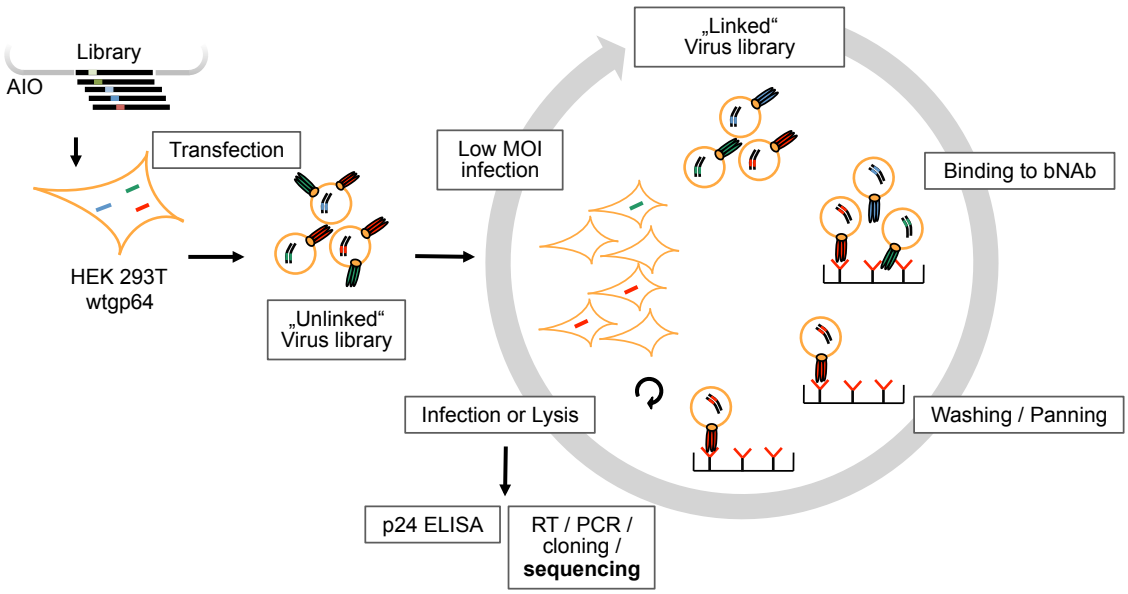

Fig. 3.2 Schematic overview of the AIO display and panning procedure
Starting on the left, HEK 293T wtgp64 cells are transfected with lentiviral vector based constructs (i.e. AIO). The produced virus is pseudotyped with wtgp64 and displays envelopes of the library. The linkage between genotype and phenotype is not given initially (“unlinked” virus library). By low MOI infection of new cells, a linkage between genotype and phenotype is achieved for the infected cells. The virus formed by these cells is pseudotyped with wtgp64 and displays the envelope coded in its genome (top). Broadly neutralizing antibodies (bNab) immobilized on a microtiterplate are used to bind virus-displaying envelopes of interest (upper right). The envelopes with the highest affinity to the bNab are selected by a stringent washing procedure (lower right). The bound viruses are used to infect fresh HEK293Twtgp64 cells with low MOI and / or are lysed to perform multiple analyses (bottom left). If fresh cells are infected, an enriched virus library is produced and another round of selection starts.

The procedure design comprises several steps starting with the production of HIV-1 virus particles by transfection of HEK293T-wtgp64 cells constitutively expressing wtgp64 [180] with proviral DNA. The wtgp64 envelope glycoprotein of the baculovirus *Autographa californica* was chosen, as it is known to mediate infection into 293T cells and concurrently not to be toxic (see 2.3.5). The virus particles pseudotyped with wtgp64 are used for a low MOI (multiplicity of infection) infection of fresh cells to achieve a linkage between genotype and phenotype through infection of only one virus per cell (see 5.3). Viruses budding from low MOI infected cells are called “linked” virus. A broadly neutralizing antibody (bNAb) is coated on a microtiterplate to bind virus particles applied. After several washing steps the remaining virus is either used for low MOI infection of fresh cells to start another round of selection or analyzed after lysis by p24 ELISA or sequencing.

3.2.2 Construction of pTN-AIO and pTN-AIOHSA plasmids

For the construction of a viral vector with a unique cloning site for the insertion of different envelope genes (library), the context of an envelope-deficient NL4-3 derived HIV-1 provirus was chosen. This initial construct is called pTN7-Stop (kindly provided by Dittmar et al.) and bears the marker gene *Renilla Luciferase* (*R.Luciferase*) at the position of Nef which is therefore substituted [181,182]. In earlier publications [183] it was shown that the substitution of Nef by a reporter gene leads to functional, replicating viruses. The plasmid pTN7-Stop was further modified by K.Schilling with a G7069C mutation to leave a unique KpnI site 3' of *R.Luciferase* [184]. This plasmid was chosen as a starting construct (Fig. 3.3).

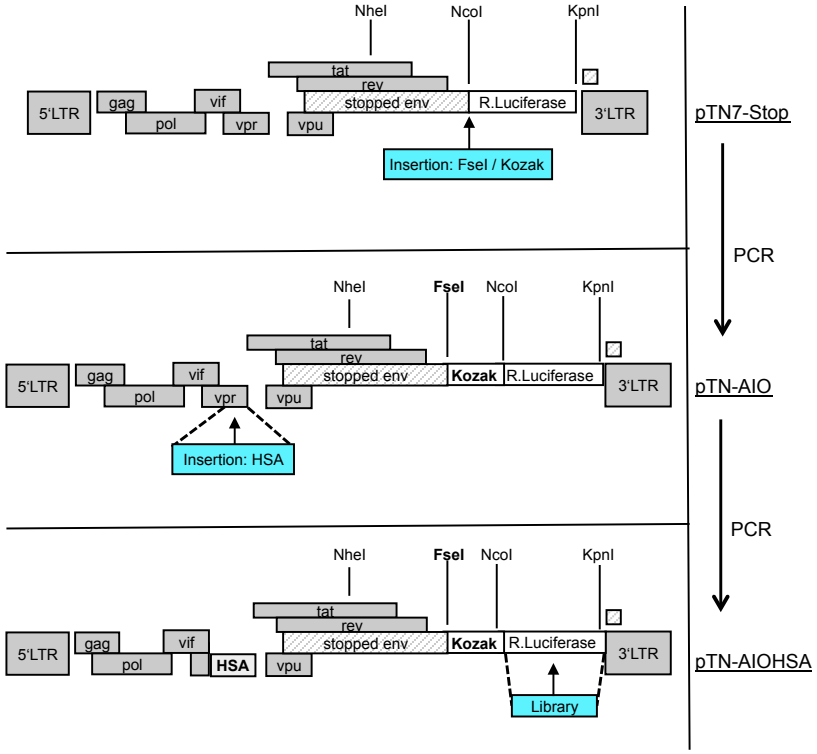

Fig. 3.3 Schematic overview of the construction of pTN-AIO and pTN-AIOHSA
The plasmid pTN7-Stop was used as starting construct. By PCR amplification between NheI and NcoI another unique restriction site and a Kozak consensus sequence were integrated as illustrated by the scheme. The resulting construct was termed pTN-AIO. Another marker gene (HSA) was inserted into the ORF of Vpr by PCR modification. The resulting construct was named pTN-AIOHSA. Screening of envelope libraries was proposed by replacing the *R.Luciferase* gene by envelope genes.

The unique restriction sites flanking the *R.Luciferase* were intended to become the integration sites of the envelope library. Thus, another unique restriction site, FseI, was introduced 5' of NcoI and the integration of a Kozak consensus sequence was done to enhance the expression [185] of a prospective library represented by the *R.Luciferase* reporter gene (data not shown). Since all components necessary for the formation of

an enveloped virus, packaged with its genome, were encoded on one proviral construct, the resulting vector was called pTN-All-in-One (pTN-AIO) (Fig.3.3). Through the integration of FseI, it was also possible to introduce a series of enhancer or promoter sequences 5' of the *R.luciferase* gene. However, no further increase of the expression rates of either *R.luciferase* or envelopes integrated were achieved (data not shown). After integration of an envelope, the substituted marker would not be available anymore. To probe for successfully transduced cells after infection (needed to determine, e.g. low MOI) another marker gene (HSA) was integrated into the ORF of Vpr and therefore substituted it, as described by Ali and colleagues [186,187] and the resulting virus was termed pTN-AIOHSA.

3.2.3 Characterization of pTN-AIO- and pTN-AIOHSA-based viruses

The small (231 bp) murine heat stable antigen (HSA) intended to be present on the surface of pTN-AIOHSA transfected cells and was efficiently detectable with an anti-HSA antibody in flow cytometry (Fig. 3.4 A). The viruses produced with pTN-AIO and pTN-AIOHSA were tested for replicative capacity in comparison to its predecessor pNL4-3 (Fig. 3.4 B) by measuring particle release over time with p24-ELISA.

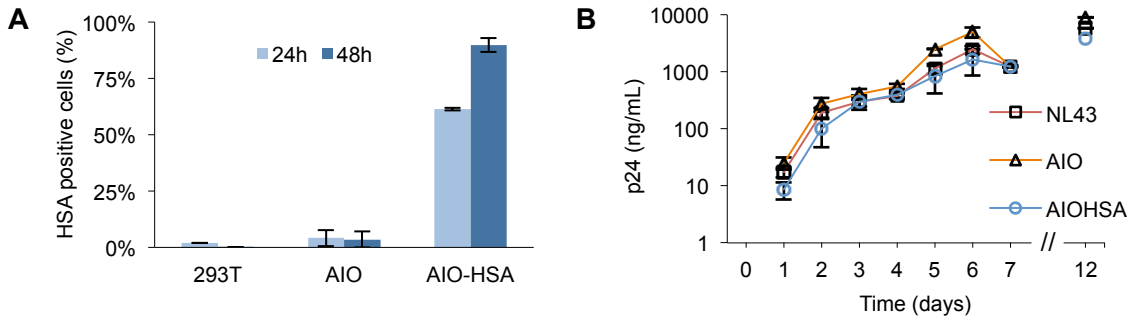

Fig. 3.4 Characterization of virus variants
The functionality of the reporter HSA as well as the replication capacities of the virus variants was tested. All results are given as the mean of two independent experiments. **A** Equal amounts of HEK293T cells (5 x 10^5) were transfected with 2 µg of the indicated provirus. The cells were stained with anti-HSA-PE antibody and probed for HSA expression by FACS, 24 h and 48 h post transfection. **B** HEK293T-wtgp64 cells (5 x 10^5), which constitutively express wtgp64 envelopes, were infected with equal amounts (MOI 0.1) of the indicated viruses. Replication was assayed every 24 h by measuring the p24-amounts in the supernatant.

HEK293T cells transfected with pTN-AIO showed for both, 24 h and 48h after transfection, only background levels of HSA positive cells, similar to an un-transfected control of 293T cells. Whereas, pTN-AIOHSA transfected cells were approximately 60% positive after 24 h, and 90 % positive after 48h post transfection (Fig. 3.4 A). Measurements of p24-amounts, which were obtained over time, in the supernatant of

NL4-3, AIO or AIOHSA infected cells, revealed no differences in the particle release between the respective virus derivatives (Fig. 3.4 B).
In conclusion, the specific detection of pTN-AIOHSA positive cells as well as similar viral replication capacities of AIO and AIOHSA compared to the predecessor NL4-3 virus was demonstrated.

3.2.4 Binding assay to quantify the amount of viruses captured by bNAb

To establish the AIO panning procedure, parameters were optimized for antibody coating, virus capture and washing procedures. Both magnetic beads and microtiterplates were evaluated as solid phase for antibody immobilization. Eventually, Nunc-Maxisorp microtiter plates performed best in specifically capturing bNAbs. The coating conditions of the antibody were tested concerning the composition of buffers and antibody concentration. The best results were obtained using 100mM $NaHCO_3$ pH 9.5 as coating buffer and 10 µg/mL (1µg/well) of antibody. Furthermore, the best conditions for viral incubations were 200 ng/well of virus, 2 h incubation time at room temperature and 3 washing steps (see Fig. 3.5). The various conditions tested (data not shown) are summarized in Table 3.1.

Table 3.1 Parameters tested to capture virus by bNAbs.

Parameter	Values tested	Optimal values
Plate type	Nunc Maxisorp, Nunc untreated (with magnetic beads)	Nunc Maxisorp
Solid phase	plates, magnetic beads	plate
Coating	direct coating of bNAb, pre-coating with anti-human IgG, use of protein-G magnetic beads	direct coating
Coating buffer	100mM $NaHCO_3$ pH 9.5, 50mM $NaHCO_3$ pH 9.5, PBS pH 7.0	100mM $NaHCO_3$ pH 9.5
Capture antibody concentration	2, 5, 10 µg/mL	10 µg/mL (1µg/well)
Virus concentration	50, 150, 200, 300 ng/well	200 ng/well
Virus incubation time	1, 2, 4 h	2
Virus incubation temperature	4°C, RT, 37°C	RT
Number of washing steps	3, 6, 10	3

The bNAb 2G12 [188] was chosen to optimize parameters of capturing viruses to antibodies immobilized on a microtiterplate. Probing for the amounts of virus captured by 2G12, a binding assay (see 2.2.2) was performed using the optimal parameters found (Table 3.1). The NL4-3 virus was used for a proof-of-concept because of its

known binding properties towards 2G12 antibody [189]. The amount of captured virus was analyzed by p24-ELISA for two different amounts of virus applied (Fig. 3.5).

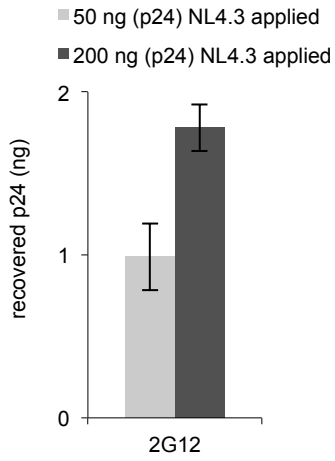

Fig. 3.5
Binding assay
A proof-of-concept for the binding and recovery of viruses was performed by using NL4-3 virus and 2G12 antibody. The results are given as the mean of two independent experiments. In order to capture virus, 2G12 was coated on a Maxisorp plate. NL4-3 viruses were applied to get captured by the immobilized antibody 2G12. After washing steps, the bound virus was lysed and applied to an ELISA assay to probe for the recovered amount of viruses. The amounts are shown in ng (p24) normalized to the amount of unspecific bound virus.

The loss of viruses applied was between 98 – 99 ± 0.5 %. This nearly complete loss of virus could not be prevented by any means in the binding assays done. We usually found 5 x 10^3 transforming units (TU) / ng p24 within our NL-43 virus preparations, which is within a common range of values found in the literature [190]. Since the virus particles in a binding assay are subject to different incubations and washing steps, a further decrease of infectivity was expected. At this stage of development, the decision was made to not pursue the AIO virus based panning strategy any longer, but to focus on transduced cells for displaying membrane-coupled envelopes.

3.2.5 Summary

The principle of a panning procedure using complete HIV-1 particles was designed. Replication competent NL4-3 derived virus derivatives AIO and AIOHSA were constructed and tested. Antibody immobilization and virus capture parameters were evaluated. A proof-of-concept using immobilized bNAb 2G12 and HIV-1 NL4-3 virus in a binding assay led to unsatisfactory amounts of recoverable virus. Thus a panning concept based on cellular display of envelopes was designed (see 3.3).

3.3 Construction of an HIV-1 envelope V3 Library

The development of a display and panning method prerequisites an environment of defined parameters. On the basis of a library of few, well characterized envelope proteins with known affinities towards the V3-binding antibody 447-52D [113,117,191], parameters for a successful display and panning were explored. To avoid selection-preferences that result from other origins than the binding toward the bNAb, a non-binding envelope of HIV-1, 96ZM651 (Accession number: AF286224) [192] was chosen as backbone for substituting the Env-V3 region with those of different 447-52D binding HIV-1 isolates [117].

3.3.1 Cloning of V3 substituted HIV-1 96ZM651 envelope variants

The DNA sequences resembling complete V3 regions of different HIV-1 isolates were adapted to human codon usage and synthesized as oligonucleotides. The plasmid pcDNA3.1-96ZMgp145HA (5.2.2) was used as template consisting of a human codon adapted gp145 envelope coding region of 96ZM651 extended by an HA tag cloned into the MCS of pcDNA3.1(+) (5.2.2). The V3 region of the envelope 96ZM651 was substituted by fusion PCR, inserting V3 regions of different isolates (5.2.1). Finally five different 96ZM651 based V3 envelope variants were chosen to form a library of envelopes that only differ in the small region of V3. The constructs were also cloned into the lentiviral QL9 vector system (see 3.5; 5.2.3). The plasmids were validated by restriction and sequence analysis (data not shown).

3.3.2 Binding of 447-52D antibody towards V3 envelope variants

Previously published experiments of Gorny and colleagues [117] determined a differential binding of 447-52D towards peptides of the V3 regions of different HIV-1 clades (Fig. 3.6 A). The differences in binding capacity were the basis for the decision to choose these V3 regions to generate a library with discriminable variants (3.3.1). After transfection of HEK293T cells with the different V3 constructs and staining with 447-52D antibody, cells were analyzed by flow cytometry. Un-transfected HEK 293T cells were used as negative control (neg.). The mean fluorescence intensity values (MFI) were corrected according to different expression levels of envelopes with the use of the antibody 5F3 [188], which is targeted towards an epitope not inside the V3 region. Thus, the epitope is equally available on all constructs used (see 2.3.7). The corrected values are shown as % of total MFI. The differential binding of 447-52D

antibody towards cell membrane displayed envelope V3 variants is shown in Fig. 3.6 B.

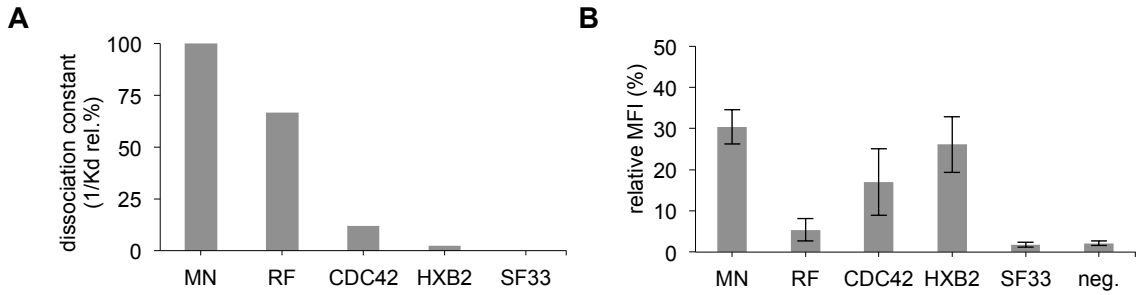

Fig. 3.6 Comparison of 447-52D antibody binding towards envelopes displayed on eukaryotic cells versus plate bound peptides
A V3 peptides of corresponding HIV-1 strains were shown by Gorny and colleagues [117] to bind with different relative Kd values. The reciprocal values are given and sorted from strong binding to non binding peptides (left to right) **B** $5x10^6$ HEK293T cells were transfected with pcDNA3.1(+) based V3 variant plasmids (2 µg each) and stained with 10 µg/mL 447-52D antibody 48 h after transfection. FACS analyses were done and the means of three independent experiments are shown. The differential binding pattern for the V3 variants is represented by the mean fluorescence intensities (MFI) normalized to equal envelope expression by an additional staining step with 10 µg/mL 5F3 antibody. Secondary stains were done with anti human antibodies coupled with APC or PE.

The obvious differences in binding capabilities in comparison between peptides and envelopes displayed on cells were notably distinct. The variant MN showed the highest, and SF33 the lowest affinity as demonstrated in both assays. However, according to the variants RF, CDC42 and HXB2 the depicted order in decreasing binding capacity of the used peptides, is diametrically opposed to the assay using envelopes displayed on cells (Fig. 3.6 A/B). Thus, reproduction of the binding-strength ranking obtained by the use of peptides was not achieved. It is known that the binding towards the linear epitope of V3 is also conformation-dependent [119]. Thus, it is not unreasonable to assume that an envelope displayed on a eukaryotic cell is differently targeted, than a linear peptide. However, it was not the aim to reproduce the data demonstrated by Gorny et al., but to generate discriminable variants of envelopes, which forms a feasible test-library for panning procedures.

3.3.3 Summary

A library of envelope variants differing only in their V3 region was constructed. The V3 variants were tested for differential binding towards the bNAbs 447-52D with flow cytometry after transfection into HEK293T cells. The MN and SF33 variants were the strongest and the weakest binding V3 variants respectively, whereas the performance

of RF, CDC42 and HXB2 variants differed from the reported experiments made with peptides. An envelope V3-variant library with distinct binding strengths toward the antibody 447-52D was successfully generated.

3.4 Cellular display and MACS-mediated panning

3.4.1 Cellular display and panning procedure (MACS-panning)

Any infected cell, from which an HIV-1 virion has been released, originally produces, like all other viral proteins, the viral envelopes that are subsequently displayed on the virus particle. Thus, after infection of target cells, HIV-1 envelope glycoproteins are expressed and displayed on the cellular plasma membrane [14]. Therefore a mammalian cell surface display was established to present envelope variants in a native, trimeric, membrane-bound environment. Hence, no virus particles were involved into the display and selection process itself and were further only used as a vector for the transduction of cells (Fig. 3.7).

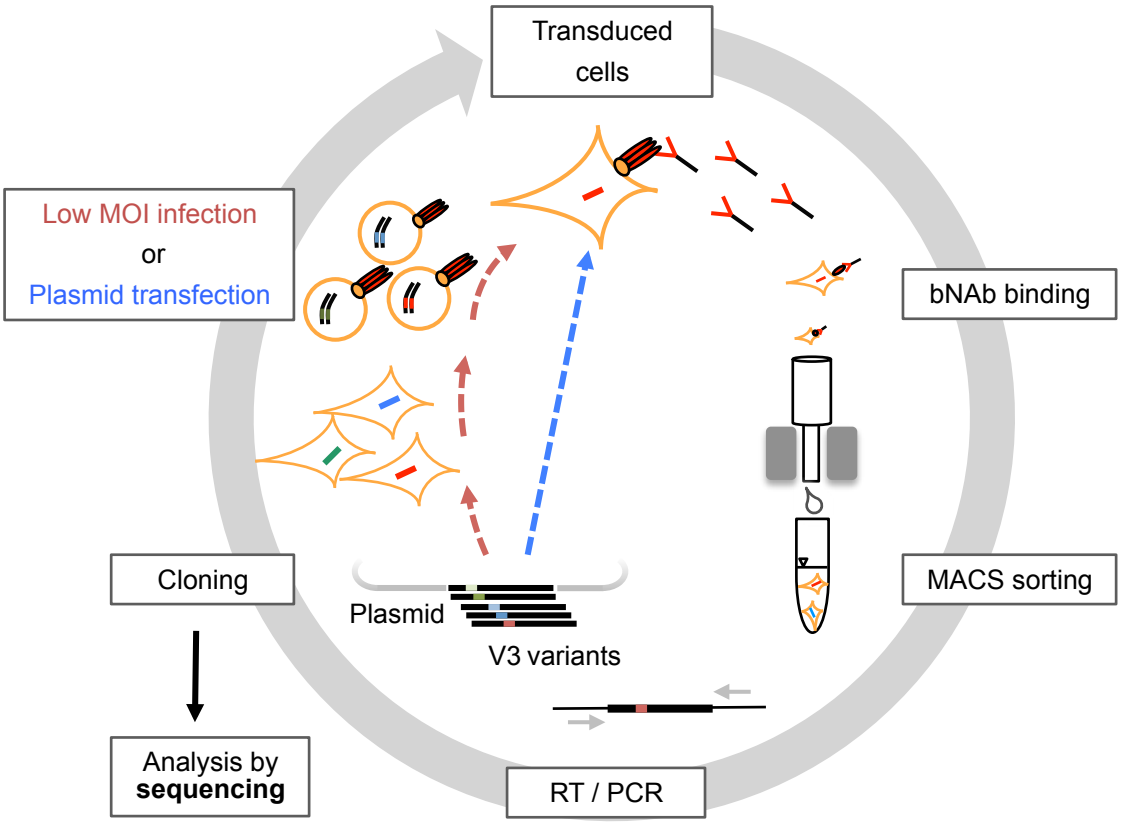

Fig. 3.7 Schematic overview of the MACS-panning procedure
Vectors coding for different envelope variants are introduced into HEK 293T cells either by transfection or infection. The linkage between genotype and phenotype is only given if the cells are infected by low MOI infection or if the cells are transfected separately by each variant (top). Broadly neutralizing antibodies (bNab) are applied to bind to cells displaying envelopes of interest (upper right). The envelopes with the highest affinity to the bNab are selected by a MACS selection procedure (lower right). The bound cells are eluted and lysed to amplify the envelope genes. Amplification is either done from mRNA (by RT / PCR) if cells are transfected, or from genomic DNA (by PCR) if infected. The recovered envelope genes are cloned into an appropriate vector and analyzed by sequencing (bottom left). Fresh cells are transfected (together with packaging and VSV-G constructs) to produce virus for low MOI infection of fresh cells. Or the vector is used to directly transfect fresh cells and enter a new round of selection.

The MACS-panning procedure design comprises several steps starting with either the production of HIV-1 virus particles by triple-transfection (envelope expressing-, packaging-, VSV-G- plasmid; see 2.3.3) and subsequent low MOI infection or with direct transfection of HEK293T cells with envelope expressing plasmids. The linkage between genotype and phenotype is reached by low MOI infection (see 5.3). Viruses budding from low MOI infected cells are called “linked” viruses. In the case of direct transfection, multiple different plasmids are expected to be expressed in one cell, and a less strong enrichment is anticipated. A broadly neutralizing antibody (bNAb) is applied to the envelope expressing cells to bind towards the envelopes anchored on the plasma membrane surface. Those cells expressing envelopes with highest affinity towards the bNAb applied are intended to bind more antibodies, thus facilitating

selection by a MACS enrichment procedure. After several washing steps the remaining cells are eluted and the envelope genes are amplified either from mRNA (RT followed by PCR) if cells are transfected, or from genomic DNA (PCR) if infected. The recovered envelope genes are cloned into an appropriate plasmid and analyzed by sequencing. To begin another round of panning the plasmids are either used to produce virus once more, or to transfect fresh cells directly, and another round is started.

3.4.2 MACS panning using one binding and one non-binding V3 variant

A proof-of-concept for MACS-mediated enrichment of envelopes binding towards 447-52D antibody was done by separately testing the selectivity of the system against transfected HEK293T cells expressing the MN (binding) or SF33 (non binding) envelope (see 2.3.6). With FACS analysis of collected samples of cells drawn at each step during MACS panning (Fig. 3.8 A), the status of enrichment was recorded. Samples of cells directly before addition to the columns were analyzed as well as samples of the washing fraction (negative) and the finally eluted fraction (positive). Un-transfected HEK293T cells were used as a background subtraction sample. An similar transfection-efficiency (MN = 60 %, SF33 = 55 %) and Env expression-rate (MFI: MN = 18, SF33 = 18) was separately determined by staining samples of both MN and SF33 transfected cells, with 5F3- and anti-human-PE -antibody respectively (data not shown). The MFI of eluted cells transfected with MN more than doubled to 113, compared to the sample before enrichment with 46.4, whereas the MFI of cells transfected with SF33 stays the same in every sample (Fig. 3.8 B). Only cells expressing envelopes that bind towards the applied 447-52D antibody were enriched.

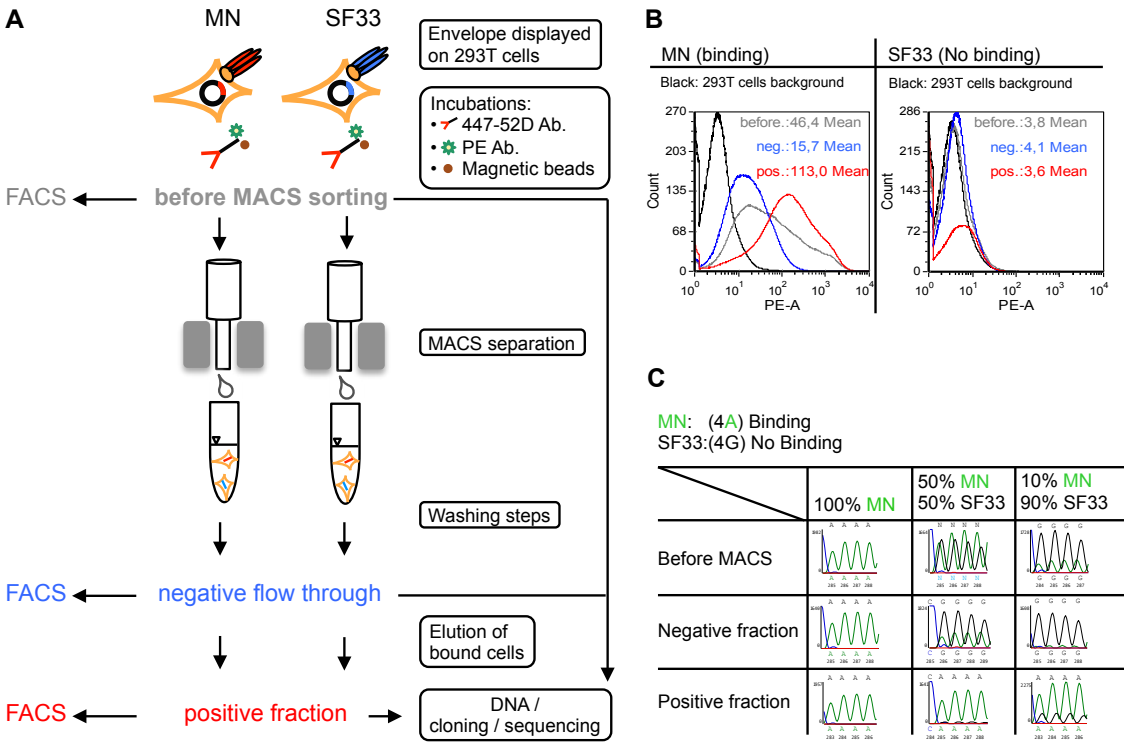

Fig. 3.8 MACS-mediated enrichment of envelopes displayed on HEK293T cells
A Schematic overview of the MACS separation procedure using separately transfected HEK293T cells displaying either the MN or SF33 envelope derivate. The cells are first stained with 447-52D antibody and subsequently in that order with anti-human magnetic beads and anti-human-PE antibody. The enrichment of cells, presenting envelopes with high affinity to 447-52D, is achieved by the use of magnetic bead separation. Cells bound by the 447-52D antibody are also labeled with magnetic beads and are immobilized within a magnetic field. After stringent washing steps the magnetic force is removed and cells are eluted. Envelope genes of different fractions are recovered and cloned into an appropriate vector, to enter a new round of selection by transfecting fresh HEK293T cells. **B** FACS analysis of separately enriched cells using MACS-panning with MN (binding) and SF33 (non binding) displaying cells. HEK293T cells (5 x 10^5) were transfected with pcDNA3.1 -based MN or SF33 constructs (2 µg each). A sample of both cells was stained with 5F3 antibody (10 µg/mL). An equally transfection efficiency (% positive cells) and Env expression-rate (MFI) was determined, 48 h after transfection (data not shown). Remaining cells were equally stained for MACS-panning with primary antibody 447-52D (10 µg/mL) and subsequently with anti-human magnetic beads and anti-human-PE antibody. Fractions before (grey), negative (blue) and positive (red) were collected separately and analyzed by FACS. The envelope expression is illustrated in colored histograms representing the MFI (Mean) compared to un-transfected HEK293T cells (black). **C** HEK293T cells (5 x 10^6) were transfected with pcDNA3.1-based MN or SF33 constructs (10 µg each). Cells were mixed 48 h after transfection as indicated. Separate MACS Panning procedures for every mixture were performed and fractions were collected as described in (B). Cells of each fraction were lysed; envelope genes were PCR amplified and cloned into pcDNA3.1. Mixed sequence analysis directed to a distinct sequence range was used to monitor the enrichment of envelopes in the different fractions. The chromatograms of the sequence range relevant to discriminate between MN and SF33 are shown respectively.

Different amounts of separately transfected and subsequently manually mixed cells were screened with MACS-panning. Separate MACS-panning procedures for every mixture were performed and fractions were collected as described before. A sample of cells from every fraction was lysed; envelope genes were amplified by PCR and cloned into pcDNA3.1(+). A polyclonal sequence analysis tailored to a distinct

sequence region, which is unique for MN and SF33 was used to monitor their enrichment in the different fractions. The relevant unique sequences to discriminate between MN and SF33 are shown for every mixture and fraction. Every mixture was screened for one round and even with lowest amount of MN (10%) the sequence representing MN clearly was enriched demonstrated by the sequence switch from GGGG (SF33) to AAAA (MN) (Fig. 3.8 C).

3.4.3 MACS-panning using the V3 library

The complete V3 envelope library was screened in MACS-panning with separately transfected cells. Equal amounts of 447-52D antibody stained cells of every variant were mixed directly before the MACS procedure. After one round of enrichment the envelope genes recovered from the eluted cells were cloned into pcDNA3.1(+) and DNA was prepared. The enrichment after one round was determined by sequencing one MTP of separately grown bacterial clones (Fig. 3.9 A). The distribution of identified clones after one round was similar to the binding strength pattern observed in Fig. 3.6 B. For a subsequent second round, the cells were no longer separately transfected with each V3 variant. Instead of that, the plasmid DNA mixture obtained from the pooled bacterial colonies after the first round were transfected directly, in order to proof whether a strict phenotype and genotype linkage is still needed. Although representing the enrichment status after one round, a further increase of the binding and a decrease of the non-binding envelope variants was not achieved by such a second round of panning, due to the absence of a linkage between genotype and phenotype (see 1.6). Hence, the counts per V3 variant were equally balanced again with only SF33 not being subject to any change in amount. The positive trend of enrichment was not enhanced, but nearly completely abolished (Fig. 3.9. B).

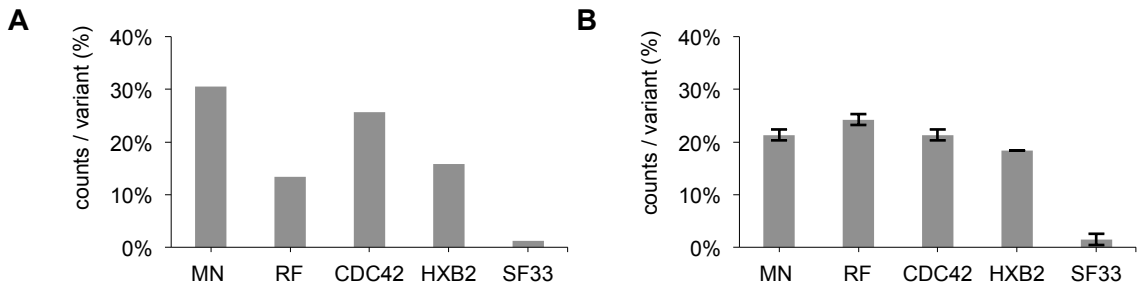

Fig. 3.9 MACS mediated enrichment of envelopes displayed on HEK293T cells
A HEK293T cells (5 x 10^6) were transfected separately with pcDNA3.1 based envelope constructs as indicated (10 µg each). Subsequently the cells were mixed together in equal parts of 1/5 and applied to a MACS Panning procedure 48 h after transfection. The envelope genes after one round of Panning were amplified from mRNA (RT/PCR) and cloned into pcDNA3.1. The DNA was prepared from an overnight culture of transformed bacteria. 94 (one MTP) separate clones were sequence analyzed, and assigned to the different variants. The relative amount of every variant is shown. **B** The obtained plasmid DNA mixture of part (A) was used to enter a second, "unlinked" round of panning by directly transfection of fresh cells. Sequence analysis of one MTP plate of bacterial clones after completion the second round of panning is shown as the mean of two separate experiments.

The enrichment of binding envelopes (i.e. MN) was only observed as long as separate transfections of the V3 variants were done. The intention of a panning procedure, however, is to screen libraries of many mixed variants at once (phage display: >10^9) [193]. Using separate transfections at this scale were not feasible. Thus, the possibility to obtain a "linked" library, although cells are transduced with a mixture of variants directly from the beginning of the panning procedure, was explored.

Therefore, virus was produced by a "triple-transfection" of a mixture of equal amounts of the envelope V3-variants that were cloned into a lentiviral vector (QL1; see 3.5), transfected together with packaging and VSV-G plasmids (see 2.3.3). Subsequently, target cells were infected with low MOI (0.1) as verified by staining of infected cells with 5F3 antibody (data not shown). Equal amounts of infected cells were subjected to MACS-panning and the eluted cells were analyzed by sequencing (Fig. 3.10).

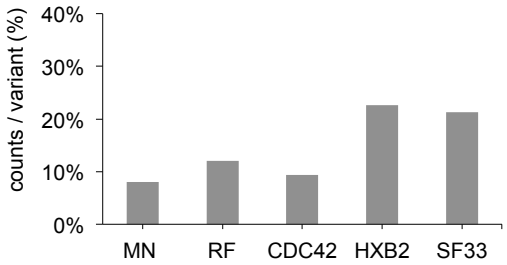

Fig. 3.10 MACS Panning with low MOI infected HEK293T cells
Virus, pseudotyped with VSV-G was produced using a mixture of equal amounts of QL1 (see 3.5) based envelope V3 constructs (see 2.3.3). HEK293T cells (5 x 10^5) were infected with low MOI (0.1) verified by 5F3 antibody staining (data not shown). Subsequently the cells were applied to a MACS Panning procedure 48 h after infection. The envelope genes were amplified from the genomic DNA of the eluted cells, cloned into pcDNA3.1, sequences were analyzed and assigned to the different variants similar to Fig. 3.9.

Neither the MACS-panning using mixed-transfected (Fig. 3.9 B), nor with mixed-virus-infected cells (Fig. 3.10) achieved an enrichment of the binding envelopes (e.g. MN), or a depletion of the non-binding envelope (SF33). Although the low MOI infection with mixed viruses should have most likely led to a separate infection of the cells, the obtained results differed to an enrichment experiment with separately transfected cells (see Fig. 3.9 A). Hence, two possible vulnerabilities of the MACS-panning procedure were considered: (I) The calculations to get low MOI infections were done using 5F3 antibody, binding towards cells that express envelopes. Assuming, that cells get infected but remain anyhow inaccessible for 5F3 antibody (weak expression, unusual folding or no display of envelopes), some cells would be miss-interpreted as un-infected cells. This would have caused an underestimation of infected cells and result in a higher MOI than desired. Infections with higher MOI are equivalent for having a higher probability to get more than one integration event per cell (see 5.3). Multiple variants of envelopes per cell were shown to reverse the enrichment effect of binders in the MACS-panning (Fig. 3.9 B); (II) Infected cells, that exhibit higher expression of envelopes than others, were probably preferentially selected, due to the presence of more binding partners towards the applied antibody on their surface. Using a MACS-based, polyclonal enrichment-process the discrimination between single cells with different envelope expression rates is impossible.

Thus, (I) a marker for infected cells only dependent on successful integration of the viral genome is desirable. (II) The selection with MACS columns had to be replaced by FACS-sorting that permits for the simultaneously determination of the Env expression strength on a single cell basis. Therefore, a new vector system (pQL) was designed and established to introduce GFP for accurate measurements of the MOI of infected cells (see 3.5).

3.4.4 Summary

The MACS-panning procedure was designed and a proof-of-concept was successfully shown for HEK293T cells that were separately transfected. No success in enrichment of binding envelopes (i.e. MN) and depletion of non-binding variants (i.e. SF33) was observed, when cells were transduced with a mixture of variants. This was also the case when “low-MOI conditions” were used to create an effect of separately transduced cells. Two weaknesses of the MACS-panning design concerning the determination of low-MOI infections and a possible bias towards high envelope expressing cells were noticed and reconsidered.

3.5 QL vector development

3.5.1 Design and construction of QL vectors

As described above, the determination of transduced cells and the accuracy of low MOI infection are crucial to ensure a high probability for singly infected cells and a linkage of phenotype and genotype. Furthermore, an accurate marker and method to control the envelope expression rates of transduced cells is needed. Staining cells with 5F3 antibody turned out to be neither an accurate marker for infection nor for the expression of envelopes, because 5F3 antibody is not binding all infected and envelope expressing cells (see Fig. 3.13 B). Furthermore, being addicted to appropriate expression and display of envelopes with equal efficiency is a hindrance that is immanent to the use of antibodies as a marker. This is especially true if such an antibody is expected to bind equally to every envelope in a more complex library. Therefore, a new lentiviral vector was designed to overcome this limitation. The integration of GFP into the lentiviral part of the plasmids introduced a marker suitable for direct identification of infected cells (Table 3.2/ 3).

Table 3.2 Components of the lentiviral starting construct
The plasmid pWPXLd (Addgene) was used as the starting construct. The construct consists of a plasmid backbone (not shown) and carries a lentiviral expression cassette consisting of the listed elements.

Element	Properties
5'LTR	Long terminal repeat: HIV-1 regulatory elements, transcriptional control and promoter region [194].
RRE	Comprises parts of the Env sequence encompassing the Rev response element (RRE) flanked by splice signals (not shown): Increased packaging of RNA into virions, increased transcription and cytoplasmic export of full-length RNA [195]
EF1α	Human elongation factor 1 aplpha (EF1α) promoter [196]: Constitutive promoter less susceptible to down regulation [197,198]
cPPT	Central polypurin tract: Involved in forming a central DNA flap: Increases the transduction efficiency by completing the nuclear import process to wild type levels [195,199]
GFP	Green fluorscent protein and its derivatives eGFP and YFP are used as fluorescence marker genes [200]
WPRE	The posttranscriptional regulatory element of woodchuck hepatitis virus, increases the level of expression [201]
3'LTR	A truncated version of 3'LTR is used resulting in a self-inactivating viral vector (SIN) [202].

Furthermore, a CcdB positive selection marker (killer-gene [168]) was integrated to enable a convenient and efficient cloning [167] (see 2.1.4) of envelope variants.
The lentiviral plasmid pWPXLd [203] (5.2.2) was used as a starting construct. Because of the presence of Esp3I sites, the original backbone of pWPXLd was substituted by non- Esp3I containing plasmid backbones, PCR-Script-Amp (5.2.2) with its derivatives pQL1-5, as well as by pcDNA3.1(+) (5.2.2) with its derivatives pQL6-11 (Table 3.3).

Table 3.3 Vector pQL: stages of development
The eGFP cassette of pWPXLd was substituted by a CcdB expression cassette flanked by two Esp3I restriction sites (see Fig. 3.11) enabling for the QL cloning procedure (pQL1/ 6) described in part 2.1.4. Besides the integration of the CcdB cloning cassette, several attempts were necessary to integrate an again functional expression cassette of GFP or YFP using standard PCR and cloning techniques.

Plasmid	Map of the lentiviral part
pWPXLd	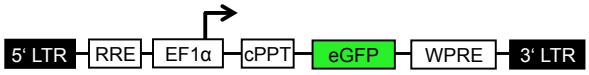 Basic lentiviral vector
pQL1 / pQL6*	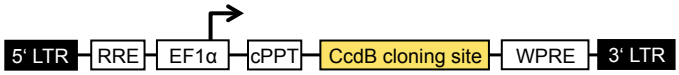 The CcdB cloning element was integrated. *QL1 versus QL6: plasmid backbones were switched (not shown/ see main text).
pQL2	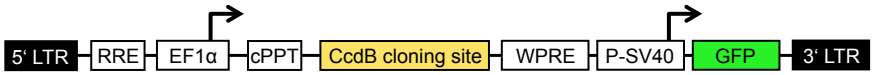 An expression cassette consisting of SV40 early promoter and GFP was cloned upstream of the 3' LTR sequence
pQL3	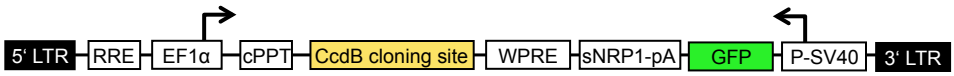 The orientation of the GFP expression cassette was switched compared to QL2 and a sNRP-1 poly adenylation site [204] was added
pQL4	 The same orientation as in QL3, but YFP (Clonetech, see 5.2.2) and a SV40 poly-adenylation sequence were chosen
pQL5 / pQL7*	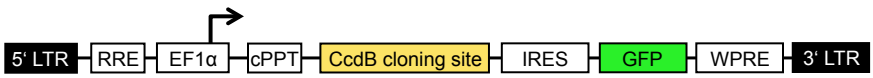 IRES (internal ribosome entry site, implemented from pMACS LNGFR-IRES, (see 5.2.2) and GFP were introduced downstream of the CcdB cloning site. *switched plasmid backbones (see above and main text)
pQL8	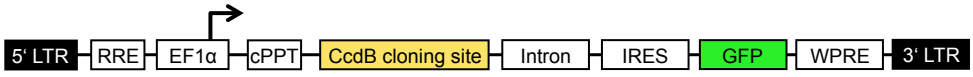 An artificial Intron [205] was cloned upstream of the IRES site
pQL9	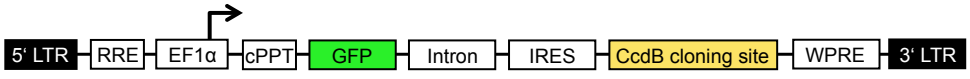 GFP and CcdB cloning site were switched in positions
pQL10	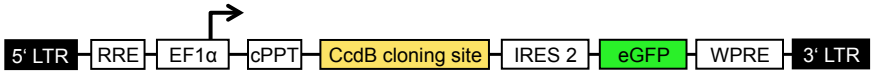 Equals pQL5/7 except for using IRES2-eGFP from pIRES2-eGFP (Clonetech, see 5.2.2)
pQL11	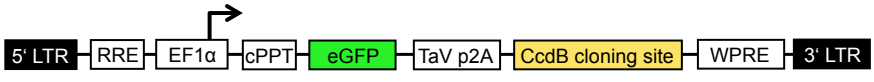 Equals QL9 except that the TaV p2A peptide [206] substitutes the Intron-IRES

The construction of pQL1 and 6 was sequentially performed by (I) PCR amplification of the MCS (multiple cloning site) of pcDNA3.1(+) (primer pair 4A1/1A4) and blunt-end ligation with pPCR-Script-Amp linearized with EcoRV. (II) Subsequently, the plasmid was linearized with EcoRV/XbaI within the MCS and ligated with the lentiviral part of pWPXLd obtained by restriction with SspI/XbaI (5.7 kb fragment). (III) The substitution of eGFP within the WPXLd part by a CcdB expression cassette flanked by two Esp3I restriction sites, cloned via MluI/NdeI and propagation in DB3.1 bacteria (CcdB resistant) resulted in the pQL1 plasmid. The vector pQL6 was constructed by another substitution of the plasmid backbone. Here, the lentiviral part of pQL1 (EcoRI; blunt-ended; 5.4 kb) was ligated with the plasmid backbone of pcDNA3.1(+) (PciI/MfeI; blunt-ended; dephosphorylated; 1.9 kb). Particularly, pQL9 was created by cloning a GFP gene into the MCS of pMACS LNGFR-IRES (#130-091-887, Miltenyi Biotech) via EcoRI/BamHI. Subsequently, an expression cassette consisting of GFP, synthetic Intron [205] and an IRES site (internal ribosome entry site) was introduced upstream of the CcdB cloning site of pQL6 (via PCR, 8B2 / B3) resulting in the final pQL9 plasmid. The elimination of Esp3I sites in the original plasmids enabled the Insertion of a CcdB expression cassette with flanking Esp3I restriction sites (Typ IIS) mediating the QL cloning procedure [167] (see 2.1.4).

With the QL cloning procedure the restriction and ligation reactions were performed simultaneously in one reaction vessel. A subsequent selection for positively cloned plasmids was done by transformation of the CcdB sensitive bacterial strain DH10B (Fig. 3.11).

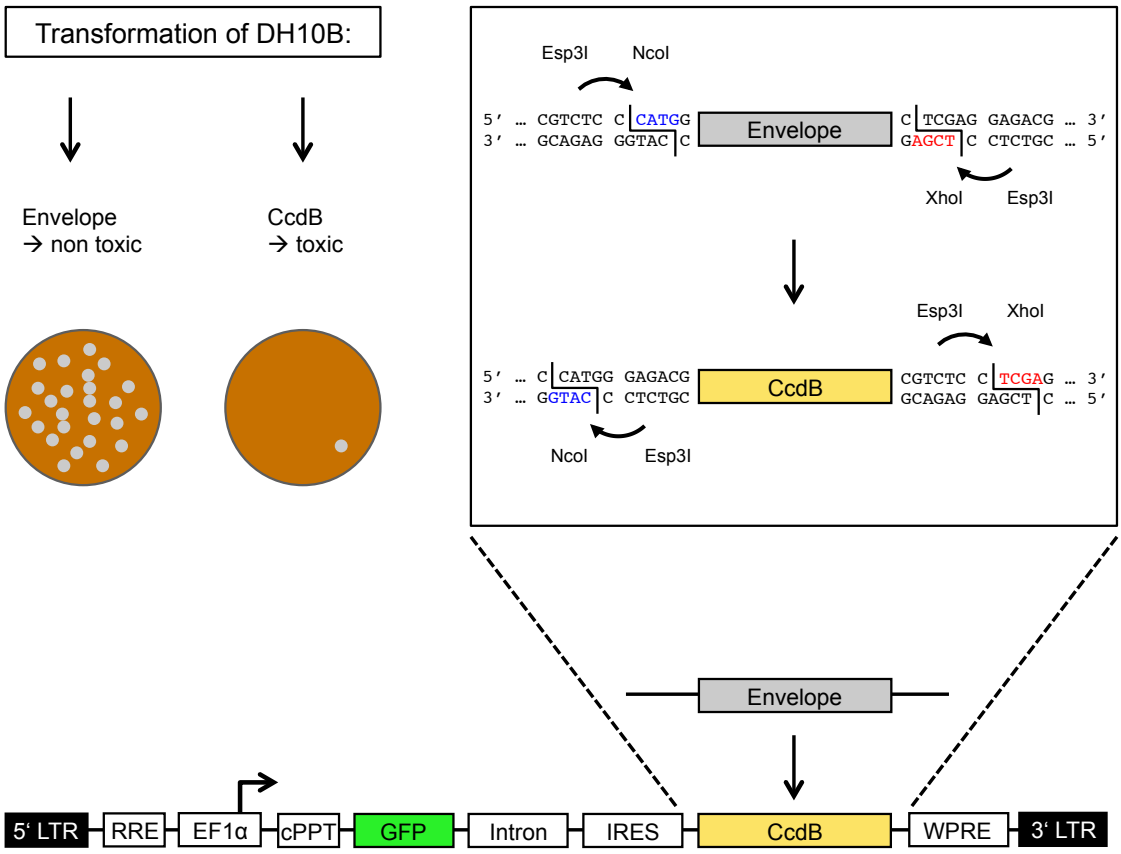

Fig. 3.11 Schematic overview of the QL cloning procedure
An envelope or envelope library is amplified with primers (see 5.2.1) extending the envelope gene by the restriction sites Esp3I followed in 5'→3' by NcoI with the forward primer (e.g. 5I3) and XhoI for the reverse primer (e.g. 5I4) (top right). The amplified envelope gene and a QL plasmid (e.g. pQL9) are jointly incubated with the Esp3I restriction enzyme and T4-Ligase (see 2.1.4). Only the equally colored "sticky-ends" are compatible and can be ligated successfully (right). After transformation of CcdB sensitive bacteria like DH10B, only bacteria bearing a plasmid without CcdB are able to form colonies (left). Only few (<0.01%) bacteria are seen on control plates where no envelope insert was applied to the reaction due to irregularly ligated "empty" plasmids.

As Esp3I cleaves downstream of its recognition site, NcoI and XhoI sites were chosen as adjacent restriction sites. After restriction with Esp3I the resulting DNA bears fully compatible NcoI and XhoI "sticky-ends" allowing an easy introduction of inserts using the QL method (see 2.1.4). With subsequent derivatives of pQL1 and pQL6, envelope and GFP genes were introduced differently into the lentiviral part of the vector (Table 3.3) to achieve both, envelope and GFP expression (3.5.2).

3.5.2 Characterization of the QL vectors

Multiple derivatives were created and tested to achieve GFP expression in the presence and absence of an envelope (MN) expression cassette (Fig. 3.12 A). Cells transfected with QL vectors (with and without cloned envelope) that showed GFP

expression and at the same time could be successfully stained with 447-52D antibody towards the envelope variant MN, were compared for equal GFP and 447-52D antibody signals by FACS analysis (Fig. 3.12 B).

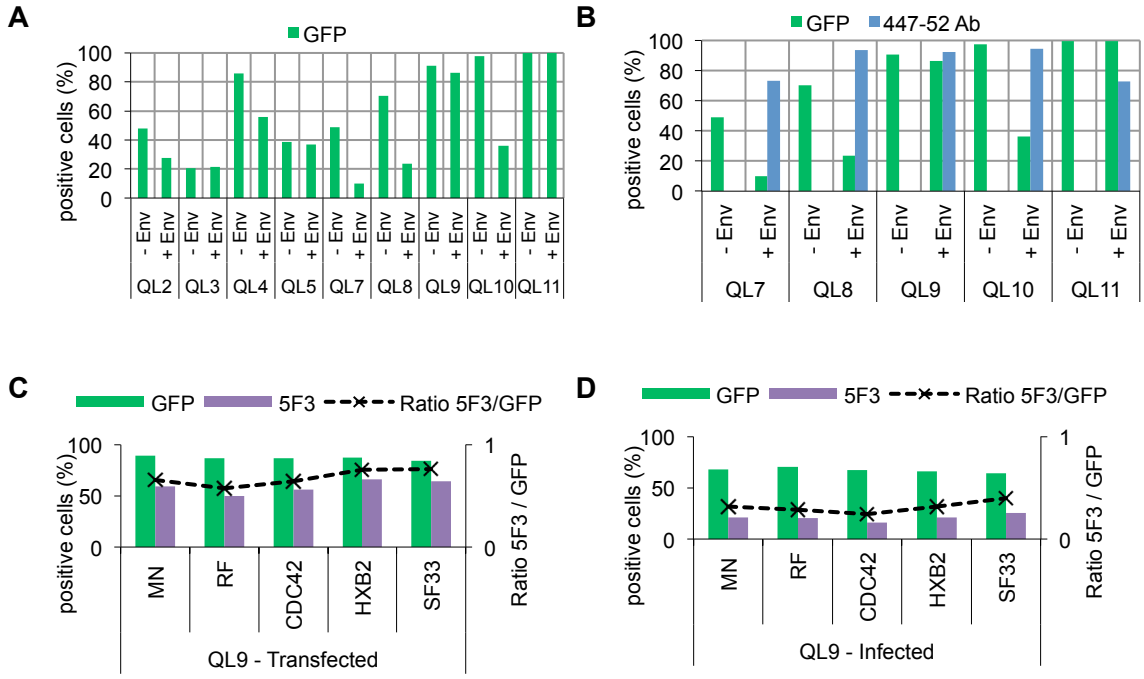

Fig. 3.12 Evaluation of the QL vector development

A / B HEK293T cells (3 x 10^5) were transfected with equal amounts (1 µg each) of the QL based constructs with or without an MN envelope V3 gene as indicated. 48 h after transfection all cells were stained with 50 µL 447-52D (10 µg/mL) and subsequently anti-human APC (1:500) antibodies. The cells were analyzed by FACS for co-expression of GFP in presence or absences of MN envelope. Values are shown as percent positive cells after histogram subtraction of un-transfected HEK293T cells (A); Cells that are both positive for GFP and 447-52D staining (B). **C / D** HEK293T cells (3 x 10^5) were either transfected (1 µg) or infected (MOI 1) with a QL9 based V3 envelope construct. The cells were stained with 5F3 (10 µg/mL) and anti-human APC (1:500) antibodies, 48 h after transduction. In FACS analyzes the cells were probed for GFP and 5F3 expression. The ratio of 5F3 and GFP positive cells is indicated.

Only cells transfected with QL9 and QL11 showed GFP expression correlating with the expression of the MN envelopes stained with 447-52D antibody. In both plasmids GFP is cloned upstream of the envelope gene. In QL9 an IRES site [207], in QL11 a p2A peptide [206] is used to couple the expression of GFP and envelope. Since QL9 was the first functional vector variant, all following characterizations were based on this vector. A QL9-based set of the V3 library envelopes (3.3.1) was compared for GFP versus 5F3 antibody binding after transfection, as well as after infection of 293T cells. The binding of 5F3 antibody differs between transfection and infection, which is shown by the ratio of 5F3/GFP illustrated with the dotted line (Fig. 3.12 C/D). This effect was

further analyzed, since 5F3 antibody was used in earlier experiments (3.4) to determine positively infected cells and to calculate low MOI.

3.5.3 A marker for transduction and envelope expression

Since GFP was initially introduced as a marker (3.5.1) only for successful transductions, antibodies were explored to serve as a marker for equal amounts of envelopes anchored on the plasma membrane of transduced cells. Therefore, antibodies were chosen that binds the envelope variants outside of their differing V3 regions (Fig. 3.13).

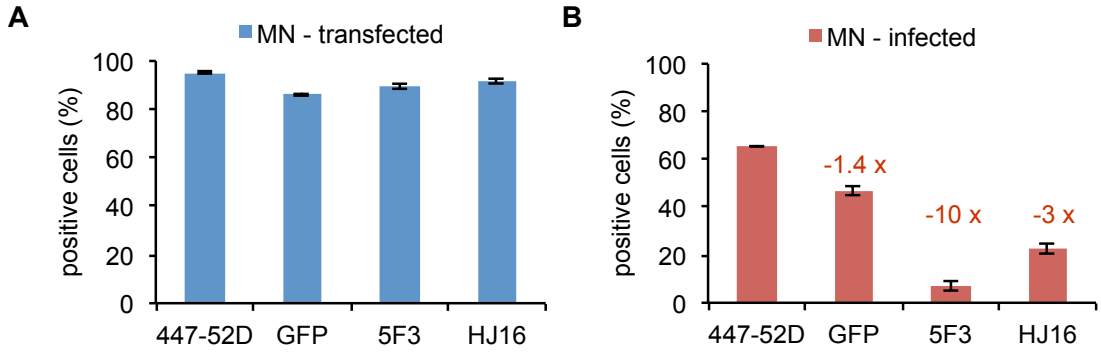

Fig. 3.13 Comparison of antibody binding to MN envelope transfected or infected cells
Petridishes with 1.5 x 10^6 HEK293T cells were either transfected (5 µg; blue) or infected (red) with an MOI 0.5 (according to GFP) with QL9-MN, which encodes for the strongest 447-52D binding envelope V3 variant MN. Cells were split into four portions and stained with 0.5 mL 10 µg/mL primary antibody (i.e. 447-52D, 5F3, HJ16) and APC conjugated secondary antibody (1:500) 48 h after transduction. FACS analysis is shown for each antibody as positive cells (%) gated in relation to un-transduced HEK293T control cells. The factor of reduction (colored numbers) between equal cell populations, either **A** transfected or **B** infected, using different primary staining antibodies is shown. GFP is co-expressed on QL9 and served as a marker for transduction. The mean values of two separate experiments are shown.

Two separate petri-dishes with HEK293T cells were either transfected or infected with QL9-MN and analyzed by FACS. Un-transduced cells were used for background subtractions in each measurement. The expression of GFP was used as a marker for transfected as well as infected cells. Equal amounts of cells were separately stained 48 h after either transfection or infection, using 447-52D antibody as a positive control for Env expression (MFI: transfected cells 876, infected cells 39). The antibodies 5F3 and HJ16 were tested whether they were capable to stain the same amount of cells (%) compared to the 447-52D positive control. Only in the case of transfected cells an equal result compared to the positive control was achieved for 5F3 and HJ16 antibodies (Fig. 3.13 A). Whereas, the infected cells showed a discrepancy of 10-fold (5F3) and 3-fold (HJ16) reduction of the amount of positive cells compared to the

positive control (Fig. 3.13 B). Notably, only the signals for GFP positive cells seemed to correspond to similar levels (-1.4 fold, Fig. 3.13. B) of positive cells compared to 447-52D antibody for both transfected and infected cells (Fig. 3.13 A/ B). Consequently, GFP was further explored to serve as a marker for Env expression as well.

3.5.4 Correlation of GFP and envelope expression after infection

Apart from using GFP as a marker for transduction, it was analyzed for the suitability as a marker for expression. HEK293T cells were infected with various amounts of QL9-MN and assayed for the correlation of GFP and envelope expression 48 h after infection. Cells were stained with 447-52D antibody, un-transduced cells were used for background subtraction and both GFP and 447-52D signals were analyzed by FACS (Fig. 3.14).

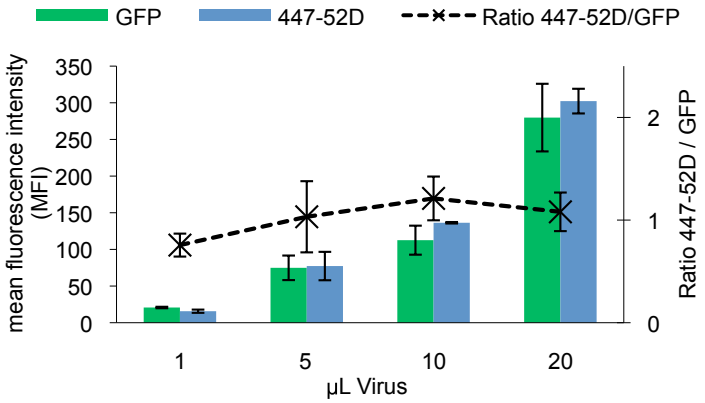

Fig. 3.14 Ratio of 447-52D and GFP of infected cells
HEK293T cells (3 x 10^5) were infected with QL9-MN viruses with the volume indicated (MOI: 0.05 – 0.5) and stained with 50 µL 447-52D antibody (10 µg/mL) 48 h after infection. FACS analysis is shown for the different volumes of the applied virus as the MFI of gated living cells. The ratio of 447-52D/GFP is shown with a secondary axis to indicate the connection between the expression levels of the envelope and GFP. The mean values of two independent experiments are shown.

Even though GFP is not directly coupled with the envelope expression and especially not with its display, it was shown that the correlation to Env-expressing cells was more reliable compared to a 5F3 antibody staining (Fig. 3.13 B). Furthermore a constant correlation between GFP expression and the amount of envelopes displayed on the cells (MFI) was seen independently of the amount of infecting virus (range of MOI: 0.05 – 0.5). The dashed line in Fig. 3.14 illustrates that the calculated ratio of GFP expression and displayed envelope bound by 447-52D antibody is constant. Therefore, GFP was further on used as both, a marker for the transduction of cells and the expression level of envelopes.

3.5.5 V3 variant affinities and optimal discrimination

The parameters for an equilibrium binding and optimal discrimination of cells expressing envelope V3 variants by 447-52D antibody were determined by a time course and a series of antibody dilutions (Fig. 3.15).

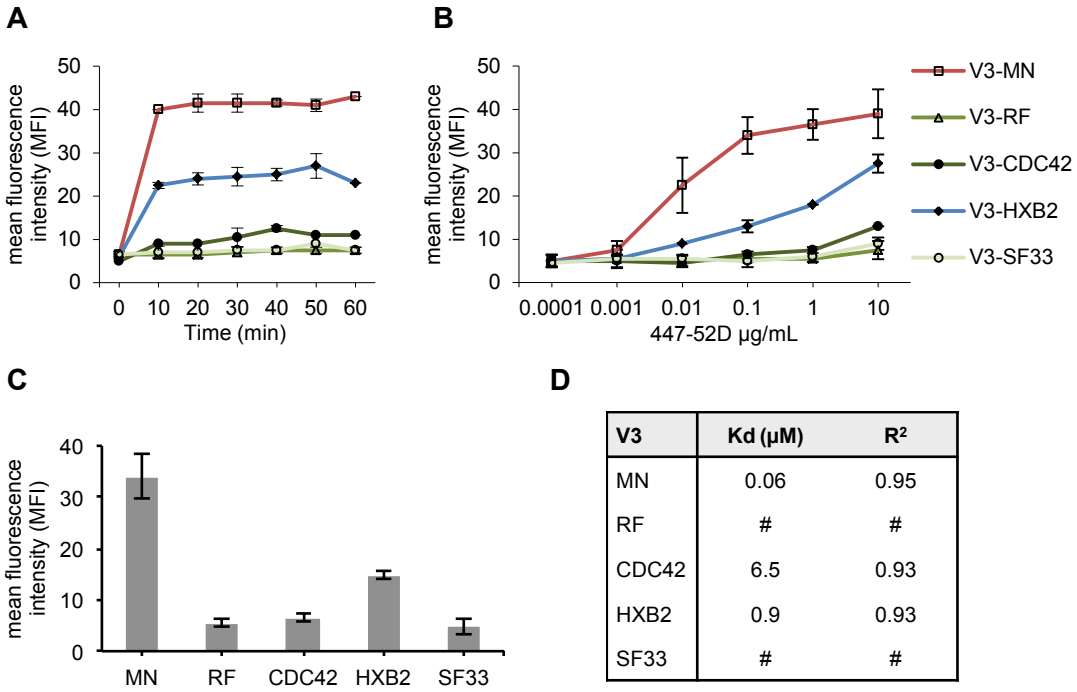

V3	Kd (µM)	R^2
MN	0.06	0.95
RF	#	#
CDC42	6.5	0.93
HXB2	0.9	0.93
SF33	#	#

Fig. 3.15 Optimization of 447-52D antibody binding conditions
HEK293T cells were infected with an MOI of 0.3 by one of the respective QL9-V3 variants. The cells were stained with 447-52D antibody and APC secondary antibody 48 h after infection. All FACS analyses were gated in relation to un-infected HEK293T cells. The mean values of two independent experiments corrected for equal GFP expression are shown (see 3.5.4). **A** The staining with 447-52D antibody (10 µg/mL) was scheduled to obtain an equilibrium binding profile with 10 min increments. FACS analyses are shown as the MFI of every V3 construct for the different staining times. **B** The 447-52D antibody was serially diluted and incubated on cells for 1 h at 4°C to get a concentration-dependent binding profile. FACS analyses are shown as the MFI of every V3 construct stained with different 447-52D antibody concentrations. **C** Cell populations stained with 0.1 µg/mL 447-52D antibodies are separately shown to illustrate the differential binding at this concentration. **D** The dissociation constants Kd were determined from the equilibrium binding titration curves shown in (B). Data points were fitted by nonlinear least squares regression (One site / Fit total and nonspecific binding, Graphpad, Prism 5), and the resulting Kd as well as R^2 values are depicted (#, non-calculable).

HEK293T cells were infected separately with one of the respective QL9 based virus V3 envelope variants. The cells were stained with 447-52D antibody in samples with equal amounts of cells and different incubation times (Fig. 3.15 A) or different antibody concentrations (Fig. 3.15 B). Longer incubation than 10 min did not lead to higher staining signals (MFI), thus equilibrium binding is assumed as measured by FACS. An

optimal antibody concentration of 0.1 µg/mL was observed (Fig. 3.15 C), which showed the best discrimination between the different variants. A similar general binding profile compared to the library binding profile described in an earlier section (Fig. 3.6 B) was observed. The equilibrium dissociation constant Kd, was calculated by fitting the data obtained by titration of 447-52D antibody using a nonlinear least squares regression [208,209]. The affinity of the V3 variant MN (Kd = 0.06 µM) was determined to have the highest affinity to 447-52D antibody, followed by HXB2 (Kd = 0.9 µM) and CDC42 (Kd = 6.5 µM) (Fig. 3.15 D).
To ensure optimal binding conditions in further experiments incubation times of 15 min and 447-52D antibody concentrations of 0.2 µg/ml, were chosen as standard parameters.

3.5.6 Growth kinetics of bacteria transformed with V3 constructs

The influence of a respective plasmid on bacterial growth after transformation is one possible issue for an unspecific bias in an enrichment procedure like panning. Although all V3 constructs share the same molecular background, a bias in the selection of variants remains possible if the bacterial growth rate is influenced by the differences in the V3 coding region of the plasmids. To rule this out, the growth-rate and accuracy of the plasmids prepared after an over-night culture were analyzed. Therefore the pQL9 V3 constructs were used to transform DH10B cells (2.1.5), which subsequently were cultivated for a DNA preparation in MTP (2.1.6). At different time points, the OD(600) was measured and compared for differential growth by calculating the individual bacterial doubling-times. The bacterial growth-rates were measured in five replicates. All strains consistently had a doubling-time of 78 ± 4 min. The subsequently, and additionally from separate overnight-cultures, isolated plasmid DNA were tested for correctly sized bands (data not shown) after preparation and restriction (1 µg each) with AleI at 37°C for 2 h on a 1 % Agarosegel (see 2.1). All samples consistently showed correctly sized restriction patterns, as well as equal plasmid DNA yields (data not shown). Thus, a bias resulting from a varying bacterial plasmid propagation of the different V3 variants was excluded.

3.5.7 Realtime PCR analyzes

Evaluating the status of enrichment on the basis of sequencing randomly chosen samples of single bacterial clones is dependent and therefore limited by the sample size. A practically sample size for manual processing was considered to be one MTP

(94 single clones) per round of enrichment. These generated values were accurate related to the parent population with ± 10 %, within a confidence level of 95% [210,211]. A Realtime PCR reaction was established to increase the statistical accuracy by analyzing the relative portion of any out of five V3 envelope variants in a plasmid DNA sample of usually 0.05 ng DNA (≈ 4 x 10^6 plasmids) after every round of enrichment. Within a confidence level of 95%, the generated values were accurate related to the parent population with ± 0.05 %. Thus, a higher accuracy in the readout of the enrichment status was possible. Besides, providing a tool for the confirmation of the enrichment status, determined by sequencing. However, a Realtime-PCR-based method is only practicable for the limited number of variants used within the V3 library and not for any proposed larger libraries. A critical parameter for PCR based experiments is the efficiency with which a primer pair is able to amplify a DNA sequence [212]. Therefore, efficiency values of primer pairs (reference and specific primers) designed for analytical purposes as well as for primer pairs used to amplify the complete envelope genes within the panning procedure (8H1/H2) were determined (Fig. 3.16 A/B). Different PCR efficiencies would result in a biased PCR amplification in favor of one of the V3 constructs. The calculated efficiency values were taken into account for the calculations of relative amounts of V3 variants probed in section 3.6. The amplification of the complete V3 envelope by PCR was un-biased according to the 8H1/H2 primer pair, which performed with similar efficiencies on all tested V3 envelope variants within the given margin of error (Fig. 3.16 B).

A

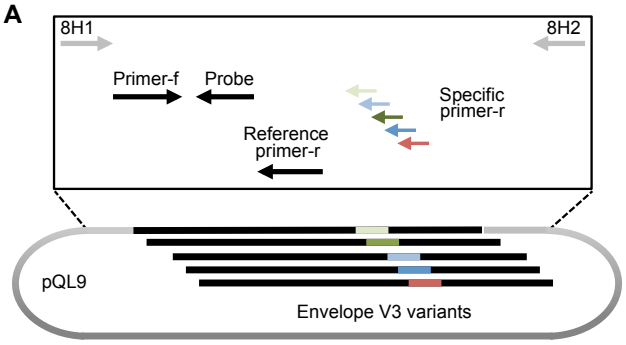

B

	Efficiency (%)		
	Primerpair		
V3 variant	8H1/8H2	Reference	Specific
MN	57 ± 7	104	106
RF	50 ± 11	109	104
CDC42	57 ± 6	106	101
HXB2	50 ± 7	101	100
SF33	55 ± 5	103	100

C

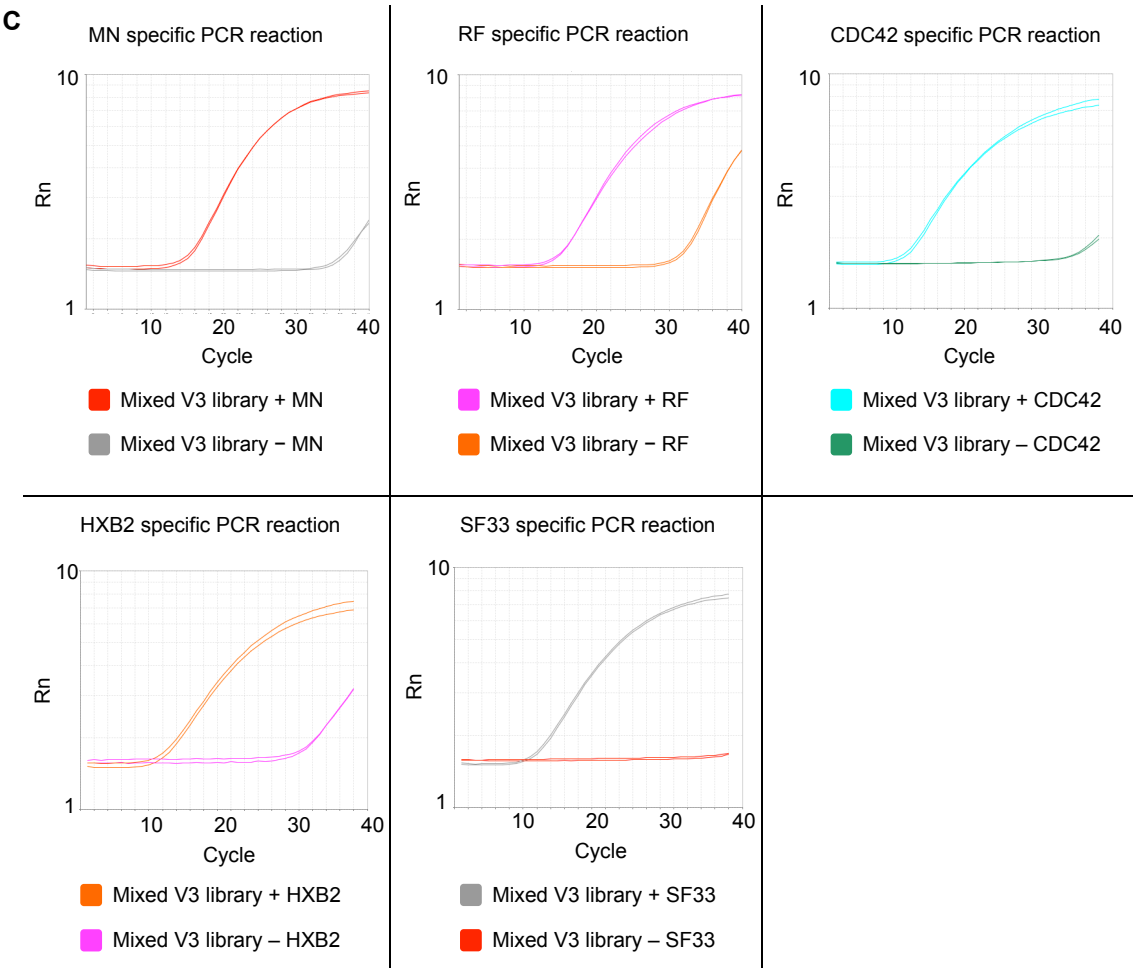

Fig. 3.16 Efficiency and verification of the specificity of Realtime PCR analyses
A Schematic overview of the Realtime PCR components. Consensus sequences are color-coded. Sequences corresponding to the envelope are black and to the QL9 plasmid are grey. Oligonucleotides like primers or probes are grey, black or colored arrows. The colors and orientation visually connect the plasmid sequence to its oligonucleotide binding area. The Probe is 5' labeled with FAM and 3' quenched by BHQ1. **B** PCR efficiencies for all primer pairs used on the V3 plasmids were calculated to demonstrate comparable efficiencies between the different V3 constructs. Efficiencies for primer 8H1 and 8H2 were tested with SYBR Green (mean and SD of two separate experiments). The other primers were tested with probe based Realtime PCR. **C** Probe based Realtime PCR amplifications on plasmid mixtures were done to verify the specificity of every possible combination of the V3 variants used. The name of the colored samples indicates whether the tested V3 variant is present or absent. Technically, triplicates of 5 µL of every sample

mixture (1 ng/µL) were tested with its corresponding specific Primer-r, but with equal Primer-f and Probe. Rn values (normalized Reporter) are the ratio of the fluorescence emission intensity of the reporter (Probe) to the fluorescence emission intensity of the passive reference dye (i.e. ROX). Rn is plotted against the PCR cycle number to illustrate the amplification of PCR products.

Realtime PCRs using plasmid mixtures of QL9 V3 envelope variants confirmed the specificity of the primer pairs designed for analytical experiments (Fig. 3.16 C). Each primer pair was probed using a mixture of plasmid with (positive) and without (negative) the appropriate V3 envelope. All tested primer pairs specifically interacted only with the V3 envelope variant for which they were designed.

3.5.8 Summary

A new lentiviral vector (QL9) was designed and characterized. With the integration of GFP into QL9, a marker for transduction and equal envelope expression was introduced. Optimal parameters for the discrimination of QL9 infected V3 envelope-expressing cells were determined. Realtime PCR was introduced in addition to sequence analyzes of single bacterial clones, as a statistically more reliant analytical tool to analyze the amount of distinct V3 variants in a mixture of plasmids. A bias in the enrichment of V3 variants with the benefit to one of the constructs was excluded concerning differing bacterial growth as well as differing PCR efficiencies primer pairs used.

3.6 Lenti-cellular display and FACS-mediated panning

3.6.1 Lenti-cellular display and panning procedure (FACS-panning)

A lenti-cellular display and FACS-panning procedure was designed considering the experiences of earlier developed panning procedures (see 3.2 / 3.4) and addition of new techniques addressing the discovered weaknesses. With the development of pQL9, a reliable determination of low MOI infection and normalization of envelope expression of cells is possible. Furthermore the CcdB-mediated QL cloning strategy enabled a convenient, standardized and efficient process for the cloning of envelope genes. Utilizing Realtime PCR a second tool besides sequencing of single bacterial clones is available to specifically determine the amount of each V3 variant within a mixture of DNA (3.5). Although this PCR-based assay is only practicable for the development stage using limited numbers of V3 variants, the increased accuracy and validation of the obtained results by a separate analysis tool, is of advantage. Further on, the previous MACS-mediated enrichment process was substituted with a single cell FACS sorting procedure. This essential modification enabled the selection of cells based on their individual properties. Hence, unwanted avidity effects were avoided by (I) gating for cells that display Env in equal amounts, and (II) the separation of cells displaying Env that bind with the desired higher affinity towards the applied 447-52D antibody (Fig. 3.17).

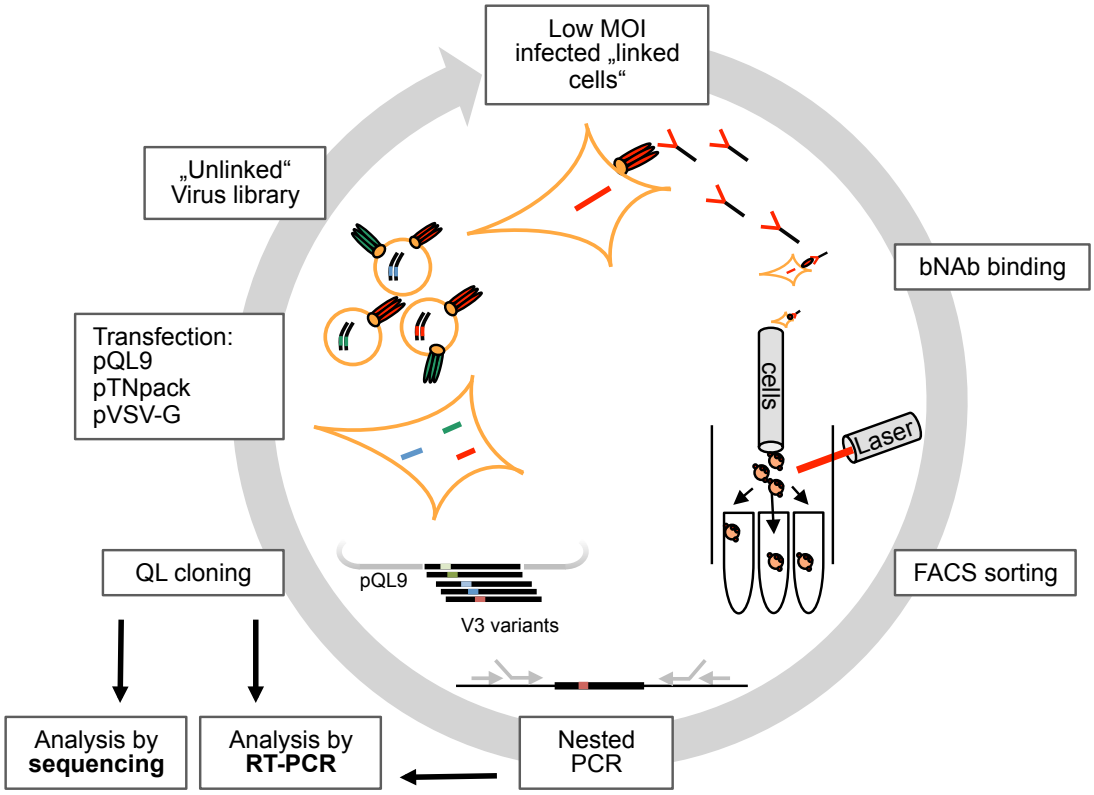

Fig. 3.17 Schematic overview of the FACS-panning procedure
HEK293T cells are transfected with lentiviral-vector-based constructs (QL9 + pTN pack, pVSV-G) (left). The produced virus is pseudotyped with VSV-G and displays envelopes coded on QL9. The linkage between its genotype and phenotype is not given (“unlinked” virus library). By low MOI infection of new cells, a linkage between genotype and phenotype is achieved for the infected cells (top). Broadly neutralizing antibodies (bNab) are applied to bind to these cells, expressing envelopes of interest (upper right). The envelopes with the highest affinity to the bNab are selected by a FACS-sorting procedure (lower right). The selected cells are collected and lysed, before amplifying the envelope genes. Amplification is done from genomic DNA (Nested PCR). The recovered envelope genes are cloned into QL9 plasmid and analyzed by sequencing and Realtime-PCR (RT-PCR) (bottom left). Fresh cells are transfected (together with pTN pack and pVSV-G) to produce new virus for Low MOI infection of fresh cells, thus entering a new round of selection.

The FACS-panning procedure starts with the production of viruses by a triple-transfection of pQL9-V3-library, packaging-, and VSV-G- plasmid (see 2.3.3). Any transfected cell receives multiple library variants at once. Therefore, arising viruses displays diverse Env variants that not stringently coincide with the Env gene encoded on their genome (unlinked virus library). A linkage between genotype and phenotype is reached by a low MOI (0.1) infection (see 5.3). Consequently, infected cells receive only one viral genome and express only one V3 Env variant. Thus, low MOI infected cells are called “linked cells”. The broadly neutralizing antibody (bNAb) 447-52D is applied to the envelope expressing cells to bind towards the envelopes anchored on the plasma membrane surface. The marker GFP is used to gate for equally Env expressing cells (see 3.5.4). A FACS sorting procedure selects cells expressing

envelopes with high affinity towards the bNAb applied (see 3.6.2). The sorted cells are lysed and the envelope genes are amplified from genomic DNA (Nested-PCR; 2.1.1). The recovered envelope genes are cloned (2.1.4) into pQL9, and bacteria are transformed. Single bacterial clones are analyzed by sequencing, and plasmid DNA is analyzed by Realtime PCR (RT-PCR; 2.1.2). The obtained plasmids are used to produce a new batch of VSV-G pseudotyped viruses and to begin another round of panning.

3.6.2 FACS sorting strategy

A series of different gating strategies was tested using pQL9 based V3 library transfections and infections of cells, in order to evaluate parameters for an optimal discrimination of envelope V3 variants (data not shown). Gating for living, single cells and choosing populations with an even GFP expression yielded the best results. Therefore, a VSV-G pseudotyped batch of virus was produced by triple transfection (see 2.3.3) of HEK293T cells using a QL9 plasmid (-mixture, see 3.6.3), packaging- and VSV-G- plasmids. Subsequently, fresh HEK293T cells were infected with low MOI (0.1) as measured by counting GFP expressing cells. Subsequently a FACS-panning (3.6.1) was performed using ~ 4 x 10^7 cells. One typical sorting experiment is shown to illustrate the FACS sorting strategy. Therefore, 50,000 events were recorded and a series of hierarchical gates were applied to isolate single, high affinity, Env displaying cells (Fig. 3.18 A-B).

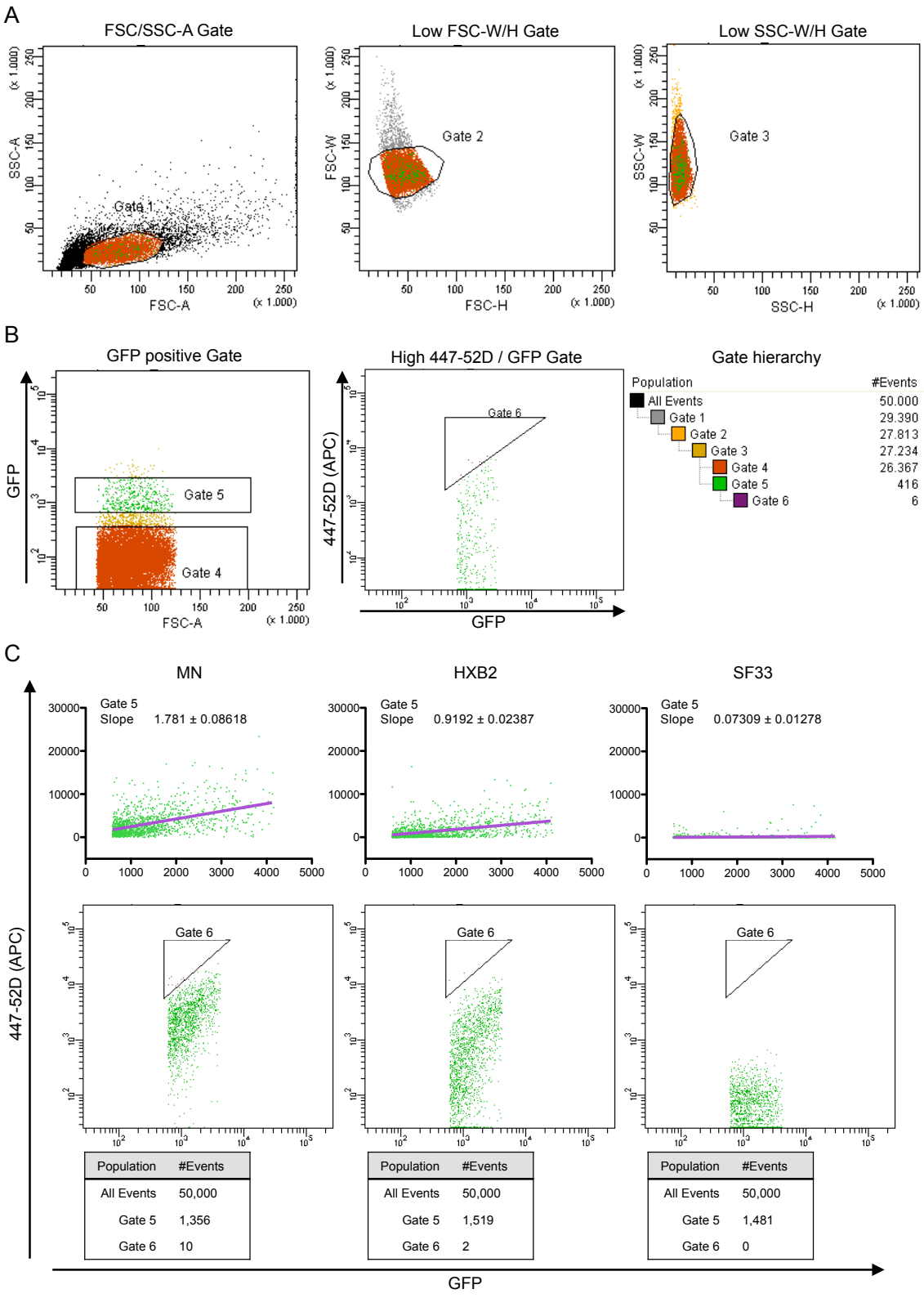

Fig. 3.18 FACS-sorting strategy

A The living population of infected cells (see main text) was gated according to their size (FSC-A) and granularity (SSC-A) (left). Further gates were applied to eliminate doublets by adjusting the parameters of FSC (middle) and SSC (right) according to height and width. **B** GFP positive cells were gated within their main population to avoid highest (possibly multiply infected) and lowest (possibly background noise) GFP expressing cells (left). Sorting population is gated for highest APC (447-52D

antibody) signals in relation to GFP signals. Therefore a triangle shaped Gate (Gate 6) was chosen. Cells which appear in the upper left corner are supposed to have the highest APC to GFP ratio and may therefore display an envelope with high affinity to the tested antibody (447-52D) (middle). The complete Gate hierarchy starting from all events, to the events sorted (Gate 6) is shown (right). **C** Evaluation of the triangle gate strategy: HEK293T cells (13 x 10^6) were infected with low MOI (0.1) by each QL9-V3 variant, respectively. The cells were stained with 447-52D antibody and APC secondary antibody 48 h after infection. Cells were analyzed by FACS according to the gating strategy described in part A and B. Cells that appeared in Gate 5 are shown in a linear dot plot and were further analyzed by calculating a linear regression curve (purple). Representative variants MN, HXB2, and SF33 illustrate that with increasing affinities cells shift to the upper left direction of the gate as demonstrated by an increasing slope value. The triangle shaped Gate 6 is shown in a log-scale dot plot. The numbers of events counted for Gate 5 and Gate 6 are shown below each plot, respectively. Consequently, decreasing amounts of cells equals decreasing affinities of Env, as detected in the sorting Gate 6, ranging from 10 counts of MN, 2 of HXB2 and 0 of SF33.

The applied gating strategy selects for (I) the living fraction of cells according to their size, as measured by the forward (FSC) and side (SSC) scatter area (A). (II) Since cells tend to rotate while measuring the height (H) and width (W) parameters for both, FSC and SSC were adjusted to select for the lower, main population, to discriminate single cells (Fig. 3.18 A). (III) In order to decrease the chance for selecting multiply infected cells, as well as to avoid background noise, the highest and lowest GFP expressing cells were excluded in choosing the main population of GFP positive cells (Gate 5, Fig. 3.18 B).
A triangle shape was chosen for the FACS-sorting gate (Fig. 3.18 B, Gate 6) to select cells with the highest ratio of 447-52D binding related to envelope expression (represented by GFP). Thus, it is assured that primarily envelope variants with high affinity towards 447-52D antibody and not with unusually high expression are selected.

A separate experiment was performed to evaluate the proposed triangle gating strategy for high affinity Env selection. Therefore 13 x 10^6 HEK293T cells were infected with low MOI (0.1) by each QL9-V3 variant, respectively. The FACS-sorting strategy was performed individually for each variant as described above. The cells were probed for high affinity towards 447-52D antibody by calculating a linear regression curve for cells that appeared in Gate 5. Representative variants of the model V3 library are shown (Fig. 3.18 C). The distinct slopes of the regression curves illustrate the varying ratio of 447-52D / GFP for each Env variant, respectively. A higher ratio equals a higher affinity of 447-52D towards the respective Env [138]. A high stringency for selecting only high affinity Envs was proposed by gating only for the top < 10 events out of 50.000 counts, using the triangle shaped selection Gate 6 (Fig.

3.18 B, C) [138,209]. According to the evaluation experiments a distinct difference in cell counts for MN (10), HXB2 (2) and SF33 (0) suggested a stringent discrimination between the V3 variants. As this encouraging evaluation was done with separate infected cells, a proof-of-concept experiment using a mixture of MN and SF33 followed.

3.6.3 FACS-panning using one binding and one non-binding V3 variant

A proof-of-concept for the FACS-panning procedure of envelopes binding towards 447-52D antibody was done with mixtures of QL9-MN (binding) or QL9-SF33 (non binding) V3 envelope variants. VSV-G pseudotyped virus batches were produced by triple transfection (see 2.3.3) of HEK293T cells with three different QL9-MN and QL9-SF33 plasmid ratios (MN / SF33: (I) 5 % / 95 %, (II) 25 % / 75 %, (III) 50 % / 50 %), each with packaging-, and VSV-G- plasmids. Subsequently, fresh HEK293T cells were infected with low MOI (0.1) and FACS-panning (3.6.1) was performed using ~ 4 x 10^7 cells for each of the three samples. The envelope genes of sorted cells (~ 1000 cells per sample) were recovered and cloned into pQL9 plasmids. The distribution of V3 variants during two rounds of selection were monitored by sequencing plasmids from single bacterial clones (one MTP) and performing Realtime PCR (RT-PCR) with plasmid preparations. The V3 envelope distributions were analyzed with samples directly before FACS-sorting (Input) and after the enrichment rounds (1^{st}, 2^{nd}). The amount of each V3 variant is shown as the count of identified single bacterial clones out of sequencing 94 clones (one MTP) and additionally by calculating the relative amount of every V3 variant in the respective plasmid preparations by RT-PCR (Fig. 3.19 – 22 A). RT-PCR reactions with primer pairs specific for each V3 variant (3.5.7) were performed in triplicates and the mean C_t (crossing point, also known as C_P) values were determined by the usage of the StepOne software (Life technologies corporation). The portions of V3 envelope variants (%) in a mixture of plasmids were determined by calculating relative amounts. Individual amounts of plasmids were calculated by the formula E^{-Ct} (E = Efficiency of PCR) for each V3 specific PCR. Subsequently, the portion of each V3 variant in a mixture was calculated in relation to the sum of all variants detected [213-215]. The total amounts of plasmids in each sample were calculated using a reference primer pair (3.5.7) that independently of the respective V3 variant amplifies a region on the plasmids used. To depict conformity of the used relative quantification method the relation of the calculated reference values to the sum of the V3 variants values are shown (%) (Fig. 3.19 – 22 B).

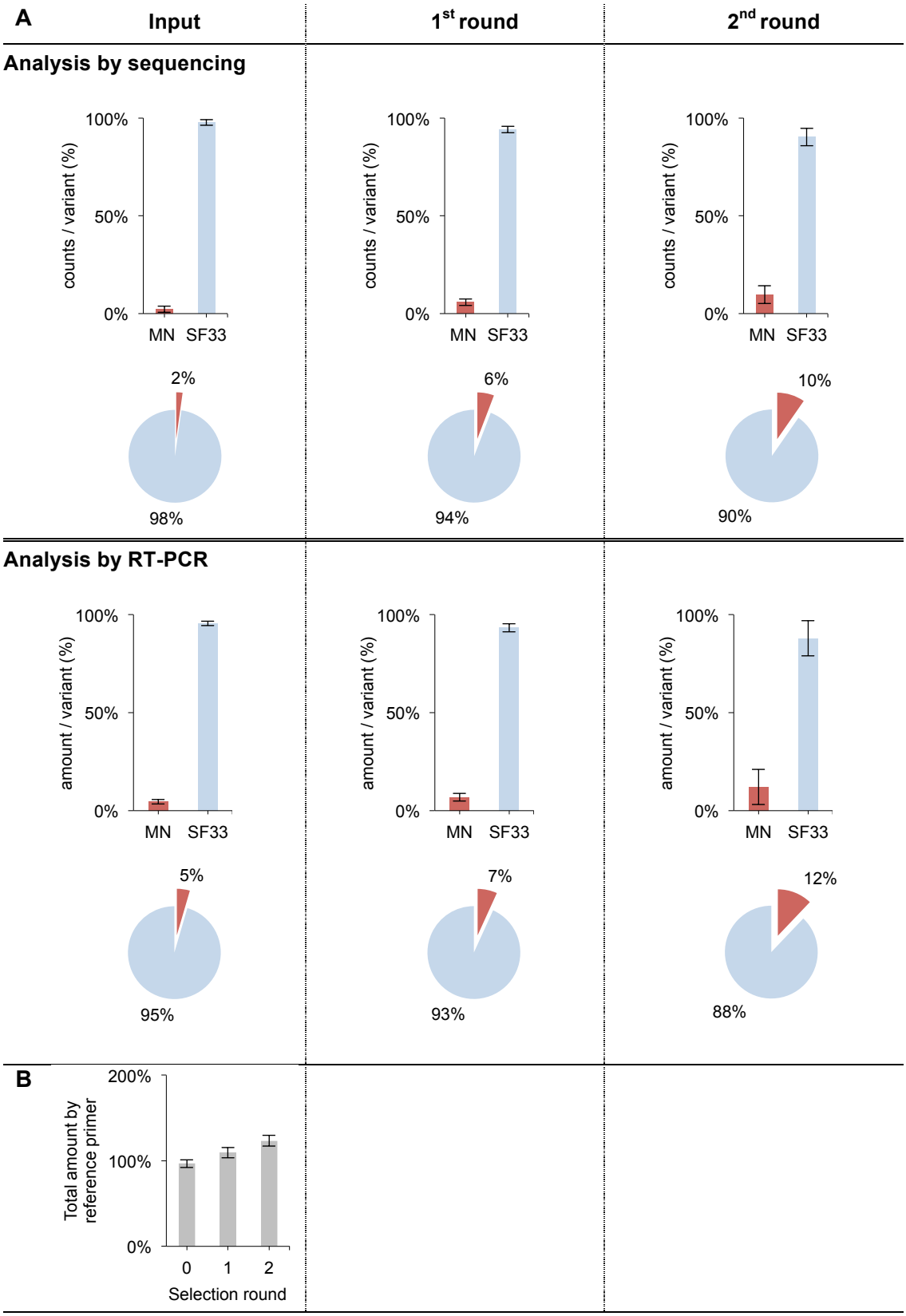

Fig. 3.19 FACS-panning-mediated enrichment of V3 envelope variants displayed on HEK293T cells
Description overleaf.

Fig. 3.19 FACS-panning-mediated enrichment of V3 envelope variants displayed on HEK293T cells

A pQL9 plasmid mixture of envelope V3 variants containing 5% MN and 95% SF33 was prepared. HEK293T cells (13 x 10^6) were transfected (pQL9-mixture, pTN pack, pVSV-G) to form an un-linked virus library. Fresh HEK293T cells (13 x 10^6) were infected with low MOI (0.1). The infected "linked" cells were applied to a FACS-sorting procedure 48 h after infection. The envelope genes were amplified from the genomic DNA of the collected cells, cloned into pQL9 and analyzed by sequencing and Real-time-PCR. Fresh cells were transfected with the new pQL9 mixture (together with pTN pack and pVSV-G) to produce new virus for Low MOI infection of fresh cells and to enter another round of selection. The mean values of two independent experiments are shown. **A** The relative counts (upper panels) or amount (lower panel) per variant of the input mixture, 1^{st} and 2^{nd} round are shown for analyzes by sequencing (one MTP) and RT-PCR (Efficiency^{-Ct} as % of each variant) respectively. **B** For every RT-PCR sample the total amount of pQL9 plasmids was probed. A reference primer pair was used that amplifies a sequence independent of the envelope gene inserted into pQL9.

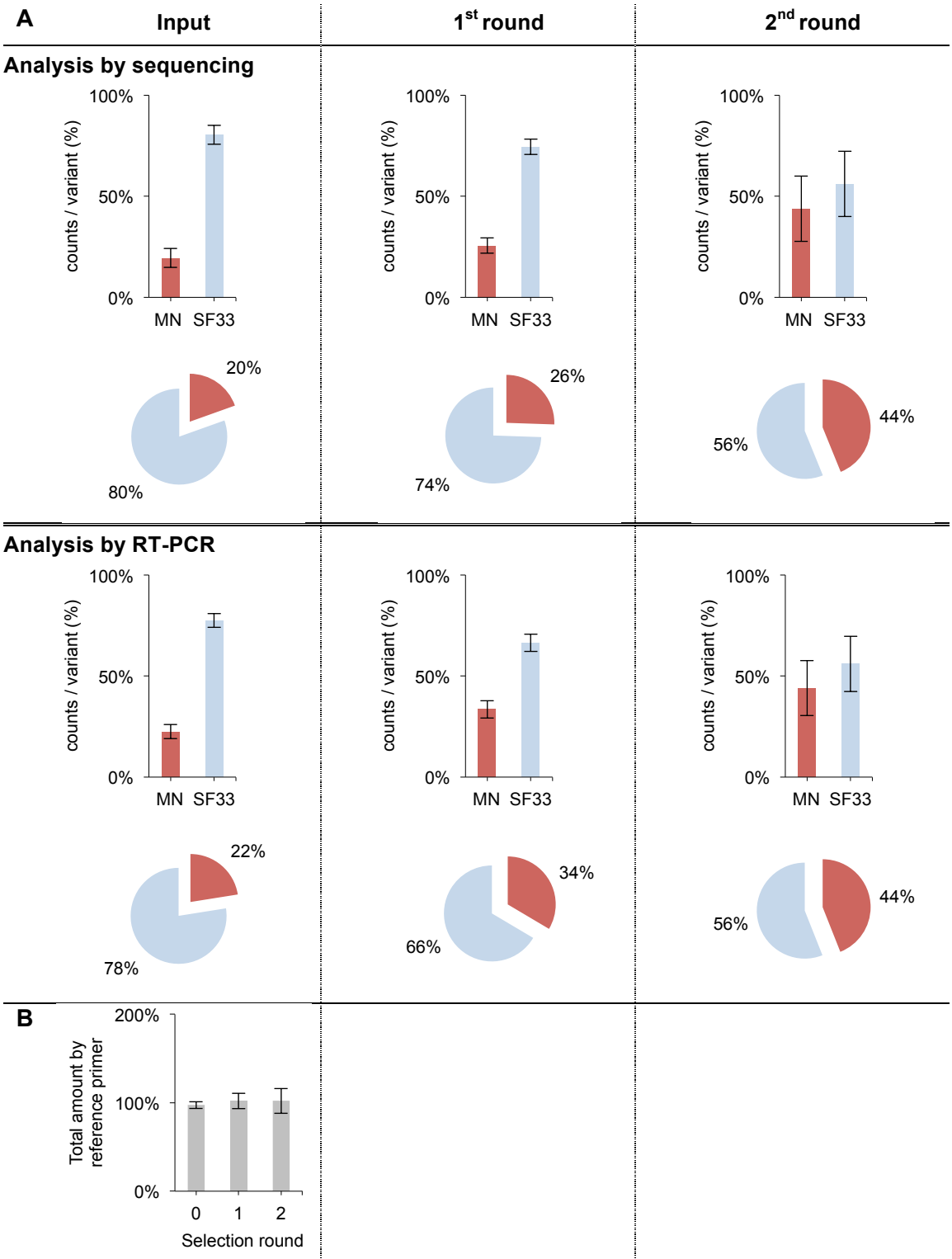

Fig. 3.20 FACS-panning-mediated enrichment of V3 envelope variants displayed on HEK293T cells

A pQL9 plasmid mixture of envelope V3 variants containing 25% MN and 75% SF33 was prepared. The Panning procedure was performed and results were calculated as described in Fig. 3.19. **A** The relative counts or amount per variant of the input mixture, 1st and 2nd round are shown. **B** Total amount of pQL9 plasmids.

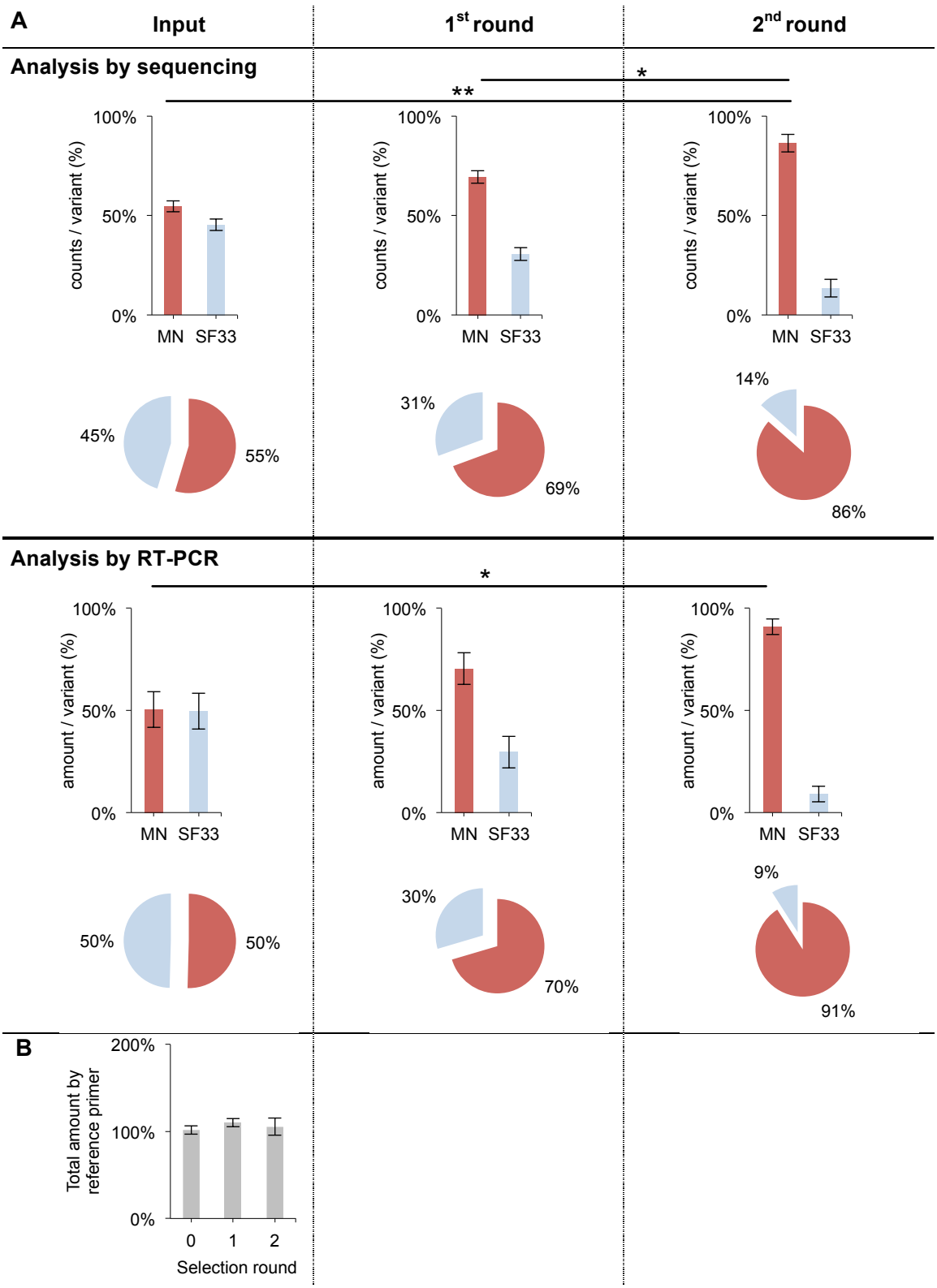

Fig. 3.21 FACS-panning-mediated enrichment of V3 envelope variants displayed on HEK293T cells

A pQL9 plasmid mixture of envelope V3 variants containing 50% MN and 50% SF33 was prepared. The Panning procedure was performed and results were calculated as described in Fig. 3.19. Statistics are calculated using the unpaired t-test or 1way-ANOVA followed by "Tukey's Multiple Comparison" test if groups were compared (* P<0.05; ** P<0.01; *** P<0.001). **A** The relative counts or amount per variant of the input mixture, 1st and 2nd round are shown. **B** Total amount of pQL9 plasmids.

The enrichment of the MN variant out of differently proportioned mixtures starting with 5% MN (Fig. 3.19), 25% MN (Fig. 3.20) and 50% MN (Fig. 3.21) could be demonstrated. Significant (*) differences were calculated either by an unpaired t-test if two columns in one group were compared or using the 1way-ANOVA test followed by "Tukey's Multiple Comparison Test" if columns between all groups were compared (* $P<0.05$; ** $P<0.01$; *** $P<0.001$). The mean values of two independent experiments are shown.

Within the panning targeted for an input value of 5% MN, at least a doubling of the amount of MN within 2 rounds was achieved. Both analysis methods showed a consistent increase of MN throughout the panning rounds as analyzed by sequencing (2%, 6%, 10%) and RT-PCR (5%, 7%, 12%). However, concerning both methods, no statistically significant enrichment was achieved, thus only a trend towards higher relative amounts of MN could be observed (Fig. 3.19 A). The trend for a higher deviation of the total plasmid amounts calculated relative to the sum of both individually detected plasmids throughout the panning rounds was noted (Fig. 3.19 B). This implies an increasing discrepancy to the V3 specific measurements and may explain the increasing standard deviation of the measured V3 values appearing in the second round.

During the panning starting with 25% MN, at least a doubling of the amount of MN within 2 rounds was achieved again. Both analysis methods showed a consistent increase of MN throughout the panning rounds as analyzed by sequencing (20%, 26%, 44%) and RT-PCR (22%, 34%, 44%). Again only an enrichment trend of the V3 variant MN is observable still lacking statistical significance, when comparing Input to first and second round (Fig. 3.20 A). The total amount of plasmid was calculated relative to the sum of both specifically detected plasmids and consistently resulted in values of ~100% throughout the panning rounds (Fig. 3.20 B).

Within the panning starting with 50% MN, a statistically significant enrichment of the V3 variant MN was observed as indicated. A consistent increase of MN throughout the rounds of panning, as analyzed by sequencing (55%, 69%, 86%) and RT-PCR (50%, 70%, 91%) was demonstrated. The trend of a doubling rate of MN within 2 rounds of panning was almost achieved again. A statistically significant enrichment of MN was obtained, when comparing Input to the second panning round as calculated for both analysis methods. Additionally, a statistically significant enrichment of MN was observed comparing first to second round, but remained restricted to the calculations of the sequencing method (Fig. 3.21 A). Moreover, the total amount of plasmids detected, consistently corresponded to the amounts detected by the specific V3 related primers (Fig. 3.21 B). This “proof-of-concept” study demonstrates the ability to

enrich a binding envelope at the cost of a non-binding envelope, by applying the FACS-based panning procedure.

3.6.4 FACS-panning using the complete V3-library

The complete V3 envelope library was screened with the FACS-panning procedure. A VSV-G pseudotyped batch of virus was produced by triple transfection (see 2.3.3) of HEK293T cells with a QL9 plasmid mixture (20% of each V3 variant), packaging- and VSV-G- plasmids. Subsequently, fresh HEK293T cells were infected with low MOI (0.1) and a FACS-panning (3.6.1) was performed using ~ 4 x 10^7 cells. The envelope genes of sorted cells (1300 ± 600 cells each round) were recovered and cloned into pQL9 plasmids. The distribution of the different V3 variants throughout the selection rounds are calculated and illustrated similar to the descriptions in section 3.6.3. The enrichment of the variant MN out of an equally proportioned mixture was proven. Significant (*) differences of V3 envelope amounts were calculated by the 1way-ANOVA test followed by "Dunnett's Multiple Comparison" test (* $P<0.05$; ** $P<0.01$; *** $P<0.001$). The mean values of four independent experiments are shown (Fig. 3.22).

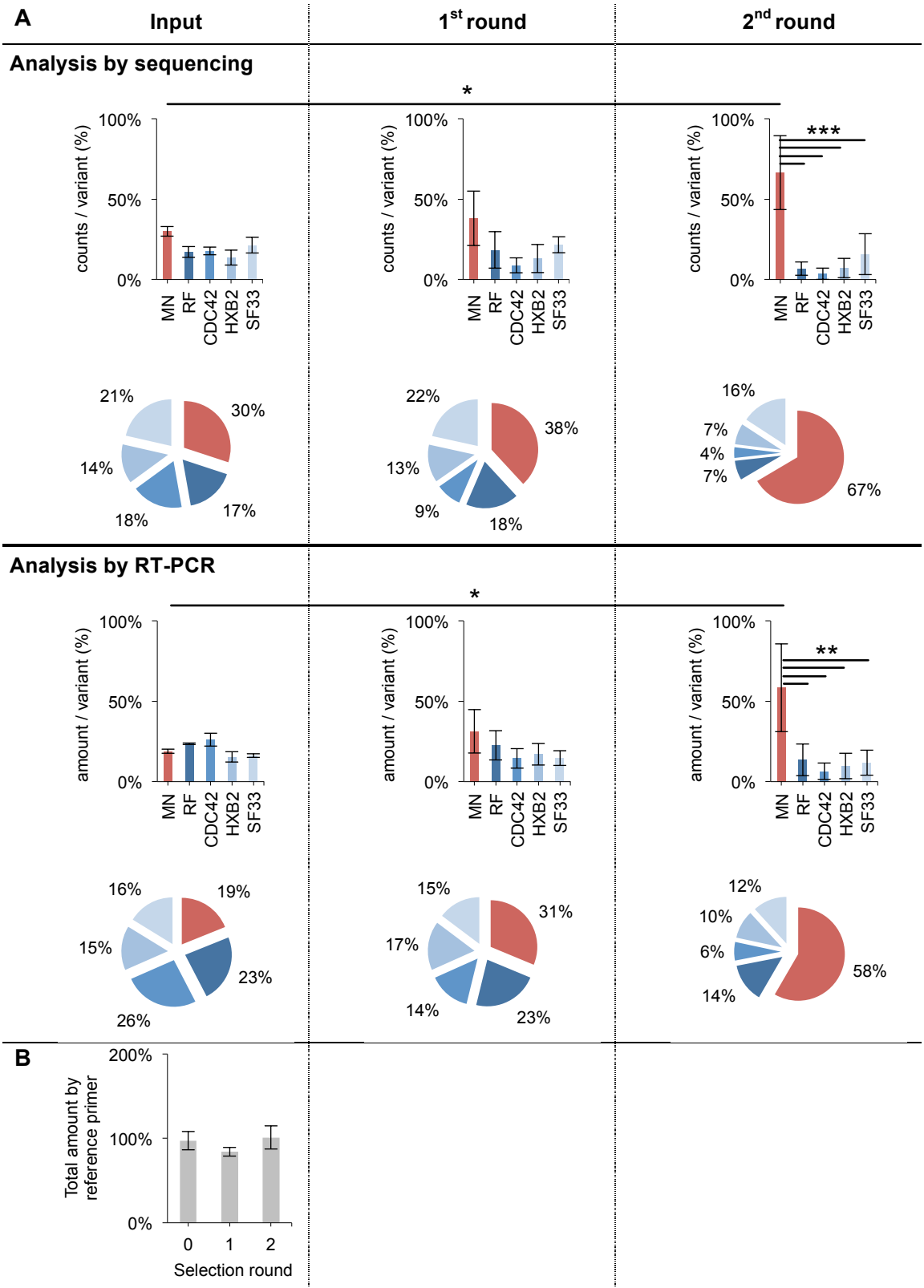

Fig. 3.22 FACS-sorting-mediated enrichment of V3 envelope variants displayed on HEK293T cells

A pQL9 plasmid mixture of envelope V3 variants containing equal amounts of MN, RF, CDC42, HXB2, and SF33 was prepared. The Panning procedure experiments were done similar to Fig. 3.19. Statistics are calculated using the one way ANOVA test and "Dunnett's" post test (n.s. P>0.05; * P<0.05; ** P<0.01; *** P<0.001). **A** The relative counts or amount per variant of the input mixture, 1st and 2nd round are shown. **B** Total amount of pQL9 plasmids.

The panning described above, aimed at an Input value of 20% for each Env variant. Roughly, a similar Input distribution of Env was achieved (Fig. 3.22 A, Input). Both analysis methods showed a consistent increase of MN throughout the rounds of panning as analyzed by sequencing (30%, 38%, 67%) and RT-PCR (19%, 31%, 58%). Thus, at least doubling the amount of MN within 2 rounds was achieved, consistently to the preliminary experiments shown in section 3.6.3. Comparing the rounds of panning as separate groups, MN was significantly enriched, as indicated for both analysis methods. Additionally, regarding the second round of selection, a significant enrichment of MN in relation to all other V3 variants was observed as indicated (Fig. 3.22 A). The total amount of plasmids (reference primer pair) was calculated relative to the sum of the individually detected V3 plasmids (specific primer pairs) throughout the rounds of panning. In every panning round nearby ~100% plasmid total amounts were measured, thus a consistent detection of all individual plasmids was proven (Fig. 3.22 B). With this extended "proof-of-concept" study the ability to enrich a binding envelope not only in presence of one non-binding envelope (3.6.3), but also in presence of various envelopes with distinct binding capabilities (3.5.5) was demonstrated. Taken together, the applied panning procedure resulted in enrichment rates of ~ 3-10 fold after 2 rounds of selection (Table 3.4).

Table 3.4 Enrichment of Env variant MN[a]
The specific enrichment of the V3 variant MN is calculated for each FACS-panning.

Panning		Ratio[a] of Env recovered after 2 rounds (%) / Env Input (%)		Fold enrichment[b]
		MN	Non-MN	
5% MN	(Fig. 3.19)	2.68	0.92	2.91
25% MN	(Fig. 3.20)	1.97	0.72	2.71
50% MN	(Fig. 3.21)	1.8	0.18	9.88
Library Screen	(Fig. 3.22)	3.09	0.51	6.01

a Only values obtained by Realtime PCR were considered
b Calculations were made according to the formula $\frac{Amount\ MN\ \#\ 2}{Amount\ MN\ \#\ 0} / \frac{Amount\ Non{-}MN\ \#2}{Amount\ Non{-}MN\ \#0}$ [149]
round of panning

The amounts of Env recovered after 2 rounds of selection in relation to Input amounts were summarized. An enrichment of ~3-fold was calculated for the panning procedures starting with 5% MN or 25% MN, and ~10-fold for the panning starting with 50% Input amounts of MN. The enrichment rate of MN as calculated for the model library screen is ~6-fold. Thus, the capability of the developed panning procedure to enrich the highest affinity Env variant was demonstrated, even in the presence of several competitive Envs such as the HXB2 variant.

3.6.5 Summary

A lenti-cellular display and FACS-panning procedure was designed and evaluated. A FACS sorting strategy was established by gating for single cells with average GFP expression (= envelope expression) and sorting by a triangle shaped gate for cells with a high 447-52D / GFP signal, allowing the sorting of high affinity Env variants. With proof-of-concept studies comprising different proportions of either binding- and non-binding V3 envelope variants, or the use of a panel of five V3 envelope variants with different affinities, the enrichment of a V3 variant (MN) with highest binding affinity towards 447-52D bNAb was demonstrated. Statistical tests approved that after two rounds of selection with the V3 library, a significant enrichment of the V3 variant MN was achieved ($P<0.05$).

4. Discussion

4.1 Development of a display and panning platform

It was shown that vaccination trials using monomeric Env [216] were inferior in eliciting presumptive correlates of protection [94] such as bNAbs or cellular immunity. Requirements of a proposed protective vaccine comprise both almost sterilizing antibody-mediated immunity, and rapid CTL-mediated elimination of infected cells [217]. Since bNAbs were discovered, the properties of their exact target sites have been subject to ongoing examination, and been used as a guideline for vaccine design efforts (reverse vaccinology) [108,120-125]. Therefore, optimally representing immunogenic bNAb epitopes, excluding non-neutralizing epitopes, and displaying distinct native states of Env, including quaternary epitopes, represent some of the desired properties of an ideal trimeric immunogen [218].

In this thesis, techniques were developed to identify HIV-1 envelope variants intended to be displayed in trimeric, membrane-bound states that bind with high affinity towards a given bNAb (e.g. 447-52D). The resulting “lenti-cellular display” and FACS-mediated panning procedures enable the selection of Env in a mammalian context, intended to display Env natively, and providing access to quaternary structures [219]. Existing, well-established display and selection techniques such as phage display [130], retroviral display [149] and others [144] were considered, and the overriding strategy was adapted to be consistent with the proposed requirements of a trimeric, membrane-bound state of Env.

4.1.1 Viral display and panning (AIO-platform)

The already described [149] avian leukemia virus (ALV) display is based on chimeric envelope proteins. In the proposed HIV-1 library, Env variants are intended to be displayed in a mostly native state to ensure proper access to bNAb binding sites. Therefore, the obvious method of choice to display such Env variants, considering the criteria above, was using the HIV-1 virus itself. In close analogy to the ALV display method [149] (see 1.6), a technique was designed based on HIV-1 (AIO; see 3.2.1). The NL4-3 derived proviral vector pTN7stop was chosen as a basis for developing pTN-AIO, since it was already proven to form replication competent, but Env negative virions. Furthermore, it expresses an integrated reporter protein (*R.Luciferase*), which was considered a suitable integration site for a prospective Env library. Therefore, two further modifications were made: (I) enhancing the expression level at the reporter site

by integrating a Kozak consensus sequence upstream of the reporter protein; and (II) integrating another reporter protein (HSA) into the ORF of vpr, which becomes incorporated into the cellular membrane [186,187]. Thus, infected cells were easily detected by anti-HSA antibody staining (Fig 3.4 A).

Besides the detection of infected cells, HSA should enable potential virion and cell precipitation or enrichment assays. Despite initial successful steps in developing the AIO platform, in terms of detection and replication of AIO-HSA (see 3.2.1-3), only unsatisfactory amounts of virus bound to immobilized antibody were recoverable (~1-2 %, 5-10 x 10^3 particles). Therefore, any proposed Env library would be limited to the number of virions that can be bound. The variability of a prospective library of Env variants would have to be limited in order to ensure proper representation of each variant. Usually over-representation of approximately 20-fold is estimated to reach 95% statistical confidence of screening every variant at least once [220]. Hence, the efficacy of a library screening method strongly depends on being able to represent the variability of a library several-fold [221,222].

Despite testing several conditions, only low amounts of virions were regularly captured. Since the produced batches of virions were found to be infectious, and therefore stable over a usual range (5 x 10^3 TU/ng p24) [190], a loss of stability is thought to occur during the panning procedure. Several incubation and washing steps are applied during panning and may lead to unspecific disruption of virions applied. Despite these problems, increasing stringency of washing conditions is required to efficiently enrich the strongest binders [223]. Enhancing the amount of bound HIV-1 virions was not possible, and simply scaling up the amounts used is uneconomical, as well as technically limited.

As an alternative to using virions, cellular display was considered as the basis for developing an Env display system. HEK293T cells, which were formerly used to produce HIV-1 viruses, were considered to meet the proposed requirements for Env display, especially since these cells have been used for cellular display purposes [138,139]. Thus, the AIO-platform was abandoned in favor of a cellular display technique. To enable thorough testing of the conditions needed for successful screening, a model Env library and corresponding bNAb partner were selected.

4.1.2 An HIV-1 envelope V3 library to adjust panning parameters

The well-characterized bNAb 447-52D [113,117,191] was chosen, since former experiments of Gorny et al. [117] using V3 peptides from different HIV-1 strains, resulted in distinct binding patterns with different Kd values. It was therefore likely that different V3-bearing Env variants would be bound by 447-52D antibody in a manner that allows discrimination by affinity. The complete V3 region of a 96ZM651-derived gp145 Env (see 3.3) was exchanged by the V3 regions of the mentioned isolates with different Kd values towards 447-52D. After transient expression in 293T cells, binding by 447-52D antibody was tested. Interestingly, the cellular-based membrane-bound Env binding pattern (for variants RF, CDC42, HXB2; Fig. 3.6) differed from the reported peptide-based binding pattern, with the exception of the best binding (MN) and non-binding (SF33) V3 variants.

Considering that a peptide-based assay differs greatly from a cellular-based assay, the observed discrepancy is not unexpected. Since there are many putative structural or steric differences in accessing epitopes on peptides compared to membrane-bound Env, neither a reproduction, nor the exact binding profile was anticipated, or needed. Furthermore, different readout strategies were used to determine a binding pattern. The peptide-based assay used a modified ELISA technique [117,224] to calculate specific Kd values, whereas the cellular-based FACS assay compared MFI values. However, the 447-52D antibody binding pattern obtained for cellular-based, membrane-bound Env was considered a feasible challenge for a panning procedure aiming to enrich the best 447-52D antibody binding Env variants.

4.1.3 Cellular display and MACS-mediated panning

Since Env is expressed and integrated into the cellular membrane prior to the budding of virions (see 1.2), cellular display probably also closely mimics the properties of a membrane-bound, trimeric Env. Although viral-based display theoretically has the advantage of representing greater variabilities in small volumes (~10^7 TU/mL), this was confounded by the massive loss (98-99%, see 3.2.4) of particles during the panning process. Cellular display, in comparison, is rather more restricted in terms of propagating practicable clone numbers (e.g. 10^4 - 10^6 infected cells, see 3.4.3, 3.6), but has superior performance in terms of sufficient recovery and reliable analysis after the enrichment steps (see 3.4.2). Since the MACS system is a widely used application for enriching fragile and rare cells [225,226] the recovery rates for positive cells were adequate (Fig. 3.8). Although initial separation experiments (Fig. 3.9. A) showed

successful enrichment of binders according to the previously determined binding pattern, this was only true in the case of separately transfected cell mixtures. In other words, MACS panning succeeded if cells were transfected separately, each with one of the V3 variants of the model library, and subsequently mixed in a 1:1 ratio, but failed if cells were transduced with a mixture of V3 variants. Even an attempt to mimic conditions of separately transfected cells by using low MOI infections (according to 5F3 staining, see 3.4.3), ensuring phenotype and genotype linkage, failed with non-specific enrichments (see Fig. 3.10).

To explain these findings, potential drawbacks were hypothesized: (I) If cells express and display Env in different amounts, MACS may mediate selection in favor of a higher level of expression (avidity), instead of the intended higher affinity of Env. (II) An underestimation of the 5F3 antibody determined low MOI would have resulted in an unlinked-library display, and consequently similar failure in selecting the strong binder, as has been documented. However, neither hypothesis was assessable within the MACS system, which is rather like a “black-box” in terms of having no option to adjust selection parameters, such as distinct expression levels of Env during the selection process. Furthermore, the viral vector used so far, lacks a separate marker gene. Thus, MOI and display of Env on cells were determined jointly by staining Env on infected cells using the antibody 5F3 in a FACS based readout in separate samples. Therefore, the precision of determining low MOI depended on the accuracy of 5F3 antibody staining all infected cells (% pos. cells). If cells were infected and expressed Env that is disrupted in terms of 5F3 antibody binding, the determined MOI would be biased. To disconnect determining the MOI from the antibody 5F3, new viral vectors (Table 3.3) were developed, bearing a separate marker gene (GFP) to instantly determine the MOI after infection of cells.

4.1.4 QL viral vector development

During the design of viral vectors, a more convenient strategy for the cloning of Env library genes was introduced. The “QL” (Quick-Ligation) procedure involves using the Esp3I restriction enzyme (Typ IIS) and CcdB [168] selection marker (see Fig. 3.11). A conceptually similar technique was recently applied for a cloning vector called pINITIAL by Geertsma et al. [167]. Correspondingly, using a Typ-IIS restriction enzyme together with standard T4 ligase enabled a one-step restriction and directed-ligation reaction. Moreover, with QL-mediated cloning the CcdB marker gene, which is toxic for the DH10B *E.coli* strain used, ensured reliable growth only if Env successfully

substituted CcdB. Taken together, the QL procedure simplified (one-step) and therefore improved the ligation and cloning process of Env genes (see Fig. 3.11). Another desired feature was using a marker (GFP) for infection that is directly encoded on the viral vector and easy to detect. Thus, the MOI can be determined independently of an indicator cell line or staining with an antibody.

It required several approaches (see 3.5.2) to successfully implement GFP as a separate marker gene into the viral vector that reliably indicates a transformed cell. Two criteria had to be met: First, expression of GFP had to be independent of the cloned Env gene (Fig. 3.12 A). Second, expression of both the Env V3 variant MN bound by 447-52D antibody and a similar signal of GFP corresponding to the amount of positive cells (%) was desired (Fig. 3.12 B). Interestingly, only the pQL variants that encoded the GFP marker upstream of Env (pQL9 and 11) successfully passed the selection criteria. All other variants were either almost undetectable, or positive only for GFP or Env, or GFP expression decreased drastically once Env was expressed from the same vector. Those effects were not the subject of further experiments, but might be due to promoter interference as demonstrated by Curtin et al. [227], when heterologous promoters were used (pQL2, -3, -4, see Table 3.3). Although Curtin et al. particularly chose the widely used promoters CMV in combination with EF1α, they hypothesized that interference between heterologous promoters occurs relatively often.

Consequently, an IRES site was explored in subsequent pQL vectors (pQL5 – 10, see Table 3.3). Since lower IRES-dependent second gene expression is known in many cases [228], various pQL designs were made in order to express Env as the first gene and the known strong fluorescent GFP as the second gene. Interestingly, when Env was successfully expressed, these vectors (pQL5, 7, 8, 10; see Fig. 3.12) mediated a consistently strong reduction in detectable GFP positive cell numbers, instead of the proposed tolerable decrease in GFP (second gene) expression strength.

Eventually, the switch of gene positioning accomplished in the vector pQL9 resulted in homogenous expression of both GFP (first gene) and Env (second gene). The particular effect was not the subject of further experiments, but is consistent with prior studies, which have shown that the expression of the gene downstream of IRES inconsistently depends on the first gene sequence upstream of IRES [229,230]. Thus, GFP was successfully expressed if positioned as the first gene and a model Env library with differing sequences as the second genes (see Fig 3.12 C/D). Besides, the varying, unpredictable influence on the second gene expression mediated by different gene sequences located at the first position was excluded, since GFP would be constantly used at this critical first position.

Another homologous GFP and Env expressing vector was developed, pQL11, by introducing the TaV (Thosea asigna virus) p2A peptide. Where p2A sequences occur within an ORF, the formation of the peptide bond at the C-terminus of (each) 2A does not occur. Thus each protein is stoichiometrically produced as a discrete translational product [206]. For this widely used type of peptide sequence [206,231] it was shown that genes containing an N-terminal signal sequence can inhibit the functionality of p2A sequences, if positioned as the first gene [232]. Thus, Env was again positioned as the second gene to avoid any possible interference (see Table 3.3).

Since pQL9 was constructed earlier than pQL11, it was chosen as the standard viral vector in the following experiments. After the V3 Env library had been cloned into QL9, determining the MOI using GFP and 5F3 antibody was compared following transfection or infection. The ratio of positively stained cells using 5F3 antibody versus GFP should ideally be 1:1, due to a QL9-carrying cell (GFP^+) expressing GFP as well as Env. This was nearly achieved after transfection (Fig. 3.12 C), but not after infection (Fig. 3.12 D) with any of the QL9 variants.

In fact, this was the first strong evidence supporting the proposed underestimation of low MOIs determined (see 3.4.4 / 4.1.3) by the antibody 5F3 in earlier experiments (see 3.4). For clarification, a separate experiment was performed using cells either transfected or infected with the QL9-MN variant. Both batches of cells were analyzed for the expression of GFP as well as staining of Env using 447-52D (positive control), 5F3 and HJ16 antibodies. No differences in cells assessed as positive were observed for cells that had been transfected (Fig. 3.13 A). However, in the case of infected cells, it was confirmed that using the 5F3 antibody had led to an up to 10-fold gap between the accuracy in determining the number of positive cells (%) compared to the 447-52D antibody (Fig. 3.13 B). This means a desired low MOI of 0.1 calculated using data obtained from 5F3 antibody staining, was actually a MOI of 1. According to the Poisson distribution (see 5.3) this is equivalent to 37% uninfected, 37% singly infected and 26% multiply infected cells.

The accuracy gap was only detectable in the case of infected cells and not after transfections, which is most likely due to a much higher level of Env expression in transfected cells (22-fold, see 3.5.3). Such a high level of Env expression probably overburdened the host furin-protease processing, resulting in a higher amount of uncleaved Env [233-236] displayed on transfected cells. As it was shown that antibodies directed against gp41-epitopes bind more strongly to uncleaved Env [237,238], this effect could have contributed to the transfection- / infection-dependent binding accuracy of the gp41-specific 5F3 antibody.

Nevertheless, it was clearly shown that the 5F3 antibody-based determination of the MOI was strongly biased. Therefore, a high number of multiply infected cells had probably contributed to the failure of enrichment using MACS Panning (Fig 3.10).
However, according to the performance of GFP as a marker for transduction, further experiments confirmed a stable correlation of GFP and Env, also in terms of expression levels (MFI) (see Fig. 3.14). Thus, GFP was validated as a marker for both, transduction and Env expression. Therefore, the second proposed vulnerability of MACS-panning (see 3.4.3), namely cells with different expression strength of Env were not discriminable, has been solved as long as FACS analysis is used. Notably, the correlation of GFP versus Env expression (MFI) may only be valid for the V3 model library used, and might differ for prospective larger libraries, which probably contain more distinct as well as possibly disrupted Envs.

4.1.5 Basic conditions for a QL9-based V3 library panning

Parameters for an optimal binding of the 447-52D antibody, concerning the discrimination between the different V3 variants after a low MOI infection were experimentally determined. The resulting characteristic binding pattern (Fig. 3.15) was similar to earlier experiments (Fig 3.6 B) using transfected cells. Critical parameters, which probably unspecifically bias the panning procedure, were thought to be located at the amplification-steps of library processing. Therefore, the growth rates of transformed bacteria and the PCR reactions amplifying the complete Env gene were probed for differences in the performance between each V3 variant used (3.5.6. / Fig. 3.16 B). Many factors, such as plasmid sequence, medium, temperature, rpm and production vessels (here MTPs) can influence the bacterial doubling-time [239-242]. Therefore, it was not unusual to result in 78 ± 4 min, compared to a frequently suggested 30 min doubling-time, which is only achievable under ideal conditions [243]. However, consistently equal bacterial growth-rates, plasmid DNA yields, plasmid genetic stabilities and PCR efficiencies for each V3 variant were documented and constituted a promising basis for the development of an unbiased panning procedure.

4.1.6 Quantification of enrichment by sequencing and Realtime PCR

The enrichment of V3 Env variants harvested in each round of panning was evaluated by cloning the Env genes of an isolated fraction of cells into an appropriate plasmid. Subsequently, transformation of bacteria, propagation of single bacterial clone cultures and finally sequence analysis of several bacterial clones (see 2.1) were performed. This procedure was intended to work within an acceptable level of accuracy, as each clone was precisely assigned to one of the V3 variants according to its sequence. On the other hand, this method represents a tedious procedure, as all clones were manually maintained. Thus, this procedure was practically limited in the sample size of clones that were analyzed, and therefore resulted in an overall statistical accuracy of ± 10 % (see 3.5.7). A second analysis tool based on Realtime PCR was established, allowing to analyze a mixture of plasmid DNA at once (Fig. 3.16 C). The applied Realtime PCR approach was specifically designed for the usage in the context of the developed model V3 library. It is not intended to be, in that arrangement, a manageable method for any proposed larger Env library comprising a great variety of sequences. Other techniques such as the comparison of DNA fragment patterns during several panning rounds, received after the digestion with a restriction enzyme ("fingerprinting") would be more reasonable in such a case [131].

Specificity was proven, using manually compounded QL9 V3 library plasmid mixtures. Adept primer design allowed performing Realtime PCR reactions, which exclusively amplified one desired V3 variant in such a mixture. When the desired variant was absent, no or only late (Cycle > 30) unspecific signals were detectable. Since the amounts of DNA used in the analyses of panning rounds are about 100-fold less, the unspecific signals are supposed to rise at even later cycles (Cycle > 40), and were considered negligible. Thus, the theoretical sample size depicted by the calculated number of plasmids per ng DNA was dramatically increased, and the statistical accuracy was improved up to ± 0.05 % (3.5.7). Moreover, Realtime PCR is less time-consuming than sequencing. Asides, assembling several Realtime PCR reactions turned out to be less tedious than picking and processing several hundred bacterial clones.

Hence, the high consistency of the Realtime PCR results, compared to the clonal sequencing analyses, provided a crucial contribution to the validity of the obtained V3 library panning results (see 3.6).

4.1.7 FACS-mediated panning

As discussed in section 4.1.3, several drawbacks were mentioned, which potentially circumvented a successful, specific enrichment of V3 variants using the MACS-panning. Some of these, such as the determination of MOI and the correlation of Env presented on cells, were solved with the implementation of the marker gene GFP. One particular issue mentioned earlier (4.1.3), was a general drawback, appearing with the usage of MACS, namely the “black-boxed” process of MACS-separations itself (see Fig. 3.7/ 8). Particularly, adjusting parameters to compensate avidity effects, triggered through varying amounts of displayed Env, was not possible. Thus, the complete MACS-mediated selection was switched to a FACS-based selection of cells. The improvement made with this decision was mainly constituted in taking the control of the selection process on a single cell basis. The combination of a consecutive gating strategy, seeking for living, singly and GFP positive cells, and a triangle shaped sorting gate, ensured the selection of high 447-52D binding cells (see Fig. 3.18). As GFP was shown to correspond with the expression level of Env, the triangle shape of the sorting gate was a tool to discriminate between avidity and affinity effects. It was aimed not to select for highly expressing cells (avidity effect) with the highest signals in general, but to select for a higher ratio of antibody signals in relation to the level of Env expression (affinity effect).

In contrast to the previous experiments made with MACS, Input mixtures of cells as well as the mixtures of following rounds, were produced in the same manner. Therefore, a two-step process facilitating the linkage of phenotype and genotype was applied: (I) The plasmid DNA mixture of V3 variants was transfected jointly with packaging and VSV-G plasmids to produce virus particles, (II) Low MOI infections with these viruses were made to generate singly infected cells. Utilizing such a procedure already for the first round of panning depicts a realistic scenario, as any proposed large library (> 1x 10^3 variants) of Env would not be generated as single plasmid clones, but as a mixture of plasmids. Simulating such realistic conditions, the challenging probability of undesired multiple infections could be present alongside the first infection of cells. However, a valuable evaluation of the FACS-panning system was only feasible by using a realistic scenario.

Preliminary panning experiments were made to demonstrate that in principle the discrimination between at least two V3 variants is possible. Therefore, one binding (MN) and one non-binding (SF33) variant were chosen as a minimal model library for a panning procedure (see 3.6.3). Three different ratios of MN/SF33 infected cells were chosen as Input mixtures to evaluate the performance of separation within two rounds

of panning. Both, the 5 % and 25 % MN leveled Input mixtures, showed a consistent trend of a ~3-fold enrichment of MN cells throughout two rounds of panning (Fig. 3.19/ 20). Asides a nearly ~10-fold enrichment of MN, the first statistical significant enrichment was achieved using 50% MN Input mixtures (see Fig. 3.21).

Taken together, considering the relation of enriched MN to depleted SF33 variants an overall enrichment rate of up to ~10-fold after 2 rounds (#) of panning was achieved (see Table 3.4). The calculations are based on the formula $\frac{Amount\ MN\ \#\ 2}{Amount\ MN\ \#\ 0} / \frac{Amount\ SF33\ \#2}{Amount\ SF33\ \#0}$ = x-fold enrichment of MN [149].

4.1.8 FACS-panning: V3 library screening

The complete V3 model library, consisting of five V3 variants representing Envs with different 447-52D binding capacities (see 3.5.5), was screened by the FACS-panning procedure (see 3.6.4). The complete procedure was performed analogously to preliminary experiments, in which two V3 variants were used (see 3.6.3). The Input mixtures were generated with viruses produced by mixtures of the QL9 based V3 library (see 2.3.3), resulting in an overall even distribution of ~1:1 for each V3 variant, with only slight differences depending on the analysis tool used.

After the first round of selection a small trend in favor of MN was measurable, which continually rose to a statistically significant enrichment of the V3 variant MN after the second round of panning. Notably, the enrichment of the desired variant MN was strongly significant ($P < 0.01$) in relation to any other depleted V3 variant after the second round of panning. An overall enrichment rate of 6-fold was achieved as calculated by the formula previously discussed (4.1.7), but using the amount of all non-MN Env variants instead of SF33 only (see Table 3.4). Thus, the enrichment rate is within the same range as achieved by preliminary experiments (see 3.6.3/ 4.1.7), although more competitive Env variants for the binding to 447-52D were present.

These encouraging results suggest that with the FACS panning procedure a successful screening of larger Env libraries is feasible.

The only similar lentiviral display system published so far, is represented by that of Taube et al. [139]. They used bivalent scFv antibody fragments fused to gp41 and presented them on virions as well as on HEK293T cells. By performing a combined selection of a first magnetic-bead and second FACS-sorting step, the authors claimed to reach a 10^6-fold enrichment between a binding and non-binding mixture of cells. Besides some similarity according to the approach for the selection of cells, Taube et

al. strictly produced both examined variants as separate virions, and performed infections separately. Thus, this strategy probably suffers from the already discussed drawback of having an artificially complete separation, which most likely depicts enrichment factors that only apply for artificial conditions. Furthermore, the described combination of MACS with the selection of high level expressing cells by a subsequent FACS-sorting procedure, most likely promotes avidity instead of affinity effects (see 4.1.3/ 4). Therefore, their approach was sufficient to discriminate between two strongly differing binders, as demonstrated in the study of Taube et al. and similar to the results obtained with MACS-panning in this thesis (3.4.2). Actually, the limitations in using only separately infected cells, as well as the sorting of mixtures containing more than two variants, was resolved by the FACS-panning procedure described in this thesis.

Interestingly, the enrichment of MN in relation to other Env variants (e.g. HXB2 or SF33) was not as efficient, as separately detected binding capabilities had suggested (Fig. 3.18 C). This may be due to possibly unfavorable, but inevitable circumstances caused by the mixed virion production, in order to create the desired realistic scenario of panning: (I) Since a two-step process was applied to generate a phenotype and genotype linkage (see 3.6), in the first, unlinked step a mixture of pQL9-V3 variants is used for the production of virions, which embeds two RNA^+ strands (see 1.2). Therefore, a chimeric genome of MN joined with e.g. SF33 RNA might be formed. It has been shown that predominantly only one copy of the viral genome gets integrated [244], while more than two copies lead to apoptosis [245]. Thus a negative effect, caused by multiple integration events and a decreased efficiency of the linkage of phenotype and genotype seemed limited. Nevertheless, strictly isolating MN variants might therefore be delayed; (II) Subsequently to the mixed transfection, virions are purified from cell-culture supernatant by ultracentrifugation, leading to aggregation due to their high local concentration [246]. Thus, multiple infections of cells are imaginable, even though low MOI (0.1) conditions are applied to achieve only singly infected cells (see 5.3). Although equal limitations for the integration of more than one copy would apply as described for the first step, an influence on the efficiency of the selection process remains possible. In order to assess these possibilities in more detail, a second QL9 based virus, bearing DsRed [247] instead of GFP would be of worth. A mixed production of virus and low MOI infection as described for the panning procedure might be performed. Subsequently, FACS analysis might provide information to the distribution of multiple integration events by separating infected cells according to green, red or yellow (green+red) fluorescence; (III) Aggregates of cells were observed after infection and to some extent dissipated using a cell strainer prior

to the sorting procedure (see 2.3.8). Therefore, a more stringent single cell gating strategy, or the use of cells adapted to suspension growth might be due; (IV) An overall sorting efficiency of only 50%, as calculated from the number of sorted events / (sort conflicts + sorted events) x 100, provided by the FACS-Aria software (data not shown), was observed. Particularly, FACS-sorting may be improved for the selection of single cells by further straightening the gating strategy, lowering the concentration of applied cells, optimizing the flow-rate of cells or trying to apply alternative cell-types that are known to be less sticky (e.g. HEK293F). Though, the specific parameters that have caused sorting conflicts remained inaccessible, further efforts in order to increase the sorting efficiency could be worthwhile.

In prospective experiments the FACS-panning might be challenged by using libraries of larger diversity for the selection of Env variants featuring the desired bNAb-inducing properties.

4.2 Conclusion

A mammalian cell display and panning platform was developed and evaluated in this thesis. The ability to enrich an HIV-1 Env variant with the highest affinity to an applied antibody in the context of four, less strongly binding Env variants, was successfully demonstrated. Thus, when searching for an Env with optimal binding capacities to an applied bNAb, the FACS-panning platform provides a tool to screen libraries of trimeric, membrane-bound Env variants.

4.3 Outlook

Although a proof-of-concept was shown for the FACS-panning procedure, several issues still remain to further improve the procedure. The diversity of any proposed library to be screened is restricted to the number of cells that can be screened at once, which depends on the instrument and parameters chosen (FACSAria, up to ~70,000 events / second). For the FACS-panning procedures in this thesis acquisition rates of 10,000 events / second were applied. Therefore, efforts should focus on efficiently increasing the number of cells that can be used for FACS sorting. Particularly, using cells that can be propagated in much higher concentrations, such as HEK293F, as well as evaluating the highest possible acquisition rates for FACS sorting, as long as single cell populations and purity are not decreased, could be worthwhile.

The lenti-cellular display and FACS-mediated panning developed in this thesis offer a unique solution for bNAb-dependent, affinity-triggered enrichment of Env. Further experiments aiming at isolating unknown Env variants that are able to re-elicit bNAbs (reverse vaccinology) [122] will involve using larger libraries of Env, as well as several bNAbs.

In addition to simply seeking for an affinity-enhanced Env, neutralization-relevant, conformational states of Env will possibly be accessible by addition of cellular binding partners of Env, such as CD4 or the co-receptors CCR5 or CXCR4. As mentioned in the Introduction (Fig. 1.2) binding of CD4 induces conformational changes in Env, enabling the viral entry process, which can be blocked by several bNAbs. It will be part of future experiments to learn whether it is possible to screen for a specific Env conformation that is preferably bound and then blocked or locked [44] after bNAb binding. Therefore, isolating such Env transition state conformations would depict interesting candidates for a vaccine that may be able to elicit blocking and therefore neutralizing antibodies.

Besides HIV-1, the developed panning platform is proposed to work with other proteins. As demonstrated by e.g. Taube et al. [139], presentation of proteins such as scFv antibody fragments was successfully performed using a similar procedure. Generally, all proteins capable of being expressed and integrated into a cellular membrane are likely to operate within the developed panning platform.

5. Appendix

5.1 Abbreviations

If not stated otherwise, common abbreviations follow recommendations from the Chicago Manual of Style [248], the Gold Book of IUPAC [249] and the White Book of the Joint Commission on Biochemical Nomenclature (JCBN) [250]. References were cited following the recommendations of PloS ONE [251].

Ab	antibody
AIO	All-in-One
ALV	Avian Leukosis Virus
ART	anti-retroviral therapy
Amp	ampicillin
APC	Allophycocyanin
ATCC	American Type Culture Collection
BCR	B-cell receptor
bNAb	broadly neutralizing antibody
bp	base pairs
BSA	bovine serum albumin
CA or p24	capsid protein
CCR5	chemokine receptor type 5
CD4	cluster of differentiation 4
HR	heptad repeat
CIP	calf intestine phosphatase
(h)CMV	(human) cytomegalovirus
CT	Cytoplasmic tail
C_t	Cycle threshold
CTL	cytotoxic T lymphocyte
CXCR4	chemokine receptor type 4
DC	Dendritic cell
DMEM	Dulbecco's modified Eagle's medium
DMR	aa D474, M475, R476 of HIV-1 Env
DMSO	Dimethyl sulfoxide
ds	double strand
DTT	Dithiothreitol
EDTA	Ethylenediaminetetraacetic acid
ELISA	Enzyme-Linked Immunosorbent Assay
Env	envelope protein
Fab	Fragment antigen binding
FACS	Fluorescence-Activated Cell Sorting
Fc	Fragment, crystallizable = constant antibody region
FCS	fetal calf serum
FP	Fusion peptide
g	relative centrifugal force
Gag	group-specific antigen
gDNA	genomic DNA
GFP	Green Fluorescent Protein
gp41	glycoprotein of 41 kDa = HIV transmembrane protein
gp120	glycoprotein of 120 kDa = HIV surface protein
gp145	glycoprotein of 145 kDa = HIV envelope precursor protein with truncated CT
gp160	glycoprotein of 160 kDa = HIV envelope precursor protein
HA	Hemagglutinin, or shortly for HA-tag
HEK293T	human embryonal kidney cell line 293T
HeLa	human cervix carcinoma cell line
HIV	Human Immunodeficiency Virus
HRP	horseradish peroxidase
ID	immunodominant
IVS	Intervening sequence
IRES	Internal Ribosomal Entry Site
kb	kilobases
LANL	Los Alamos National Laboratory
LB	Lysogeny Broth medium
LTR	long terminal repeat
MACS	Magnetic Cell Separation
MCS	multiple cloning site
MFI	mean fluorescence intensity
MLV	Murine leukemia virus
MOI	Multiplicity of infection
MPER	membrane-proximal external region
mRNA	messenger RNA
MTP	Microtiterplate
NAb	neutralizing antibody
Nef	Negative factor
PBS	Phosphate buffered saline
PE	Phycoerythrin
PEI	poly-ethylenimine
Pol	Polymerase, or polymerase precursor protein
poly(A)	polyadenylation site
RT-PCR	Realtime PCR
RLU	relative light units
RLuc	*Renilla* luciferase
rpm	revolutions per minute
scFv	single-chain variable fragment
SDS	Sodium dodecyl sulfate
SIV (mac)	Simian Immunodeficiency Virus (of macaque)
Tat	Trans-Activator of Transcription
TB	Terrific Broth medium
TM	transmembrane region
Tris	tris(hydroxymethyl)aminomethane
TU	Transfducing Units
TZM-bl	HeLa-cell derivatives expressing CD4, CXCR4, CCR5 and Tat-inducible RLuc and β-Gal
U	Unit
vif	viral infectivity factor
VLP	Virus-like particle
vpr	viral protein R
vpu	viral protein U
VSV-G	Viral Stomatitis Virus Glycoprotein
WPRE	Woodchuck Hepatitis Virus Posttranscriptional Regulatory Element
wt	wild type
x	fold, in terms of multiplicity

5.2 DNA

5.2.1 Oligonucleotides

ID	Name	Sequence 5'→3'
	All-in-One	
1D1	KpnI-mut fwd	CCGTCTATTATGGGCTACCTGTGTG
1H2	THB_env_FseI-Kozak-NcoI rev	CTTATCCATGGTGGCGGCGGCCGGCCCTTATAGCAAAATCCTTTCCAAGC CCTGTCTTATTCTTC
1E6	Tat10 fwd (sequencing)	GATCCATTCGATTAGTGAACGG
1D5	RLuc rev (sequencing)	CCCTTCCAGTCCCCCTTTTC
vpr-mHSA	Insertion (via PflMI/ EcoRI)	CCATAGAATGGAGGAAAAAGAGATATAGCACACAAGTAGACCCTGACCTA GCAGACCAACTAATTCATCTGCACTATTTTGATTGTTTTTCAGAATCTGC TATAAGAAATACCATATTAGGACGTATAGTTAGTCCTAGGTGTGAATATC AAGCAGGACATAACAAGGTAGGATCTCTACAGTACTTGGCACTAGCAGCA TTAATAAAACCAAAACAGATAAAGCCACCTTTGCCTAGTGTTAGGAAACT GACAGAGGACAGGTGGAACAAGCCCCAGAAGACCAAGGGCCACAGAGGGA GCCATACACTGAATAGACACTAGAGCTTCTAGAGAGTCGCGCCGCGCGCC GACGGAGCGGACATGGGCAGAGCGATGGTGGCCAGGCTAGGGCTGGGGTT GCTGCTTCTGGCACTGCTCCTACCCACGCAGATTTACTGCAACCAAACAT CTGTTGCACCGTTTCCCGGTAACCAGAATATTTCTGCTTCCCCAAATCCA AGTAACGCTACCACCAGAGGGGGTGGCAGCTCCCTGCAGTCCACAGCTGG TCTCCTGGCTCTCTCTCTCTCTTTCTACATCTCTACTGTTAGAGAATTC
	V3 library	
5F3	THB-5F3-fwd-QL-ZM96	ATAATACGTCTCGCTAGCATGGGAGTGCGGGAGATCCTGCGG
5G5	THB-5G5-rev-QL-ZM96	ATATTCGTCTCCTCGAGCTAGTAGCCCTGCCGCACTCTGT
4B7	THB V3-InsertMN fwd	TCGGACCTGGGAGAGCTTTTTACACCACCAAAAACATCATCGGCACCATT AGACAGGCTCATTGTAACATCAGCCGGACCAACTG
4B8	THB V3-InsertMN rev	TGGTGGTGTAAAAAGCTCTCCCAGGTCCGATGTGAATCCGTTTCCGTTTG TTGTAGTTTGGTCTAGTACACACGATCTCGATGGATCTGTTC
4B9	THB V3-InsertRF fwd	AAGGACCTGGGAGAGTCATCTACGCTACTGGCCAGATCATTGGCGACATC CGAAAAGCTCACTGTAACATCAGCCGGACCAACTG
4C1	THB V3-InsertRF rev	CAGTAGCGTAGATGACTCTCCCAGGTCCTTTGGTGATGGATTTCCGGGTA TTGTTGTTGGGTCTAGTACACACGATCTCGATGGATCTGTTC
4C2	THB V3-InsertCDC42 fwd	TGGGACCTGGCCGAGTCTGGTACACAACTGGCGAGATTCTCGGAAACATT CGGCAGGCTCACTGCAACATCAGCCGGACCAACTG
4C3	THB V3-InsertCDC42 rev	CAGTTGTGTACCAGACTCGGCCAGGTCCCAGAGTGACTCGTTTTCGGGTG TGGTTGTTGGGTCTAGTACACACGATCTCGATGGATCTGTTC
4C6	THB V3-InsertHXB2 fwd	TTCAGAGAGGACCTGGACGAGCTTTTGTGACAATCGGGAAAATCGGCAAC ATGAGACAGGCTCACTGTAACATCAGCCGGACCAACTG
4C7	THB V3-InsertHXB2 rev	TCACAAAAGCTCGTCCAGGTCCTCTCTGAATTCTAATCCGTTTCCGGGTA TTGTTGTTGGGTCTAGTACACACGATCTCGATGGATCTGTTC
4C8	THB V3-InsertSF33 fwd	CTGGACCTGGCAAAGTGCTCTACACTACCGGGGAAATCATTGGAGACATT CGGAAGGCCTACTGTAACATCAGCCGGACCAACTG
4C9	THB V3-InsertSF33 rev	CGGTAGTGTAGAGCACTTTGCCAGGTCCAGATGTGATCCGTCGCCGTCTA TTGTTGTTGGGTCTAGTACACACGATCTCGATGGATCTGTTC
4D9	ZM-96-seq-For (sequencing)	GACAGACGACAGCGAGACAGG
4E1	ZM96-seq-Rev (sequencing)	CTCTCAGCAGGTTGCTCTGC
4F1	THB ZM96 seq-1-fwd (sequencing)	ATCCCCATCCACTACTGCG
	QL-plasmid construction	
4A1	T7-prom fwd	TAATACGACTCACTATA
1A4	pC-BGH-Rev	GCAACTAGAAGGCACAGTCGAGG
5G6	THB-5G6-fwd-QL-BsmB1-ccdB	ATAATAACGCGTGCTAGCGAGACGCCGGAATTGCCAGCTGGGG
5G7	THB-5G7-rev-QL-BsmB1-ccdB	TATATACATATGCTCGAGGAGACGTTATTAAATGCCCCAAAACATCAGG
6E1	THB-MluI-SV40-fwd	ATTATACGCGTCTGTGGAATGTGTGTCAGTTAGG
6E2	THB-KpnI-SV40-rev	ATTATGGTACCCGAAAATGGATATACAAGCTCC
6F4	THB-6F4-SV40-fwd	CTGTGGAATGTGTGTCAGTTAGG
6F5	THB-6F5-GFP-rev	TTACTTGTACAGCTCGTCCATGC
4E9	THB-GFP rev sNRP1	TATTGAATTCCATTTCGTATTTTATTTCTATTACTTGTACAGCTCGTCC

4G7	GFP-FOR-EcoRI	CTCTCTGAATTCATGGTGAGCAAGGGCG
4G8	GFP-Rev-XbaI	TCCTGAAGATCTTTACTTGTACAGCTCGTCC
6H1	THB-6H1-Nde1-IRES-fwd	TATTCATATGCGAGCATGCATCTAGGG
6H2	THB-6H2-Nde1-GFP-reverse	TATTCATATGTTACTTGTACAGCTCGTCCATG
6H3	THB-6H3-YFP-SV40pA-rev	GCAGTGAAAAAAATGCTTTATTTG
3D2	Seq-pLIB-For-1 (sequencing)	TCTTCCATTTCAGGTGTCGTG
5H7	THB-5H7-rev (sequencing)	TTCCACCAGATCGAGAAGGAGTTCAGCGAGGTGGAGGGCCGCATCCAGGA CCTGGAGAAGTACGTGGAGGACACCGGCAGCACCCAGGAATGGGAGCGGA AGGTCGACTTC
6H8	THB-6H8-QL5-seg-f (sequencing)	TCTGTTGAATGTCGTGAAGGAAG
6H9	THB-6H9-QL5-seq-r (sequencing)	TGCAAAGGGTCGCTACAGAC
6I1	THB-6I1-QL5-seg-f (sequencing)	GGCTACGTCCAGGAGCGC
6I7	THB-6I7 ccDB-PmeI-f	TAATAGTTTAAACGCTAGCGAGACGCCGGAATTGCCAGCTGGGG
6I8	THB-6I8 ccDB-BamHI-r	ATATAGGATCCCTCGAGGAGACGTTATTAAATGCCCCAAAACATCAGG
6I9	THB-6I9-f-NdeI-syn.Intron	TATTCATATGCTAAGTAAGGATCCACTAGTAACGG
7A1	THB-7A1-pIRES2-eGFP-f	TATTCATATGTCTGCAGTCGACGGTACCGC
8B2	THB-8B2-f-MluI-GFP	TATTACGCGTGCCATGGTGAGCAAGGGCGAGGAGCTGT
8B3	THB-8B3-r-NheI-IRES	TATTGCTAGCCGGTCCGCTTTGCGGACTGATGGGGAA
8B4	THB-8B4-r-NheI-TaV	TATTGCTAGCTGGGCCAGGATTCTCCTCGACGTCACCGCATGTTAGCAGA CTTCCTCTGCCCTCCTTGTACAGCTCGTCCATGCCGAG
8B5	THB-8B5-f-MluI-eGFP	TATTACGCGTGCCACCATGGCCACAACCATGGTGAGCAAGG
8B6	THB-8B6-f-MluI-synGag	TATTACGCGTGCCGCCAGCATGGGCGCCAGGGCCA
8B7	THB-8B7-r-SpeI-synGag	TATTACTAGTTCACTGGCTGCTGGGGTCGTTGCCG
8D5	THB-8D5-QL9-seq	AGGACATCATCAGCCTGTGGG
8D6	THB-8D6-QL9-seq	CTGGAAATCACCACCCACAG
8D7	THB-8D7-QL9-seq	AGCATCACCCTGACCGCCC
8D8	THB-8D8-QL9-seq	ACAGAACGAGAAGGACCTGC
8D9	THB-8D9-seq-f	CATGGTCCTGCTGGAGTTCGTG
9B3	THB-seq-f-9B3	TTACCGGATACCTGTCC
9B4	THB-seq-f-9B4	AGGATCTTCACCTAGATCC
9B5	THB-seq-f-9B5	ACTCATGGTTATGGCAG
9B6	THB-seq-f-9B6	TATGGTGCACTCTCAGTAC
9B7	THB-seq-f-9B7	TAAACCTGTGATTCCTCTG
9B8	THB-seq-f-9B8	AGATCCTGCATATAAGC
9B9	THB-seq-f-9B9	AACATCAGAAGGCTGTAG
9B10	THB-seq-f-9B10	ATCAAGCAGCTCCAGGC
9B11	THB-seq-f-9B11	ATCTCGACGGTATCGATG
9B12	THB-seq-f-9B12	TTCGATAAGTCTCTAGCC
9C4	THB-seq-f-9C4	CATATGATAATCAACCTCTGG
9C5	THB-seq-f-9C5	TTAAACCCGCTGATCAGC
9C6	THB-seq-f-9C6	AACAGGGACTTGAAAGCG
9C7	THB-seq-f-9C7	AACAGAGAGGAATCTTTGCAGC
	QL-cloning	
8H1	THB-8H1-for	TGAGTTGGATAGTTGTGG
8H2	THB-8H2-rev	GGATTTATACAAGGAGGAGA
5I3	THB-5I3-fwd-QL-ZM96	ATAATACGTCTCGCTAGCATGGGAGTGCGGGAGATCCTGCGGAACTGGCA GCGGTGGTGG
5I4	THB-5I4-rev-QL-ZM96	ATATTCGTCTCCTCGAGCTAGTAGCCCTGCCGCACTCTGTTCACGATGGA CAGCACGGCG
	Realtime PCR	
8H9	THB-8H9-MN-rev-2	GATGATGTTTTTGGTGGTG
8I1	THB-8I1-RF-rev-2	AGTGAGCTTTTCGGATGT
8G1	THB-8G1-CDC4-rev	TCTCGCCAGTTGTGTACC

8G3	THB-8G3-HXB2-rev	GGTCCTCTCTGAATTCTA
8G4	THB-8G4-SF33-rev	CCCGGTAGTGTAGAGC
8G5	THB-8G5-V3-for	GGAAGGCATCATCATCAG
8I2	THB-8I2-V3-rev	CGATCTCGATGGATCTGTTC
8I3	THB-8I3-V3-Sonde (FAM-BHQ1)	TTTCACGTTGTTGGTCAGGTT

5.2.2 Plasmids

Name	
pNL4-3	pUC [252] based vector, including the complete HIV-1 genome of the strain NY5/BRU (LAV-1), Accession number: AF324493.1 [253]
pTN7-Stop	Lentiviral vector based on NL4-3, autologous Env ORF interrupted, includes *R.Luciferase* inserted into the Nef ORF [181-184]
pTN-AIO	Derivative of pTN7-Stop, see 3.2.2
pTN-AIOHSA	Derivative of pTN-AIO, see 3.2.2
pTN pack	Lentiviral packaging construct [184]
pWPXLd	Lentiviral vector, Addgene plasmid #12258, Addgene Inc., Cambridge, USA
pVSVG	Envelope of vesicular stomatitis virus cloned into pcDNA3.1(+). [171]
pPCR-Script Amp	Commercially available vector, Agilent technologies # 211188
pcDNA3.1(+)	Commercially available vector, Invitrogen # V790-20
pcDNA3.1(+) QL	Derivative of pcDNA3.1(+), including a CcdB cloning cassette inserted at the MCS
pEGFP-C1	Commercially available eGFP expressing vector, Clonetech, GenBank # U55763
pEYFP-C1	Commercially available eYFP expressing vector, Clonetech, Catalog # 6005-1
pMACS LNGFR-IRES	Commercially available IRES vector, Miltenyi Biotec, Catalog # 130-091-887
pIRES2-EGFP	Commercially available IRES2-eGFP vector, Clonetech, Catalog # 6029-1
pQL1 – pQL11	Lentiviral vectors including a CcdB cloning cassette, see 3.5.1

5.2.3 V3 library sequences

V3 loop of the respective constructs

pQL9-MN

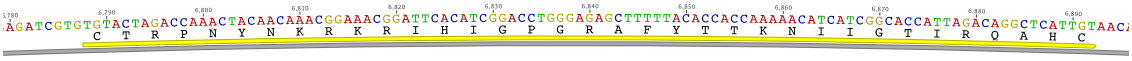

pQL9-RF

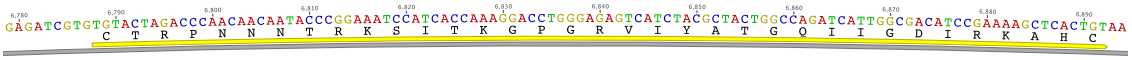

pQL9-CDC42

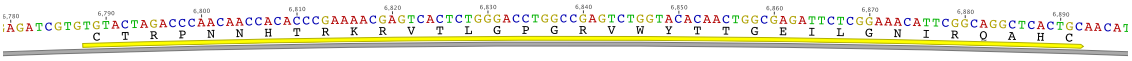

pQL9-HXB2

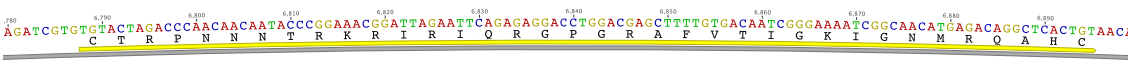

pQL9-SF33

- The respective V3 loops are underlined in yellow.
- The same variants were also cloned into pcDNA3.1(+) QL

V3 library sequence alignment

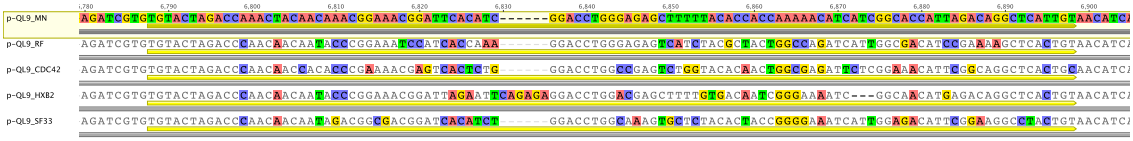

- The sequence range of the V3 loop is depicted.
- The respective V3 loops are underlined in yellow.
- The sequence of MN is set as reference. Deviating nucleotides of the other variants are highlighted.

5.3 MOI and infectivity

Poisson distribution

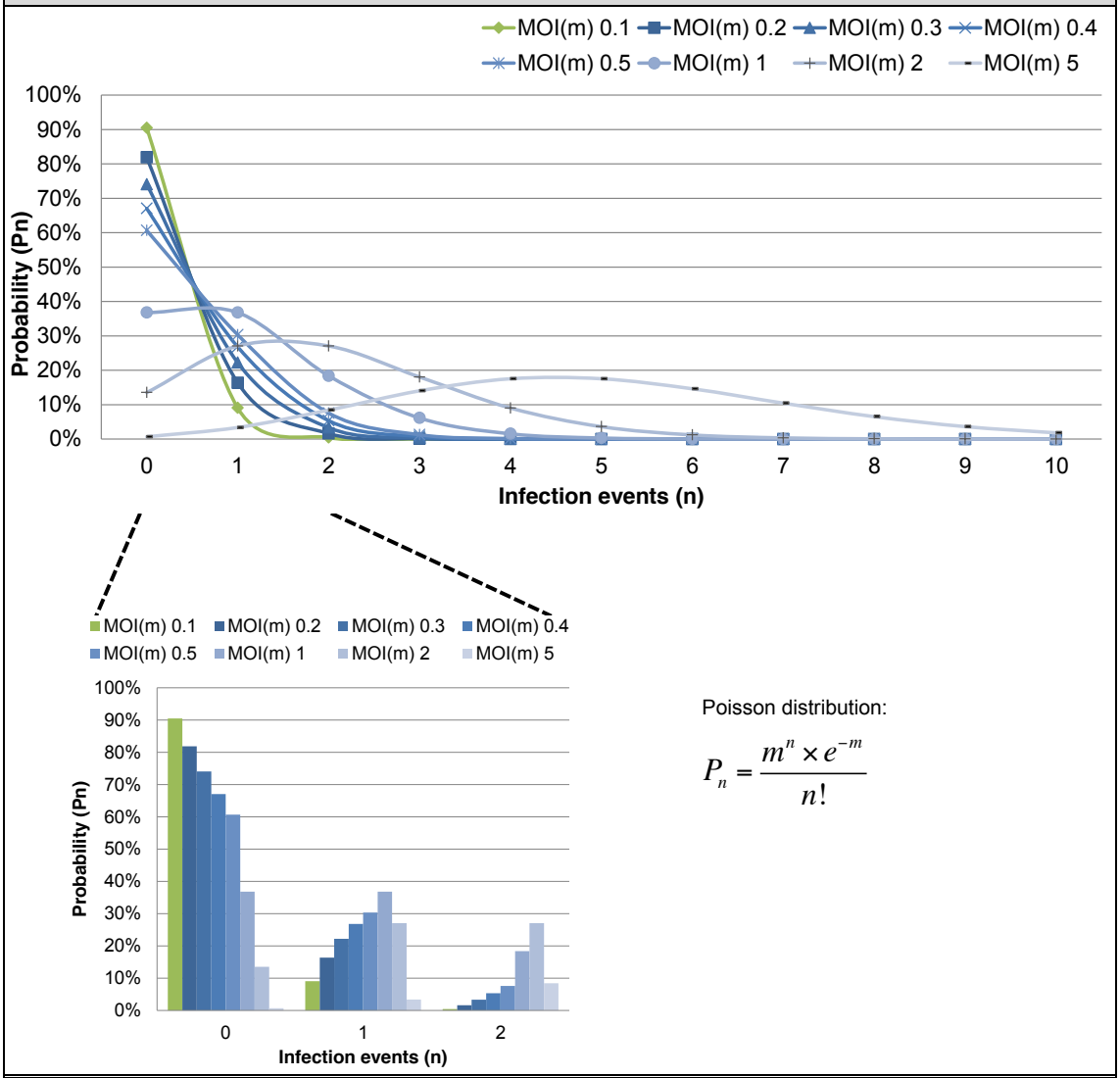

Poisson distribution:

$$P_n = \frac{m^n \times e^{-m}}{n!}$$

- e = Euler's constant
- Poisson distribution is used to determine the MOI.
- The probability P (n > 0) approximately equals MOI (m) for small values of m (m < 0.5)

5.4 References

1. Barré-Sinoussi F, Chermann J, Rey F, Nugeyre M, Chamaret S, et al. (1983) Isolation of a T-lymphotropic retrovirus from a patient at risk for acquired immune deficiency syndrome (AIDS). Science 220: 868–871. doi:10.1126/science.6189183

2. Global report (2010) Global report. Joint United Nations Programme on HIV/AIDS (UNAIDS).

3. Palella FJ, Delaney KM, Moorman AC, Loveless MO, Fuhrer J, et al. (1998) Declining morbidity and mortality among patients with advanced human immunodeficiency virus infection. HIV Outpatient Study Investigators. N Engl J Med 338: 853–860. doi:10.1056/NEJM199803263381301

4. United Nations (2011) The Millennium Development Goals Report 2011. United Nations. 68 p.

5. Dieffenbach C (2011) Thirty years of HIV and AIDS: Future challenges and opportunities. Annals of Internal Medicine.

6. Antiretroviral Therapy Cohort Collaboration (2008) Life expectancy of individuals on combination antiretroviral therapy in high-income countries: a collaborative analysis of 14 cohort studies. Lancet 372: 293–299. doi:10.1016/S0140-6736(08)61113-7

7. Abdool Karim Q, Abdool Karim SS, Frohlich JA, Grobler AC, Baxter C, et al. (2010) Effectiveness and safety of tenofovir gel, an antiretroviral microbicide, for the prevention of HIV infection in women. Science 329: 1168–1174. doi:10.1126/science.1193748

8. Munier CML, Andersen CR, Kelleher AD (2011) HIV vaccines: progress to date. Drugs 71: 387–414. doi:10.2165/11585400-000000000-00000

9. Hütter G, Nowak D, Mossner M, Ganepola S, Müssig A, et al. (2009) Long-term control of HIV by CCR5 Delta32/Delta32 stem-cell transplantation. New England Journal of Medicine 360: 692–698. doi:10.1056/NEJMoa0802905

10. Margolis DM (2011) Eradication therapies for HIV Infection: time to begin again. AIDS Research and Human Retroviruses 27: 347–353. doi:10.1089/AID.2011.0017

11. McElrath MJ, Haynes BF (2010) Induction of immunity to human immunodeficiency virus type-1 by vaccination. Immunity 33: 542–554. doi:10.1016/j.immuni.2010.09.011

12. Zhu P, Liu J, Bess J, Chertova E, Lifson JD, et al. (2006) Distribution and three-dimensional structure of AIDS virus envelope spikes. Nature 441: 847–852. doi:10.1038/nature04817

13. Sierra S, Kupfer B, Kaiser R (2005) Basics of the virology of HIV-1 and its replication. J. Clin. Virol. 34: 233–244. doi:10.1016/j.jcv.2005.09.004

14. Briggs JAG, Kräusslich H-G (2011) The Molecular Architecture of HIV. Journal of Molecular Biology 410: 491–500. doi:10.1016/j.jmb.2011.04.021

15. Ono A (2010) Relationships between plasma membrane microdomains and HIV-1 assembly. Biol. Cell 102: 335–350. doi:10.1042/BC20090165

16. Zhu P, Winkler H, Chertova E, Taylor KA, Roux KH, et al. (2008) Cryoelectron Tomography of HIV-1 Envelope Spikes: Further Evidence for Tripod-Like Legs. PLoS Pathogens 4: e1000203. doi:10.1371/journal.ppat.1000203

17. Zhu P, Chertova E, Bess J, Lifson JD, Arthur LO, et al. (2003) Electron tomography analysis of envelope glycoprotein trimers on HIV and simian immunodeficiency virus virions. Proc Natl Acad Sci USA 100: 15812–15817. doi:10.1073/pnas.2634931100

18. Ott DE (2008) Cellular proteins detected in HIV-1. Rev. Med. Virol. 18: 159–175. doi:10.1002/rmv.570

19. Miyauchi K, Kim Y, Latinovic O, Morozov V, Melikyan GB (2009) HIV Enters Cells via Endocytosis and Dynamin-Dependent Fusion with Endosomes. Cell 137: 433–444. doi:10.1016/j.cell.2009.02.046

20. Zhang X, Kondo M, Chen J, Miyoshi H (2010) Inhibitory effect of human TRIM5a on HIV-1 production. Microbes and ….

21. Peng G, Lei KJ, Jin W, Greenwell-Wild T, Wahl SM (2006) Induction of APOBEC3 family proteins, a defensive maneuver underlying interferon-induced anti-HIV-1 activity. J Exp Med 203: 41–46. doi:10.1084/jem.20051512

22. Neil SJD, Zang T, Bieniasz PD (2008) Tetherin inhibits retrovirus release and is antagonized by HIV-1 Vpu. Nature 451: 425–430. doi:10.1038/nature06553

23. Pacheco B, Finzi A, Stremlau M, Sodroski J (2010) Adaptation of HIV-1 to cells expressing rhesus monkey TRIM5α. Virology 408: 204–212. doi:10.1016/j.virol.2010.09.019

24. Wissing S, Galloway N (2010) HIV-1 Vif versus the APOBEC3 cytidine deaminases: an intracellular duel between pathogen and host restriction factors. Molecular Aspects of Medicine.

25. Richter S, Ping Y (2002) TAR RNA loop: a scaffold for the assembly of a regulatory switch in HIV replication. Proceedings of the ….

26. Schindler M, Münch J, Kutsch O, Li H, Santiago M (2006) Nef-mediated suppression of T cell activation was lost in a lentiviral lineage that gave rise to HIV-1. Cell.

27. Fischer U, Huber J, Boelens W, Mattajt L (1995) ScienceDirect - Cell : The HIV-1 Rev Activation Domain is a nuclear export signal that accesses an export pathway used by specific cellular RNAs. Cell.

28. Fukuda M, Asano S, Nakamura T, Adachi M (1997) CRM1 is responsible for intracellular transport mediated by the nuclear export signal. Nature.

29. Ludwig C, Leiherer A, Wagner R (2008) Importance of Protease Cleavage Sites within and Flanking Human Immunodeficiency Virus Type 1 Transframe Protein p6* for Spatiotemporal Regulation of Protease Activation. Journal of Virology 82: 4573. doi:10.1128/JVI.02353-07

30. Ishima R, Torchia DA, Lynch SM, Gronenborn AM, Louis JM (2003) Solution structure of the mature HIV-1 protease monomer: insight into the tertiary fold and stability of a precursor. J Biol Chem 278: 43311–43319. doi:10.1074/jbc.M307549200

31. Wyatt R, Sodroski J (1998) The HIV-1 envelope glycoproteins: fusogens, antigens, and immunogens. Science 280: 1884–1888.

32. Wei X, Decker J, Wang S, Hui H, Kappes J (2003) Antibody neutralization and escape by HIV-1. Nature.

33. Leonard CK, Spellman MW, Riddle L, Harris RJ, Thomas JN, et al. (1990) Assignment of intrachain disulfide bonds and characterization of potential glycosylation sites of the type 1 recombinant human immunodeficiency virus envelope glycoprotein (gp120) expressed in Chinese hamster ovary cells. J Biol Chem 265: 10373–10382.

34. Frey G, Chen J, Rits-Volloch S, Freeman MM, Zolla-Pazner S, et al. (2010) Distinct conformational states of HIV-1 gp41 are recognized by neutralizing and non-neutralizing antibodies. Nat Struct Mol Biol 17: 1486–1491. doi:10.1038/nsmb.1950

35. White TA, Bartesaghi A, Borgnia MJ, Meyerson JR, la Cruz de MJV, et al. (2010) Molecular architectures of trimeric SIV and HIV-1 envelope glycoproteins on intact viruses: strain-dependent variation in quaternary

structure. PLoS Pathogens 6: e1001249. doi:10.1371/journal.ppat.1001249

36. Welch BD, VanDemark AP, Heroux A, Hill CP, Kay MS (2007) Potent D-peptide inhibitors of HIV-1 entry. Proc Natl Acad Sci USA 104: 16828–16833. doi:10.1073/pnas.0708109104

37. Curlin ME, Zioni R, Hawes SE, Liu Y, Deng W, et al. (2010) HIV-1 envelope subregion length variation during disease progression. PLoS Pathogens 6: e1001228. doi:10.1371/journal.ppat.1001228

38. Allan J, Coligan J, Barin F, McLane M (1985) Major glycoprotein antigens that induce antibodies in AIDS patients are encoded by HTLV-III. Science.

39. Bernstein HB, Tucker SP, Hunter E, Schutzbach JS, Compans RW (1994) Human immunodeficiency virus type 1 envelope glycoprotein is modified by O-linked oligosaccharides. Journal of Virology 68: 463.

40. Montefiori D, Robinson W (1988) Role of protein N-glycosylation in pathogenesis of human immunodeficiency virus type 1. Proceedings of the ….

41. Li H, Chien P, Tuen M, Visciano M (2008) Identification of an N-Linked Glycosylation in the C4 Region of HIV-1 Envelope gp120 That Is Critical for Recognition of Neighboring CD4 T Cell Epitopes. The Journal of ….

42. Raska M, Novak J (2010) Involvement of envelope-glycoprotein glycans in HIV-1 biology and infection. Arch. Immunol. Ther. Exp. (Warsz.) 58: 191–208. doi:10.1007/s00005-010-0072-3

43. Pollard SR, Rosa MD, Rosa JJ, Wiley DC (1992) Truncated variants of gp120 bind CD4 with high affinity and suggest a minimum CD4 binding region. EMBO J 11: 585–591.

44. Li Y, O'Dell S, Walker LM, Wu X, Guenaga J, et al. (2011) Mechanism of Neutralization by the Broadly Neutralizing HIV-1 Monoclonal Antibody VRC01. Journal of Virology 85: 8954–8967. doi:10.1128/JVI.00754-11

45. Freed EO, Myers DJ, Risser R (1991) Identification of the principal neutralizing determinant of human immunodeficiency virus type 1 as a fusion domain. Journal of Virology 65: 190.

46. Hwang S, Boyle T, Lyerly H, Cullen B (1991) Identification of the envelope V3 loop as the primary determinant of cell tropism in HIV-1. Science 253: 71–74. doi:10.1126/science.1905842

47. Jiang X, Burke V, Totrov M, Williams C, Cardozo T, et al. (2010) Conserved structural elements in the V3 crown of HIV-1 gp120. Nat Struct Mol Biol 17: 955–961. doi:10.1038/nsmb.1861

48. Javaherian K, Langlois A (1989) Principal neutralizing domain of the human immunodeficiency virus type 1 envelope protein. Proceedings of the ….

49. Pollakis G, Abebe A, Kliphuis A, Chalaby MIM, Bakker M, et al. (2004) Phenotypic and genotypic comparisons of CCR5- and CXCR4-tropic human immunodeficiency virus type 1 biological clones isolated from subtype C-infected individuals. Journal of Virology 78: 2841–2852.

50. Freed EO, Myers DJ, Risser R (1990) Characterization of the fusion domain of the human immunodeficiency virus type 1 envelope glycoprotein gp41. Proc Natl Acad Sci USA 87: 4650–4654.

51. Weissenhorn W, Dessen A, Harrison SC, Skehel JJ, Wiley DC (1997) Atomic structure of the ectodomain from HIV-1 gp41. Nature 387: 426–430. doi:10.1038/387426a0

52. Salzwedel K, West JT, Hunter E (1999) A conserved tryptophan-rich motif in the membrane-proximal region of the human immunodeficiency virus type 1 gp41 ectodomain is important for Env-mediated fusion and virus infectivity. Journal of Virology 73: 2469–2480.

53. Yahav T, Maimon T, Grossman E, Dahan I, Medalia O (2011) Cryo-electron tomography: gaining insight into cellular processes by structural approaches. Curr Opin Struct Biol. doi:10.1016/j.sbi.2011.07.004

54. Pancera M, Majeed S, Ban Y-EA, Chen L, Huang C-C, et al. (2010) Structure of HIV-1 gp120 with gp41-interactive region reveals layered envelope architecture and basis of conformational mobility. Proceedings of the National Academy of Sciences 107: 1166–1171. doi:10.1073/pnas.0911004107

55. Kolchinsky P, Mirzabekov T, Farzan M, Kiprilov E, Cayabyab M, et al. (1999) Adaptation of a CCR5-using, primary human immunodeficiency virus type 1 isolate for CD4-independent replication. Journal of Virology 73: 8120–8126.

56. Eckert DM, Kim PS (2001) Mechanisms of viral membrane fusion and its inhibition. Annu Rev Biochem 70: 777–810. doi:10.1146/annurev.biochem.70.1.777

57. U.S. Public Health Service (2001) Updated U.S. Public Health Service Guidelines for the Management of Occupational Exposures to HBV, HCV, and HIV and Recommendations for Postexposure Prophylaxis. MMWR Recomm Rep 50: 1–52.

58. Allen CDC, Okada T, Cyster JG (2007) Germinal-center organization and cellular dynamics. Immunity 27: 190–202. doi:10.1016/j.immuni.2007.07.009

59. Tarlinton D (2000) Dissecting affinity maturation: a model explaining selection of antibody-forming cells and memory B cells in the germinal centre. Immunology Today 21: 436–441. doi:10.1016/S0167-5699(00)01687-X

60. Radbruch A, Muehlinghaus G, Luger EO, Inamine A, Smith KGC, et al. (2006) Competence and competition: the challenge of becoming a long-lived plasma cell. Nat. Rev. Immunol. 6: 741–750. doi:10.1038/nri1886

61. Pulendran B, Ahmed R (2011) Immunological mechanisms of vaccination. Nat Immunol 131: 509–517. doi:10.1038/ni.2039

62. Sallusto F, Lanzavecchia A, Araki K, Ahmed R (2010) From vaccines to memory and back. Immunity 33: 451–463. doi:10.1016/j.immuni.2010.10.008

63. Plotkin SA (2008) Vaccines: correlates of vaccine-induced immunity. Clin. Infect. Dis. 47: 401–409. doi:10.1086/589862

64. Rajewsky K (1996) Clonal selection and learning in the antibody system. Nature 381: 751–758. doi:10.1038/381751a0

65. Carsetti R, Rosado M (2004) Peripheral development of B cells in mouse and man - Carsetti - 2004 - Immunological Reviews - Wiley Online Library. Immunol. Rev..

66. William J, Euler C, Christensen S, Shlomchik MJ (2002) Evolution of autoantibody responses via somatic hypermutation outside of germinal centers. Science 297: 2066–2070. doi:10.1126/science.1073924

67. Koup RA, Safrit JT, Cao Y, Andrews CA, McLeod G, et al. (1994) Temporal association of cellular immune responses with the initial control of viremia in primary human immunodeficiency virus type 1 syndrome. Journal of Virology 68: 4650.

68. Pantaleo G, Graziosi C, Demarest JF, Cohen OJ, Vaccarezza M, et al. (1994) Role of lymphoid organs in the pathogenesis of human immunodeficiency virus (HIV) infection. Immunol. Rev. 140: 105–130.

69. Levin MJ, Oxman MN, Zhang JH, Johnson GR, Stanley H, et al. (2008) Varicella-zoster virus-specific immune responses in elderly recipients of a herpes zoster vaccine. J. Infect. Dis. 197: 825–835. doi:10.1086/528696

70. Weinberg A, Zhang JH, Oxman MN, Johnson GR, Hayward AR, et al. (2009) Varicella-zoster virus-specific immune responses to herpes zoster in elderly participants in a trial of a clinically effective zoster vaccine. J. Infect.

Dis. 200: 1068–1077. doi:10.1086/605611

71. Pulendran B, Li S, Nakaya HI (2010) Systems vaccinology. Immunity 33: 516–529. doi:10.1016/j.immuni.2010.10.006

72. Modrow S, Falke D, Schätzl H (2009) Molekulare Virologie. Springer. 752 p.

73. Murphy K, Travers P, Walport M (2011) Janeway's Immunobiology. Garland Pub. 928 p.

74. Amara R, Villinger F, Altman J, Lydy S (2001) Control of a Mucosal Challenge and Prevention of AIDS by a Multiprotein DNA/MVA Vaccine. Science.

75. Harari A, Bart P-A, Stöhr W, Tapia G, Garcia M, et al. (2008) An HIV-1 clade C DNA prime, NYVAC boost vaccine regimen induces reliable, polyfunctional, and long-lasting T cell responses. Journal of Experimental Medicine 205: 63–77. doi:10.1084/jem.20071331

76. Drexler I, Staib C, Sutter G (2004) Modified vaccinia virus Ankara as antigen delivery system: how can we best use its potential? Current Opinion in Biotechnology 15: 506–512. doi:10.1016/j.copbio.2004.09.001

77. Ludwig C, Wagner R (2007) Virus-like particles—universal molecular toolboxes. Current Opinion in Biotechnology 18: 537–545. doi:10.1016/j.copbio.2007.10.013

78. Ulmer J, Donnelly J, Parker S, Rhodes G, Felgner P, et al. (1993) Heterologous protection against influenza by injection of DNA encoding a viral protein. Science 259: 1745–1749. doi:10.1126/science.8456302

79. Montgomery DL, Shiver JW, Leander KR, Perry HC, Friedman A, et al. (1993) Heterologous and homologous protection against influenza A by DNA vaccination: optimization of DNA vectors. DNA Cell Biol 12: 777–783.

80. Ramsay AJ, Leong KH, Ramshaw IA (1997) DNA vaccination against virus infection and enhancement of antiviral immunity following consecutive immunization with DNA and viral vectors. Immunol Cell Biol 75: 382–388. doi:10.1038/icb.1997.60

81. Ramshaw IA, Ramsay AJ (2000) The prime-boost strategy: exciting prospects for improved vaccination. Immunology Today 21: 163–165.

82. Perreau M, Welles HC, Harari A, Hall O, Martin R, et al. (2011) DNA/NYVAC Vaccine Regimen Induces HIV-Specific CD4 and CD8 T-Cell Responses in Intestinal Mucosa. Journal of Virology 85: 9854–9862. doi:10.1128/JVI.00788-11

83. Eigen M (1993) Viral quasispecies. Sci Am 269: 42–49.

84. Goonetilleke N, Liu M (2009) The first T cell response to transmitted/founder virus contributes to the control of acute viremia in HIV-1 infection. The Journal of ….

85. Keele BF, Giorgi EE, Salazar-Gonzalez JF, Decker JM, Pham KT, et al. (2008) Identification and characterization of transmitted and early founder virus envelopes in primary HIV-1 infection. Proceedings of the National Academy of Sciences 105: 7552–7557. doi:10.1073/pnas.0802203105

86. Deacon NJ, Tsykin A, Solomon A, Smith K, Ludford-Menting M, et al. (1995) Genomic structure of an attenuated quasi species of HIV-1 from a blood transfusion donor and recipients. Science 270: 988–991.

87. Sodora DL, Allan JS, Apetrei C, Brenchley JM, Douek DC, et al. (2009) Toward an AIDS vaccine: lessons from natural simian immunodeficiency virus infections of African nonhuman primate hosts. Nat Med 15: 861–865. doi:10.1038/nm.2013

88. Mascola JR, Montefiori DC (2010) The role of antibodies in HIV vaccines. Annu. Rev. Immunol. 28: 413–444. doi:10.1146/annurev-immunol-030409-101256

89. Ross AL, Bråve A, Scarlatti G, Manrique A, Buonaguro L (2010) Progress towards development of an HIV vaccine: report of the AIDS Vaccine 2009 Conference. The Lancet infectious diseases.Vol. 10. pp. 305–316. doi:10.1016/S1473-3099(10)70069-4

90. McKinnon LR, Card CM, CIHR International Infectious Diseases and Global Health Training Program (IID&GHTP) (2010) HIV vaccine efficacy trials: A brief history, and options for going forward. AIDS reviews 12: 209–217.

91. Rerks-Ngarm S, Pitisuttithum P, Nitayaphan S, Kaewkungwal J, Chiu J, et al. (2009) Vaccination with ALVAC and AIDSVAX to prevent HIV-1 infection in Thailand. N Engl J Med 361: 2209–2220. doi:10.1056/NEJMoa0908492

92. Bashyam H (2008) How alum works. J Exp Med.

93. Kool M, Soullie T, van Nimwegen M, Willart MAM, Muskens F, et al. (2008) Alum adjuvant boosts adaptive immunity by inducing uric acid and activating inflammatory dendritic cells. Journal of Experimental Medicine 205: 869–882. doi:10.1084/jem.20071087

94. Lakhashe SK, Wang W, Siddappa NB, Hemashettar G, Polacino P, et al. (2011) Vaccination against Heterologous R5 Clade C SHIV: Prevention of Infection and Correlates of Protection. PLoS ONE 6: e22010.

95. Haynes BF, Montefiori DC (2006) Aiming to induce broadly reactive neutralizing antibody responses with HIV-1 vaccine candidates. Expert review of vaccines 5: 579–595. doi:10.1586/14760584.5.4.579

96. McMichael AJ, Borrow P, Tomaras GD, Goonetilleke N, Haynes BF (2009) The immune response during acute HIV-1 infection: clues for vaccine development. Nat. Rev. Immunol. 10: 11–23. doi:10.1038/nri2674

97. Haase A (2010) Targeting early infection to prevent HIV-1 mucosal transmission. Nature.

98. Walker LM, Huber M, Doores KJ, Falkowska E, Pejchal R, et al. (2011) Broad neutralization coverage of HIV by multiple highly potent antibodies. Nature. doi:10.1038/nature10373

99. Mascola JR, Stiegler G, VanCott TC, Katinger H, Carpenter CB, et al. (2000) Protection of macaques against vaginal transmission of a pathogenic HIV-1/SIV chimeric virus by passive infusion of neutralizing antibodies. Nat Med 6: 207–210. doi:10.1038/72318

100. Wu X, Yang Z-Y, Li Y, Hogerkorp C-M, Schief WR, et al. (2010) Rational design of envelope identifies broadly neutralizing human monoclonal antibodies to HIV-1. Science 329: 856–861. doi:10.1126/science.1187659

101. Walker LM, Phogat SK, Chan-Hui P-Y, Wagner D, Phung P, et al. (2009) Broad and Potent Neutralizing Antibodies from an African Donor Reveal a New HIV-1 Vaccine Target. Science 326: 285–289. doi:10.1126/science.1178746

102. Pietzsch J, Scheid JF, Mouquet H, Klein F, Seaman MS, et al. (2010) Human anti-HIV-neutralizing antibodies frequently target a conserved epitope essential for viral fitness. Journal of Experimental Medicine 207: 1995–2002. doi:10.1084/jem.20101176

103. Schief WR, Ban Y-EA, Stamatatos L (2009) Challenges for structure-based HIV vaccine design. Curr Opin HIV AIDS 4: 431–440. doi:10.1097/COH.0b013e32832e6184

104. Burton DR, Pyati J, Koduri R, Sharp SJ, Thornton GB, et al. (1994) Efficient neutralization of primary isolates of HIV-1 by a recombinant human monoclonal antibody. Science 266: 1024–1027.

105. Gilad Ofek MTASHKJRMRWPDK (2004) Structure and Mechanistic Analysis of the Anti-Human Immunodeficiency Virus Type 1 Antibody 2F5 in Complex with Its gp41 Epitope. Journal of Virology 78: 10724. doi:10.1128/JVI.78.19.10724-10737.2004

106. Cardoso RMF, Zwick MB, Stanfield RL, Kunert R, Binley JM, et al. (2005) Broadly neutralizing anti-HIV antibody

4E10 recognizes a helical conformation of a highly conserved fusion-associated motif in gp41. Immunity 22: 163–173. doi:10.1016/j.immuni.2004.12.011

107. Scanlan CN, Pantophlet R, Wormald MR, Ollmann Saphire E, Stanfield R, et al. (2002) The broadly neutralizing anti-human immunodeficiency virus type 1 antibody 2G12 recognizes a cluster of alpha1-->2 mannose residues on the outer face of gp120. Journal of Virology 76: 7306–7321.

108. Garrity RR, Rimmelzwaan G, Minassian A, Tsai WP, Lin G, et al. (1997) Refocusing neutralizing antibody response by targeted dampening of an immunodominant epitope. J Immunol 159: 279–289.

109. Tomaras GD, Yates NL, Liu P, Qin L, Fouda GG, et al. (2008) Initial B-cell responses to transmitted human immunodeficiency virus type 1: virion-binding immunoglobulin M (IgM) and IgG antibodies followed by plasma anti-gp41 antibodies with ineffective control of initial viremia. Journal of Virology 82: 12449–12463. doi:10.1128/JVI.01708-08

110. Davis KL, Gray ES, Moore PL, Decker JM, Salomon A, et al. (2009) High titer HIV-1 V3-specific antibodies with broad reactivity but low neutralizing potency in acute infection and following vaccination. Virology 387: 414–426. doi:10.1016/j.virol.2009.02.022

111. Wyatt R, Moore J, Accola M, Desjardin E, Robinson J, et al. (1995) Involvement of the V1/V2 variable loop structure in the exposure of human immunodeficiency virus type 1 gp120 epitopes induced by receptor binding. Journal of Virology 69: 5723–5733.

112. Krachmarov CP, Honnen WJ, Kayman SC, Gorny MK, Zolla-Pazner S, et al. (2006) Factors determining the breadth and potency of neutralization by V3-specific human monoclonal antibodies derived from subjects infected with clade A or clade B strains of human immunodeficiency virus type 1. Journal of Virology 80: 7127–7135. doi:10.1128/JVI.02619-05

113. Zolla-Pazner S, Zhong P, Revesz K, Volsky B, Williams C, et al. (2004) The cross-clade neutralizing activity of a human monoclonal antibody is determined by the GPGR V3 motif of HIV type 1. AIDS Research and Human Retroviruses 20: 1254–1258. doi:10.1089/0889222042545054

114. Stanfield RL, Gorny MK, Williams C, Zolla-Pazner S, Wilson IA (2004) Structural rationale for the broad neutralization of HIV-1 by human monoclonal antibody 447-52D. Structure/Folding and Design 12: 193–204. doi:10.1016/j.str.2004.01.003

115. Zolla-Pazner S, Cohen S, Pinter A, Krachmarov C, Wrin T, et al. (2009) Cross-clade neutralizing antibodies against HIV-1 induced in rabbits by focusing the immune response on a neutralizing epitope. Virology: 1–12. doi:10.1016/j.virol.2009.05.039

116. Conley AJ, Gorny MK, Kessler JA2, Boots LJ, Ossorio-Castro M, et al. (1994) Neutralization of primary human immunodeficiency virus type 1 isolates by the broadly reactive anti-V3 monoclonal antibody, 447-52D. Journal of Virology 68: 6994.

117. Gorny MK, Xu JY, Karwowska S, Buchbinder A, Zolla-Pazner S (1993) Repertoire of neutralizing human monoclonal antibodies specific for the V3 domain of HIV-1 gp120. J Immunol 150: 635–643.

118. Zolla-Pazner S, Cardozo T (2010) Structure–function relationships of HIV-1 envelope sequence-variable regions refocus vaccine design. Nature Publishing Group 10: 527–535. doi:10.1038/nri2801

119. Gorny MK, Williams C, Volsky B, Revesz K, Cohen S, et al. (2002) Human monoclonal antibodies specific for conformation-sensitive epitopes of V3 neutralize human immunodeficiency virus type 1 primary isolates from various clades. Journal of Virology 76: 9035–9045.

120. Flynn NM, Forthal DN, Harro CD, Judson FN, Mayer KH, et al. (2005) Placebo-controlled phase 3 trial of a recombinant glycoprotein 120 vaccine to prevent HIV-1 infection. J. Infect. Dis. 191: 654–665. doi:10.1086/428404

121. Hoxie JA (2010) Toward an Antibody-Based HIV-1 Vaccine. Annu. Rev. Med. 61: 135–152. doi:10.1146/annurev.med.60.042507.164323

122. Burton DR (2002) Opinion: Antibodies, viruses and vaccines. Nat. Rev. Immunol. 2: 706–713. doi:10.1038/nri891

123. Du SX, Xu L, Zhang W, Tang S, Boenig RI, et al. (2011) A Directed Molecular Evolution Approach to Improved Immunogenicity of the HIV-1 Envelope Glycoprotein. PLoS ONE 6: e20927. doi:10.1371/journal.pone.0020927.t002

124. Ching L, Stamatatos L (2010) Alterations in the Immunogenic Properties of Soluble Trimeric Human Immunodeficiency Virus Type 1 Envelope Proteins Induced by Deletion or Heterologous Substitutions of the V1 Loop. Journal of Virology 84: 9932–9946. doi:10.1128/JVI.00868-10

125. Selvarajah S, Puffer BA, Lee F-H, Zhu P, Li Y, et al. (2008) Focused Dampening of Antibody Response to the Immunodominant Variable Loops by Engineered Soluble gp140. AIDS Research and Human Retroviruses 24: 301–314. doi:10.1089/aid.2007.0158

126. Wu X, Changela A, O'Dell S, Schmidt SD, Pancera M, et al. (2011) Immunotypes of a quaternary site of HIV-1 vulnerability and their recognition by antibodies. Journal of Virology 85: 4578–4585. doi:10.1128/JVI.02585-10

127. Harris A, Borgnia MJ, Shi D, Bartesaghi A, He H, et al. (2011) Trimeric HIV-1 glycoprotein gp140 immunogens and native HIV-1 envelope glycoproteins display the same closed and open quaternary molecular architectures. Proceedings of the National Academy of Sciences 108: 11440–11445. doi:10.1073/pnas.1101414108

128. Walker LM, Burton DR (2010) Rational antibody-based HIV-1 vaccine design: current approaches and future directions. Current Opinion in Immunology: 1–9. doi:10.1016/j.coi.2010.02.012

129. Burton DR, Weiss RA (2010) AIDS/HIV. A boost for HIV vaccine design. Science 329: 770–773. doi:10.1126/science.1194693

130. Smith GP (1985) Filamentous fusion phage: novel expression vectors that display cloned antigens on the virion surface. Science 228: 1315–1317.

131. Marks JD, Hoogenboom HR, Bonnert TP, McCafferty J, Griffiths AD, et al. (1991) By-passing immunization. Human antibodies from V-gene libraries displayed on phage. Journal of Molecular Biology 222: 581–597.

132. McCafferty J, Griffiths AD, Winter G, Chiswell DJ (1990) Phage antibodies: filamentous phage displaying antibody variable domains. Nature 348: 552–554. doi:10.1038/348552a0

133. Breitling F, Dübel S, SEEHAUS T, KLEWINGHAUS I, LITTLE M (1991) A surface expression vector for antibody screening. Gene 104: 147–153.

134. Hust M, Meyer T, Voedisch B, Rülker T, Thie H, et al. (2011) A human scFv antibody generation pipeline for proteome research. Journal of Biotechnology 152: 159–170. doi:10.1016/j.jbiotec.2010.09.945

135. Boder ET, Wittrup KD (1997) Yeast surface display for screening combinatorial polypeptide libraries. Nat Biotech 15: 553–557. doi:10.1038/nbt0697-553

136. Feldhaus MJ, Siegel RW, Opresko LK, Coleman JR, Feldhaus JMW, et al. (2003) Flow-cytometric isolation of human antibodies from a nonimmune Saccharomyces cerevisiae surface display library. Nat Biotech 21: 163–170. doi:10.1038/nbt785

137. Chen G, Hayhurst A, Thomas JG, Harvey BR, Iverson BL, et al. (2001) Isolation of high-affinity ligand-binding proteins by periplasmic expression with cytometric screening (PECS). Nature Publishing Group 19: 537–542. doi:doi:10.1038/89281

138. Ho M, Nagata S, Pastan I (2006) Isolation of anti-CD22 Fv with high affinity by Fv display on human cells. Proc Natl Acad Sci USA 103: 9637–9642. doi:10.1073/pnas.0603653103

139. Taube R, Zhu Q, Xu C, Diaz-Griffero F, Sui J, et al. (2008) Lentivirus display: stable expression of human antibodies on the surface of human cells and virus particles. PLoS ONE 3: e3181. doi:10.1371/journal.pone.0003181

140. Khare PD, Russell SJ, Federspiel MJ (2003) Avian leukosis virus is a versatile eukaryotic platform for polypeptide display. Virology 315: 303–312.

141. Russell SJ, Hawkins RE, Winter G (1993) Retroviral vectors displaying functional antibody fragments. Nucleic Acids Research 21: 1081–1085.

142. Hanes J, Plückthun A (1997) In vitro selection and evolution of functional proteins by using ribosome display. Proceedings of the National ….

143. Zahnd C, Amstutz P, Plückthun A (2007) Ribosome display: selecting and evolving proteins in vitro that specifically bind to a target. Nat Meth 4: 269–279. doi:10.1038/nmeth1003

144. Sergeeva A, Kolonin MG, Molldrem JJ, Pasqualini R, Arap W (2006) Display technologies: application for the discovery of drug and gene delivery agents. Advanced Drug Delivery Reviews 58: 1622–1654. doi:10.1016/j.addr.2006.09.018

145. FitzGerald K (2000) In vitro display technologies – new tools for drug discovery. Drug Discovery Today 5: 253–258. doi:10.1016/S1359-6446(00)01501-4

146. Ja WW, Olsen BN, Roberts RW (2005) Epitope mapping using mRNA display and a unidirectional nested deletion library. Protein Engineering Design and Selection 18: 309–319. doi:10.1093/protein/gzi038

147. Reiersen H, Løbersli I, Løset GA, Hvattum E, Simonsen B, et al. (2005) Covalent antibody display--an in vitro antibody-DNA library selection system. Nucleic Acids Research 33: e10. doi:10.1093/nar/gni010

148. Hoogenboom HR, de Bruïne AP, Hufton SE, Hoet RM, Arends JW, et al. (1998) Antibody phage display technology and its applications. Immunotechnology 4: 1–20.

149. Khare PD, Rosales AG, Bailey KR, Russell SJ, Federspiel MJ (2003) Epitope selection from an uncensored peptide library displayed on avian leukosis virus. Virology 315: 313–321.

150. Lee SY, Choi JH, Xu Z (2003) Microbial cell-surface display. Trends in Biotechnology 21: 45–52.

151. Benatuil L, Perez JM, Belk J, Hsieh CM (2010) An improved yeast transformation method for the generation of very large human antibody libraries. Protein Engineering Design and Selection 23: 155–159. doi:10.1093/protein/gzq002

152. Kondo A, Ueda M (2004) Yeast cell-surface display--applications of molecular display. Appl Microbiol Biotechnol 64: 28–40. doi:10.1007/s00253-003-1492-3

153. Lipovsek D, Plückthun A (2004) In-vitro protein evolution by ribosome display and mRNA display. J Immunol Methods 290: 51–67. doi:10.1016/j.jim.2004.04.008

154. Indrawattana N, Sookrung N, Kulkeaw K, Seesuay W, Kongngoen T, et al. (2010) Human monoclonal ScFv that inhibits cellular entry and metalloprotease activity of tetanus neurotoxin. Asian Pac. J. Allergy Immunol. 28: 85–93.

155. Kotlan B, Glassy MC (2009) Methods in Molecular Biology. Aitken R, editor Totowa, NJ: Humana Press. 1–15 pp. doi:10.1007/978-1-60327-302-2_1

156. Samuelson P, Gunneriusson E, Nygren P (2002) Display of proteins on bacteria. Journal of ….

157. Lunder M, Bratkovic T, Doljak B, Kreft S, Urleb U, et al. (2005) Comparison of bacterial and phage display peptide libraries in search of target-binding motif. Appl Biochem Biotechnol 127: 125–131.

158. Beerli R, Bauer M, Buser R (2008) Isolation of human monoclonal antibodies by mammalian cell display. Proceedings of the ….

159. Alonso-Camino V, Sánchez-Martín D, Compte M, Sanz L, Alvarez-Vallina L (2009) Lymphocyte display: a novel antibody selection platform based on T cell activation. PLoS ONE 4: e7174. doi:10.1371/journal.pone.0007174

160. Wolkowicz R, Jager GC, Nolan GP (2005) A random peptide library fused to CCR5 for selection of mimetopes expressed on the mammalian cell surface via retroviral vectors. J Biol Chem 280: 15195–15201. doi:10.1074/jbc.M500254200

161. Lin W, Kurosawa K, Murayama A, Kagaya E, Ohta K (2011) B-cell display-based one-step method to generate chimeric human IgG monoclonal antibodies. Nucleic Acids Research 39: e14. doi:10.1093/nar/gkq1122

162. Urban JH, Merten CA (2011) Retroviral Display in Gene Therapy, Protein Engineering, and Vaccine Development. ACS Chem. Biol. 6: 61–74. doi:10.1021/cb100285n

163. Buchholz CJ, Duerner LJ, Funke S, Schneider IC (2008) Retroviral display and high throughput screening. Comb Chem High Throughput Screen 11: 99–110.

164. Taussig MJ, Stoevesandt O, Borrebaeck CAK, Bradbury AR, Cahill D, et al. (2007) ProteomeBinders: planning a European resource of affinity reagents for analysis of the human proteome. Nat Meth 4: 13–17. doi:10.1038/nmeth0107-13

165. Bradbury ARM, Sidhu S, Dübel S, McCafferty J (2011) Beyond natural antibodies: the power of in vitro display technologies. Nature Publishing Group 29: 245–254. doi:10.1038/nbt.1791

166. Pejchal R, Walker LM, Stanfield RL, Phogat SK, Koff WC, et al. (2010) Structure and function of broadly reactive antibody PG16 reveal an H3 subdomain that mediates potent neutralization of HIV-1. Proceedings of the National Academy of Sciences: 1–6. doi:10.1073/pnas.1004600107

167. Geertsma ER, Dutzler R (2011) A Versatile and Efficient High-Throughput Cloning Tool for Structural Biology. Biochemistry 50: 3272–3278. doi:10.1021/bi200178z

168. Bernard P, Gabant P, Bahassi EM, Couturier M (1994) Positive-selection vectors using the F plasmid ccdB killer gene. Gene 148: 71–74.

169. Hanahan D (1983) Studies on transformation of Escherichia coli with plasmids. Journal of Molecular Biology 166: 557–580.

170. Boussif O, Lezoualc'h F, Zanta MA, Mergny MD, Scherman D, et al. (1995) A versatile vector for gene and oligonucleotide transfer into cells in culture and in vivo: polyethylenimine. Proc Natl Acad Sci USA 92: 7297–7301.

171. Aiken C (1997) Pseudotyping human immunodeficiency virus type 1 (HIV-1) by the glycoprotein of vesicular stomatitis virus targets HIV-1 entry to an endocytic pathway and suppresses both the requirement for Nef and the sensitivity to cyclosporin A. Journal of Virology 71: 5871–5877.

172. Kumar M, Bradow BP, Zimmerberg J (2003) Large-scale production of pseudotyped lentiviral vectors using baculovirus GP64. Hum Gene Ther 14: 67–77. doi:10.1089/10430340360464723

173. Hefferon KL, Oomens AG, Monsma SA, Finnerty CM, Blissard GW (1999) Host cell receptor binding by baculovirus GP64 and kinetics of virion entry. Virology 258: 455–468. doi:10.1006/viro.1999.9758

174. Lybarger L, Dempsey D, Patterson GH, Piston DW, Kain SR, et al. (1998) Dual-color flow cytometric detection of

fluorescent proteins using single-laser (488-nm) excitation. Cytometry 31: 147–152.

175. Perfetto SP, Chattopadhyay PK, Roederer M (2004) Seventeen-colour flow cytometry: unravelling the immune system. Nat. Rev. Immunol. 4: 648–655. doi:10.1038/nri1416

176. Corti D, Langedijk JPM, Hinz A, Seaman MS, Vanzetta F, et al. (2010) Analysis of memory B cell responses and isolation of novel monoclonal antibodies with neutralizing breadth from HIV-1-infected individuals. PLoS ONE 5: e8805. doi:10.1371/journal.pone.0008805

177. Shapiro HM (2005) Practical Flow Cytometry. Hoboken, NJ, USA: John Wiley & Sons, Inc. i–I pp. doi:10.1002/0471722731.fmatter

178. BD (2007) BD FACSAria II User's Guide.: 1–344.

179. Scott JK, Smith GP (1990) Searching for peptide ligands with an epitope library. Science 249: 386–390.

180. Oomens AG, Monsma SA, Blissard GW (1995) The baculovirus GP64 envelope fusion protein: synthesis, oligomerization, and processing. Virology 209: 592–603. doi:10.1006/viro.1995.1291

181. Dittmar MT, Eichler S, Reinberger S, Henning L, Kräusslich HG (2001) A recombinant virus assay using full-length envelope sequences to detect changes in HIV-1 co-receptor usage. Virus Genes 23: 281–290.

182. Lohrengel S, Hermann F, Hagmann I, Oberwinkler H, Scrivano L, et al. (2005) Determinants of human immunodeficiency virus type 1 resistance to membrane-anchored gp41-derived peptides. Journal of Virology 79: 10237–10246. doi:10.1128/JVI.79.16.10237-10246.2005

183. Neumann T, Hagmann I, Lohrengel S, Heil ML, Derdeyn CA, et al. (2005) T20-insensitive HIV-1 from naive patients exhibits high viral fitness in a novel dual-color competition assay on primary cells. Virology 333: 251–262. doi:10.1016/j.virol.2004.12.035

184. Schilling K (2011) Etablierung eines lentiviralen Display-Systems mit Hilfe eines auf einer HI-viralen Verpackungszelllinie basierenden Vektorsystems: Proof of concept anhand des HIV-1 Hüllproteins. Dissertation.

185. Kozak M (1987) An analysis of 5'-noncoding sequences from 699 vertebrate messenger RNAs. Nucleic Acids Research 15: 8125–8148.

186. Ali A, Yang O (2006) A novel small reporter gene and HIV-1 fitness assay. Journal of Virological Methods 133: 41–47. doi:10.1016/j.jviromet.2005.10.016

187. Ali A (2003) Half-genome human immunodeficiency virus type 1 constructs for rapid production of reporter viruses. Journal of Virological Methods 110: 137–142. doi:10.1016/S0166-0934(03)00110-1

188. BUCHACHER A, PREDL R, STRUTZENBERGER K, STEINFELLNER W, TRKOLA A, et al. (1994) Generation of Human Monoclonal Antibodies against HIV-1 Proteins; Electrofusion and Epstein-Barr Virus Transformation for Peripheral Blood Lymphocyte Immortalization. AIDS Research and Human Retroviruses 10: 359–369. doi:10.1089/aid.1994.10.359

189. Mehandru S, Wrin T, Galovich J, Stiegler G, Vcelar B, et al. (2004) Neutralization profiles of newly transmitted human immunodeficiency virus type 1 by monoclonal antibodies 2G12, 2F5, and 4E10. Journal of Virology 78: 14039–14042. doi:10.1128/JVI.78.24.14039-14042.2004

190. McKEATING J, McKNIGHT A (1991) Differential loss of envelope glycoprotein gp120 from virions of human immunodeficiency virus type 1 isolates: effects on infectivity and neutralization. Journal of Virology.

191. Dhillon AK, Stanfield RL, Gorny MK, Williams C, Zolla-Pazner S, et al. (2008) Structure determination of an anti-HIV-1 Fab 447-52D-peptide complex from an epitaxially twinned data set. Acta Crystallogr. D Biol. Crystallogr. D64: 792–802. doi:10.1107/S0907444908013978

192. Rodenburg CM, Li Y, Trask SA, Chen Y, Decker J, et al. (2001) Near full-length clones and reference sequences for subtype C isolates of HIV type 1 from three different continents. AIDS Research and Human Retroviruses 17: 161–168. doi:10.1089/08892220150217247

193. Dübel S, Stoevesandt O, Taussig MJ, Hust M (2010) Generating recombinant antibodies to the complete human proteome. Trends in Biotechnology: 1–7. doi:10.1016/j.tibtech.2010.05.001

194. Rosen CA, Sodroski JG, Haseltine WA (1985) The location of cis-acting regulatory sequences in the human T cell lymphotropic virus type III (HTLV-III/LAV) long terminal repeat. Cell 41: 813–823. doi:10.1016/S0092-8674(85)80062-3

195. Naldini L, Blömer U, Gallay P, Ory D, Mulligan R, et al. (1996) In vivo gene delivery and stable transduction of nondividing cells by a lentiviral vector. Science 272: 263–267.

196. Kim DW, Uetsuki T, Kaziro Y, Yamaguchi N, Sugano S (1990) Use of the human elongation factor 1 alpha promoter as a versatile and efficient expression system. Gene 91: 217–223.

197. Gopalkrishnan RV, Christiansen KA, Goldstein NI, DePinho RA, Fisher PB (1999) Use of the human EF-1alpha promoter for expression can significantly increase success in establishing stable cell lines with consistent expression: a study using the tetracycline-inducible system in human cancer cells. Nucleic Acids Research 27: 4775–4782.

198. Sirven A, Ravet E, Charneau P, Zennou V, Coulombel L, et al. (2001) Enhanced transgene expression in cord blood CD34(+)-derived hematopoietic cells, including developing T cells and NOD/SCID mouse repopulating cells, following transduction with modified trip lentiviral vectors. Mol. Ther. 3: 438–448. doi:10.1006/mthe.2001.0282

199. Zennou V, Petit C, Guetard D, Nerhbass U, Montagnier L, et al. (2000) HIV-1 genome nuclear import is mediated by a central DNA flap. Cell 101: 173–185. doi:10.1016/S0092-8674(00)80828-4

200. Chalfie M, Tu Y, Euskirchen G, Ward WW, Prasher DC (1994) Green fluorescent protein as a marker for gene expression. Science 263: 802–805.

201. Zufferey R, Donello JE, Trono D, Hope TJ (1999) Woodchuck hepatitis virus posttranscriptional regulatory element enhances expression of transgenes delivered by retroviral vectors. Journal of Virology 73: 2886–2892.

202. Zufferey R, Dull T, Mandel RJ, Bukovsky A, Quiroz D, et al. (1998) Self-Inactivating Lentivirus Vector for Safe and Efficient In Vivo Gene Delivery. Journal of Virology 72: 9873.

203. Addgene - pWPXLd Plasmid Data (n.d.) Addgene - pWPXLd Plasmid Data.. Available: http://www.addgene.org/12258/. Accessed 21 Aug. 2011.

204. McFarland TJ, Zhang Y, Atchaneeyaskul L-O, Francis P, Stout JT, et al. (2006) Evaluation of a novel short polyadenylation signal as an alternative to the SV40 polyadenylation signal. Plasmid 56: 62–67. doi:10.1016/j.plasmid.2005.11.005

205. Huang M (1990) Intervening sequences increase efficiency of RNA 3'processing and accumulation of cytoplasmic RNA. Nucleic Acids Research.

206. Szymczak AL, Workman CJ, Wang Y, Vignali KM, Dilioglou S, et al. (2004) Correction of multi-gene deficiency in vivo using a single "self-cleaving" 2A peptide-based retroviral vector. Nat Biotech 22: 589–594. doi:10.1038/nbt957

207. Jang SK, Kräusslich HG, Nicklin MJ, Duke GM, Palmenberg AC, et al. (1988) A segment of the 5' nontranslated region of encephalomyocarditis virus RNA directs internal entry of ribosomes during in vitro translation. Journal of Virology 62: 2636.

208. Fu H, Wilkinson KD (2004) Protein-Protein Interactions.

New Jersey: Humana Press. 015–032 pp. doi:10.1385/1-59259-762-9:015

209. VanAntwerp JJ, Wittrup KD (2000) Fine Affinity Discrimination by Yeast Surface Display and Flow Cytometry. Biotechnol. Prog. 16: 31–37. doi:10.1021/bp990133s

210. Fleiss JL, Levin B, Paik MC, Fleiss J (2003) Statistical Methods for Rates & Proportions. 3rd ed. Wiley-Interscience. 800 p.

211. Rao SR, Rao PM (n.d.) Sample Size Calculator by Raosoft, Inc. raosoft.com. Available: http://www.raosoft.com/samplesize.html. Accessed 24 Aug. 2011.

212. Kubista M, Andrade JM, Bengtsson M, Forootan A, Jonák J, et al. (2006) The real-time polymerase chain reaction. Molecular Aspects of Medicine 27: 95–125. doi:10.1016/j.mam.2005.12.007

213. Heid CA, Stevens J, Livak KJ, Williams PM (1996) Real time quantitative PCR. Genome Research 6: 986–994. doi:10.1101/gr.6.10.986

214. Freeman WM, Walker SJ, Vrana KE (1999) Quantitative RT-PCR: pitfalls and potential. BioTechniques 26: 112–22, 124–5.

215. Livak KJ, Schmittgen TD (2001) Analysis of Relative Gene Expression Data Using Real-Time Quantitative PCR and the 2−ΔΔCT Method. Methods 25: 402–408. doi:10.1006/meth.2001.1262

216. Kim M, Qiao Z-S, Montefiori DC, Haynes BF, Reinherz EL, et al. (2005) Comparison of HIV Type 1 ADA gp120 monomers versus gp140 trimers as immunogens for the induction of neutralizing antibodies. AIDS Research and Human Retroviruses 21: 58–67. doi:10.1089/aid.2005.21.58

217. Koff WC (2010) Accelerating HIV vaccine development. Nature 464: 161–162. doi:10.1038/464161a

218. Pejchal R, Wilson IA (2010) Structure-based vaccine design in HIV: blind men and the elephant? Curr Pharm Des 16: 3744–3753.

219. Moscoso CG, Sun Y, Poon S, Xing L, Kan E, et al. (2011) Quaternary structures of HIV Env immunogen exhibit conformational vicissitudes and interface diminution elicited by ligand binding. Proceedings of the National Academy of Sciences 108: 6091–6096. doi:10.1073/pnas.1016113108

220. Brakmann S, Johnsson K (2002) Directed molecular evolution of proteins. Vch Verlagsgesellschaft Mbh. 357 p.

221. Perelson AS, Oster GF (1979) Theoretical studies of clonal selection: Minimal antibody repertoire size and reliability of self-non-self discrimination. Journal of Theoretical Biology 81: 645–670. doi:10.1016/0022-5193(79)90275-3

222. Gold L (2001) mRNA display: diversity matters during in vitro selection. Proc Natl Acad Sci USA 98: 4825–4826. doi:10.1073/pnas.091101698

223. Urban JH, Schneider RM, Compte M, Finger C, Cichutek K, et al. (2005) Selection of functional human antibodies from retroviral display libraries. Nucleic Acids Research 33: e35. doi:10.1093/nar/gni033

224. Friguet B, Chaffotte AF, Djavadi-Ohaniance L, Goldberg ME (1985) Measurements of the true affinity constant in solution of antigen-antibody complexes by enzyme-linked immunosorbent assay. J Immunol Methods 77: 305–319. doi:10.1016/0022-1759(85)90044-4

225. Grützkau A, Radbruch A (2010) Small but mighty: how the MACS-technology based on nanosized superparamagnetic particles has helped to analyze the immune system within the last 20 years. Cytometry A 77: 643–647. doi:10.1002/cyto.a.20918

226. Saiyed Z, Telang S, Ramchand C (2003) Application of magnetic techniques in the field of drug discovery and biomedicine. BioMag Res Technol 1: 2. doi:10.1186/1477-044X-1-2

227. Curtin JA, Dane AP, Swanson A, Alexander IE, Ginn SL (2008) Bidirectional promoter interference between two widely used internal heterologous promoters in a late-generation lentiviral construct. Gene Ther 15: 384–390. doi:10.1038/sj.gt.3303105

228. Mizuguchi H (2000) IRES-Dependent Second Gene Expression Is Significantly Lower Than Cap-Dependent First Gene Expression in a Bicistronic Vector. Mol Ther 1: 376–382. doi:10.1006/mthe.2000.0050

229. Yu X (2003) Lentiviral vectors with two independent internal promoters transfer high-level expression of multiple transgenes to human hematopoietic stem-progenitor cells. Mol Ther 7: 827–838. doi:10.1016/S1525-0016(03)00104-7

230. Ben-Dor I, Itsykson P, Goldenberg D, Galun E, Reubinoff BE (2006) Lentiviral vectors harboring a dual-gene system allow high and homogeneous transgene expression in selected polyclonal human embryonic stem cells. Mol. Ther. 14: 255–267. doi:10.1016/j.ymthe.2006.02.010

231. de Felipe P, Luke GA, Hughes LE, Gani D, Halpin C, et al. (2006) E unum pluribus: multiple proteins from a self-processing polyprotein. Trends in Biotechnology 24: 68–75. doi:10.1016/j.tibtech.2005.12.006

232. de Felipe P, Luke GA, Brown JD, Ryan MD (2010) Inhibition of 2A-mediated “cleavage” of certain artificial polyproteins bearing N-terminal signal sequences. Biotechnol J 5: 213–223. doi:10.1002/biot.200900134

233. Moulard M, Decroly E (2000) Maturation of HIV envelope glycoprotein precursors by cellular endoproteases. Biochim. Biophys. Acta 1469: 121–132.

234. Moulard M, Hallenberger S, Garten W, Klenk HD (1999) Processing and routage of HIV glycoproteins by furin to the cell surface. Virus Research 60: 55–65.

235. Binley JM, Sanders RW, Clas B, Schuelke N, Master A, et al. (2000) A recombinant human immunodeficiency virus type 1 envelope glycoprotein complex stabilized by an intermolecular disulfide bond between the gp120 and gp41 subunits is an antigenic mimic of the trimeric virion-associated structure. Journal of Virology 74: 627–643.

236. Binley JM, Sanders RW, Master A, Cayanan CS, Wiley CL, et al. (2002) Enhancing the Proteolytic Maturation of Human Immunodeficiency Virus Type 1 Envelope Glycoproteins. Journal of Virology 76: 2606–2616. doi:10.1128/JVI.76.6.2606-2616.2002

237. Pancera M, Wyatt R (2005) Selective recognition of oligomeric HIV-1 primary isolate envelope glycoproteins by potently neutralizing ligands requires efficient precursor cleavage. Virology 332: 145–156. doi:10.1016/j.virol.2004.10.042

238. Dey AK, David KB, Lu M, Moore JP (2009) Biochemical and biophysical comparison of cleaved and uncleaved soluble, trimeric HIV-1 envelope glycoproteins. Virology 385: 275–281. doi:10.1016/j.virol.2008.12.009

239. Carnes AE, Luke JM, Vincent JM, Schukar A, Anderson S, et al. (2011) Plasmid DNA fermentation strain and process-specific effects on vector yield, quality, and transgene expression. Biotechnol. Bioeng. 108: 354–363. doi:10.1002/bit.22936

240. Williams JA, Luke J, Langtry S, Anderson S, Hodgson CP, et al. (2009) Generic plasmid DNA production platform incorporating low metabolic burden seed-stock and fed-batch fermentation processes. Biotechnol. Bioeng. 103: 1129–1143. doi:10.1002/bit.22347

241. O'Mahony K, Freitag R, Hilbrig F, Muller P (2007) ScienceDirect - Process Biochemistry : Strategies for high titre plasmid DNA production in Escherichia coli DH5α. Process ….

242. Yau SY, Keshavarz-Moore E, Ward J (2008) Host strain

influences on supercoiled plasmid DNA production in Escherichia coli: Implications for efficient design of large-scale processes. Biotechnol. Bioeng. 101: 529–544. doi:10.1002/bit.21915

243. Madigan MT, Martinko JM, Dunlap PV, Clark DP (2005) Brock Biology Of Microorganisms. 11th ed. Benjamin Cummings. 1088 p.

244. Hu WS, Temin HM (1990) Retroviral recombination and reverse transcription. Science 250: 1227–1233.

245. Levin A, Hayouka Z, Brack-Werner R, Volsky DJ, Friedler A, et al. (2009) Novel regulation of HIV-1 replication and pathogenicity: Rev inhibition of integration. Protein Engineering Design and Selection 22: 753–763. doi:10.1093/protein/gzp060

246. Segura MM, Kamen AA, Garnier A (2011) Methods in Molecular Biology. Merten O-W, Al-Rubeai M, editors Totowa, NJ: Humana Press. 89–116 pp. doi:10.1007/978-1-61779-095-9_4

247. Matz MV, Fradkov AF, Labas YA, Savitsky AP, Zaraisky AG, et al. (1999) Fluorescent proteins from nonbioluminescent Anthozoa species. Nat Biotech 17: 969–973. doi:10.1038/13657

248. University of Chicago Press Staff ed. (2010) The Chicago Manual of Style. 16th ed. University of Chicago Press Staff, editor University Of Chicago Press. 1026 p.

249. McNaught A, Wilkinson A (1997) Compendium of chemical terminology: IUPAC.

250. Liebecq C (1992) Biochemical Nomenclature: And Related Documents.

251. PLoS ONE (n.d.) PLoS ONE. Public Library of Science.

252. Yanisch-Perron C, Vieira J, Messing J (1985) Improved M13 phage cloning vectors and host strains: nucleotide sequences of the M13mpl8 and pUC19 vectors. Gene 33: 103–119. doi:10.1016/0378-1119(85)90120-9

253. Adachi A, Gendelman HE, Koenig S, Folks T, Willey R, et al. (1986) Production of acquired immunodeficiency syndrome-associated retrovirus in human and nonhuman cells transfected with an infectious molecular clone. Journal of Virology 59: 284–291.

Acknowledgements

The success of any project depends largely on the encouragement and help of many generous people. I take this opportunity to express my gratitude to the people who have contributed considerably to the successful completion of this thesis.

I am very grateful to Prof. Dr. Ralf Wagner for his supervision, fundraising and his tremendous support at the Universitätsklinikum Regensburg. He motivated, encouraged and gave me guidance during all states of this project.

I deeply thank Prof. Dr. Stefan Dübel for mentoring my work and his cordially support at the Technische Universität Braunschweig.

I would like to express my special gratitude to Prof. Dr. Hans Wolf and Prof. Dr. Dr. André Gessner for their support at the Institut für medizinische Mikrobiologie und Hygiene, Regensburg.

I sincerely thank my laboratory supervisor Dr. Alexander Kliche for his excellent guidance and support during this work.

Thanks to Dr. Petra Hoffmann, Jaqueline Igl, Jasmin Stahl and Rüdiger Eder for their supervision and support in FACS sorting.

I am highly indebted to Dr. Alexander Kliche, Dr. Benedikt Asbach, Dr. Laura Klingseisen and Dr. Ulrike Heigl for their expertise and patience in providing advice and suggestions regarding this manuscript.

It is with immense gratitude that I acknowledge the support and help of all my colleagues who not only contributed to this work, but also facilitated the amazing experience of working with friendly, generous, thoughtful and cooperative people.

My heartfelt thanks go to my parents, my brother and sister, my friends and to Laura for their patience, love and encouragement.